TURUN YLIOPISTO
UNIVERSITY OF TURKU

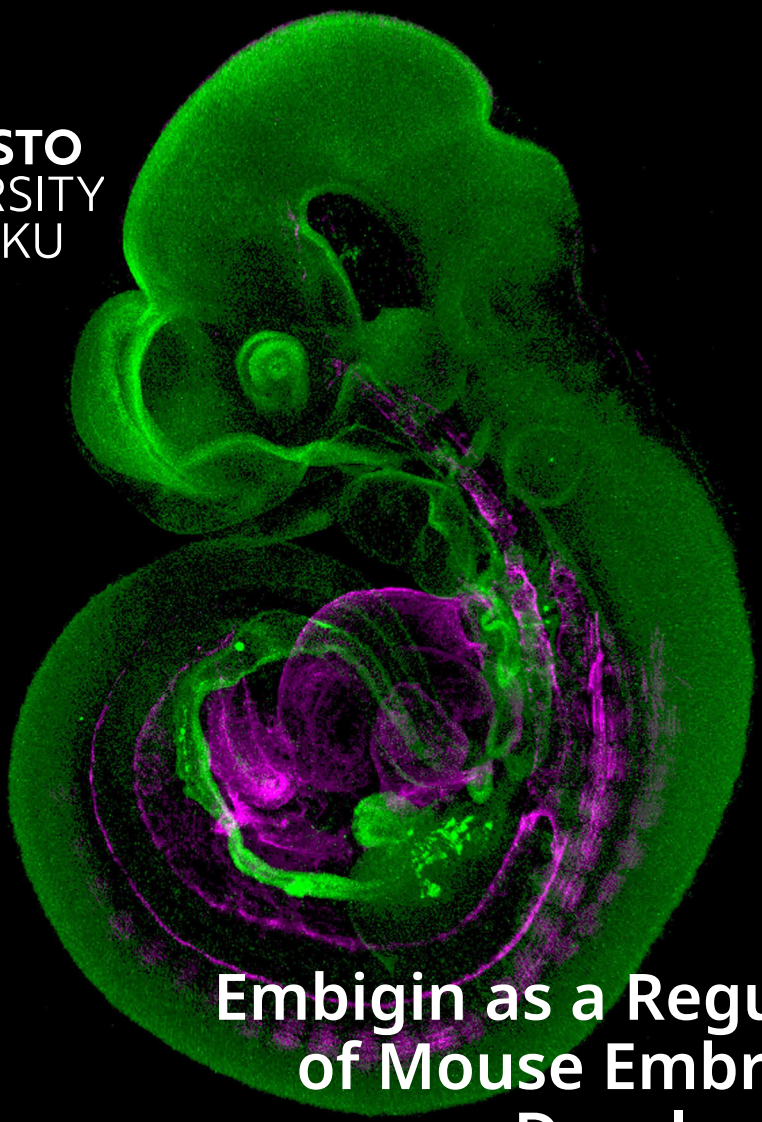

Embigin as a Regulator of Mouse Embryonic Development

Salli Talvi

TURUN YLIOPISTON JULKAISUJA – ANNALES UNIVERSITATIS TURKUENSIS
SARJA – SER. AI OSA – TOM. 750 | ASTRONOMICA – CHEMICA – PHYSICA – MATHEMATICA | TURKU 2025

TURUN
YLIOPISTO
UNIVERSITY
OF TURKU

EMBIGIN AS A REGULATOR OF MOUSE EMBRYONIC DEVELOPMENT

Salli Talvi

TURUN YLIOPISTON JULKAISUJA – ANNALES UNIVERSITATIS TURKUENSIS
SARJA – SER. AI OSA – TOM. 750 | ASTRONOMICA - CHEMICA - PHYSICA – MATHEMATICA | TURKU 2025

University of Turku

Faculty of Technology
Department of Life Technologies
Biochemistry
Doctoral Programme in Technology (DPT)

Supervised by

Professor Jyrki Heino, M.D., Ph.D.
Department of Life Technologies
InFLAMES Research Flagship
University of Turku, Finland

Johanna Jokinen, Ph.D.
Department of Life Technologies
InFLAMES Research Flagship
University of Turku, Finland

Associate Professor Pia Rantakari, Ph.D.
Turku Bioscience Centre
InFLAMES Research Flagship
University of Turku, Finland

Reviewed by

Docent Ulla Pirvola, Ph.D.
Molecular and Integrative Biosciences Research Programme
University of Helsinki, Finland

Docent Keijo Viiri, Ph.D.
Faculty of Medicine and Health Technology
Tampere University, Finland

Opponent

Professor Seppo Vainio, Ph.D.
Biocenter Oulu
University of Oulu, Finland

Cover Image: Salli Talvi

ISBN 978-952-02-0436-5 (PRINT)
ISBN 978-952-02-0437-2 (PDF)
ISSN 0082-7002 (Print)
ISSN 2343-3175 (Online)
Painosalama, Turku, Finland 2025

“Kaikki on hyvin epävarmaa, ja juuri se tekee minut levolliseksi.”

-Tuu-tikki (Tove Jansson, Taikatalvi, 1957)

UNIVERSITY OF TURKU
Faculty of Technology
Department of Life Technologies
Biochemistry
SALLI TALVI: Embigin as a regulator of mouse embryonic development
Doctoral Dissertation, 180 pp.
Doctoral Programme in Technology
November 2025

ABSTRACT

Embigin (Gp70) is a transmembrane glycoprotein belonging to the basigin subgroup of the immunoglobulin superfamily. Embigin functions as an ancillary protein for monocarboxylate transporters (MCT) and may regulate cell-extracellular matrix interactions, particularly through fibronectin. Additionally, in adult mice, embigin function has been linked to stem cell regulation. However, the role of embigin in mouse embryogenesis has remained unclear. This doctoral thesis describes embigin protein expression during embryogenesis and in adult mice and the effect of embigin deficiency ($Emb^{-/-}$) in mice, especially in lung and kidney organogenesis, and sheds some light on the function of embigin during mouse development.

First, we found that embigin protein is highly expressed during the early stages of mouse embryogenesis and later in the tubular epithelial structures of the lungs, kidneys, epididymis, and skin. The high neonatal mortality observed in $Emb^{-/-}$ mice is mainly due to delayed lung maturation and general delayed embryonic development. We noticed embigin expression in the lung primordium, suggesting the function of embigin is vital during early lung development. Furthermore, embigin was detected in adult mouse lungs in stem-like club cells. Second, we described in detail the protocol for the lung branching analysis in E12.5 mouse embryos used in the first article. Third, during mouse kidney development, we found that embigin is expressed in the kidney primordium and later in the ureteric bud (UB) and differentiating nephron precursors. The embigin deficiency retards UB branching during the early stages of kidney development, and in E13.5 $Emb^{-/-}$ kidneys, genes related to nephron development were downregulated. However, the observed delay was transient. Additionally, embigin appears to regulate directly *Pappa2*, *Acta2*, and *Tagln* genes during kidney development. Overall, embigin likely participates in early mouse development by supporting tissue-specific stem cell functions.

KEYWORDS: embigin, embryonic development, lung development, kidney development, stem cells

TURUN YLIOPISTO
Teknillinen tiedekunta
Bioteknologian laitos
Biokemia
SALLI TALVI: Embigiini hiiren alkionkehityksen säätelijänä
Väitöskirja, 180 s.
Teknologian tohtoriohjelma
Marraskuu 2025

TIIVISTELMÄ

Embigiini (Gp70) on solukalvon glykoproteiini, joka kuuluu immunoglobuliinien superperheen basigiini-alaryhmään. Embigiini toimii monokarboksylaatti-kuljettajien (MCT) apuproteiinina ja saattaa säädellä solu-soluväliaine-vuorovaikutuksia erityisesti fibronektiinin kautta. Lisäksi aikuisissa hiirissä embigiinin toiminta on yhdistetty kantasolujen säätelyyn. Embigiinin rooli hiiren alkionkehityksessä on kuitenkin jäänyt epäselväksi. Tämä väitöskirja kuvaa embigiini-proteiinin ilmentymistä alkionkehityksen aikana ja aikuisissa hiirissä sekä embigiini-puutoksen ($Emb^{-/-}$) vaikutusta hiirissä, etenkin keuhkojen ja munuaisten muodostumisessa, ja valottaa embigiinin toimintaa hiiren kehityksen aikana.

Ensinnäkin havaitsimme, että embigiini-proteiinia ilmentyy voimakkaasti hiiren alkionkehityksen alkuvaiheissa ja myöhemmin keuhkojen, munuaisten, lisäkiveksen ja ihon putkimaisissa epiteelirakenteissa. $Emb^{-/-}$ hiirillä havaittu korkea vastasyntyneiden kuolleisuus johtuu pääasiassa viivästyneestä keuhkojen kypsymisestä ja yleisestä viivästyneestä alkionkehityksestä. Havaitsimme embigiinin ilmentyvän keuhkojen primordiumissa, mikä viittaa siihen, että embigiinin toiminta on tärkeää keuhkojen varhaiskehityksen aikana. Lisäksi embigiiniä havaittiin aikuisen hiiren keuhkojen kantasolumaisissa club-soluissa. Toiseksi kuvailimme yksityiskohtaisesti ensimmäisessä artikkelissa käytetyn menetelmän keuhkojen haarautumisanalyysille E12.5-hiiren alkioissa. Kolmanneksi huomasimme hiiren munuaisten kehityksessä embigiinin ilmentyvän munuaisen primordiumissa sekä myöhemmin ureetterisilmussa (UB) ja erilaistuvissa nefronien esiasteissa. Embigiinin puutos viivästyttää UB:n haarautumista munuaisten kehityksen alussa, ja E13.5 $Emb^{-/-}$ munuaisissa nefronien kehitykseen liittyvät geenit olivat alassäädeltyjä. Havaittu viivästyminen oli kuitenkin väliaikaista. Lisäksi embigiini näyttää säätelevän suoraan *Pappa2*-, *Acta2*- ja *Tagln*-geenejä munuaisten kehityksen aikana. Kaiken kaikkiaan embigiini todennäköisesti osallistuu hiiren varhaiseen kehitykseen tukemalla kudoskohtaisia kantasolujen toimintoja.

ASIASANAT: embigiini, alkionkehitys, keuhkojen kehitys, munuaisten kehitys, kantasolut

Table of Contents

Abbreviations

α-SMA	alpha smooth muscle actin
ASC	adult stem cell
ATI cell	alveolar type I cell
ATII cell	alveolar type II cell
BASC	bronchioalveolar stem cell
BPD	bronchopulmonary dysplasia
BSA	bovine serum albumin
$Bsg^{-/-}$	basigin homozygous knockout
CAKUT	congenital anomalies of the kidney and urinary tract
cDNA	complementary DNA
E	embryonic day
ECM	extracellular matrix
Emb	embigin
$Emb^{+/-}$	embigin heterozygous knockout
$Emb^{-/-}$	embigin homozygous knockout
EMT	epithelial-to-mesenchymal transition
ESC	embryonic stem cell
FBS	fetal bovine serum
FGF	fibroblast growth factor
Fgfr2b	fibroblast growth factor receptor 2b
FN	fibronectin
GBM	glioblastoma multiforme
GF	growth factor
H&E	hematoxylin and eosin
HOXC8	Homeobox C8
HSC	hematopoietic stem cell
HSPC	hematopoietic stem and progenitor cell
ICM	inner cell mass
IF	immunofluorescence
IGF	insulin-like growth factor
IM	intermediate mesoderm

iPSC	induced pluripotent stem cell
MCT	monocarboxylate transporter
MET	mesenchymal-to-epithelial transition
MM	metanephric mesenchyme
MMP	matrix metalloproteinases
MSC	mesenchymal stem cell
NC	nephrogenic cord
ND	nephric duct
NPC	nephron progenitor cell
NSC	neural stem cell
P	postnatal day
PAPP-A2	pregnancy-associated plasma protein A2
PCR	polymerase chain reaction
PGC	primordial germ cell
R3hdml	R3h domain containing-like
RNA-seq	RNA sequencing
scRNA-seq	single-cell RNA sequencing
SPC	surfactant protein C
STAD	stomach adenocarcinoma
TEM	transmission electron microscopy
UB	ureteric bud
VNN1	vanin 1
WB	western blotting
WM	whole-mount
WT	wild type

List of Original Publications

This dissertation is based on the following original publications, which are referred to in the text by their Roman numerals:

I **Talvi S.**, Jokinen J., Sipilä K., Rappu P., Zhang F. P., Poutanen M., Rantakari P., & Heino J. Embigin deficiency leads to delayed embryonic lung development and high neonatal mortality in mice. *iScience*, 2024a; 27: 108914.

II **Talvi S.**, Jokinen J., Rantakari P., & Heino J. Protocol to study early lung developmental branching in mouse embryos using explant culture. *STAR Protocols*, 2024b; 5: 103198.

III **Talvi S.**, Jokinen J., Rappu P., Leppäkoski R., Kurtzeborn K., Rantakari P., Kuure S., & Heino J. Embigin is involved in the regulation of early mouse kidney development. Manuscript, 2025.

List of Contemporaneous Publications

- Sipilä K., Rognoni E., Jokinen J., Tewary M., Vietri Rudan M., **Talvi S.**, Jokinen V., Dahlström K. M., Liakath-Ali K., Mobasseri A., Du-Harpur X., Käpylä J., Nutt S. L., Salminen T. A., Heino J., & Watt F. M. Embigin is a fibronectin receptor that affects sebaceous gland differentiation and metabolism. *Developmental Cell*, 2022; 57: 1453-1465.e7.

1 Introduction

The laboratory mouse (*Mus musculus*) is the most commonly used mammalian model in scientific research due to its advantages in size, reproduction rate, and relatively short lifespan. On average, the protein-coding regions of the mouse and human genomes are 85% identical, and nearly all genes identified in one species have a closely related counterpart in the other. Therefore, the mouse serves as an excellent model organism for studying human biology, although there are certain limitations. The mouse has become a crucial source of information on various aspects of developmental molecular genetics and is also a valuable model for embryological studies (Alberts et al., 2002; Haque et al., 2025). Notably, our protein of interest, embigin, has been linked to early mouse development (R.-P. Huang et al., 1990; Fan et al., 1998).

1.1 Mouse embryonic development

Normal embryonic development is the result of a series of stereotypical and coordinated cell fate decisions and morphogenetic events. The mammalian embryo develops within the uterus, and the development of a placenta quickly provides nutrition from the mother, reducing the need for the developing egg cell to store large amounts of raw materials. The gestation period in mice is, on average, 18 to 22 days. Since this period is short compared to humans, the term “embryo” in this context refers to the developing mouse from fertilization to birth. The age of the embryo is referred to as embryonic day (E; embryonic age) or days post coitum (dpc; post-coital age). Mouse embryonic development can be roughly divided into two periods: preimplantation and postimplantation (Figure 1). Early mouse development depends on the tightly regulated generation and organization of cells. During the preimplantation stages of mouse development, the totipotent zygote divides to form the first 2 and 4 cells. Then the cells undergo compaction to form a morula at the 8- to 16-cell stage by three days after fertilization. Shortly after this, an internal cavity develops to form a blastocyst, in which the outer layer of cells (trophectoderm) gives rise to extraembryonic tissues, and the inner cell mass gives rise to the embryo proper and some extraembryonic structures (Alberts et al., 2002; Kojima et al., 2014; Rivera-Pérez & Hadjantonakis, 2015).

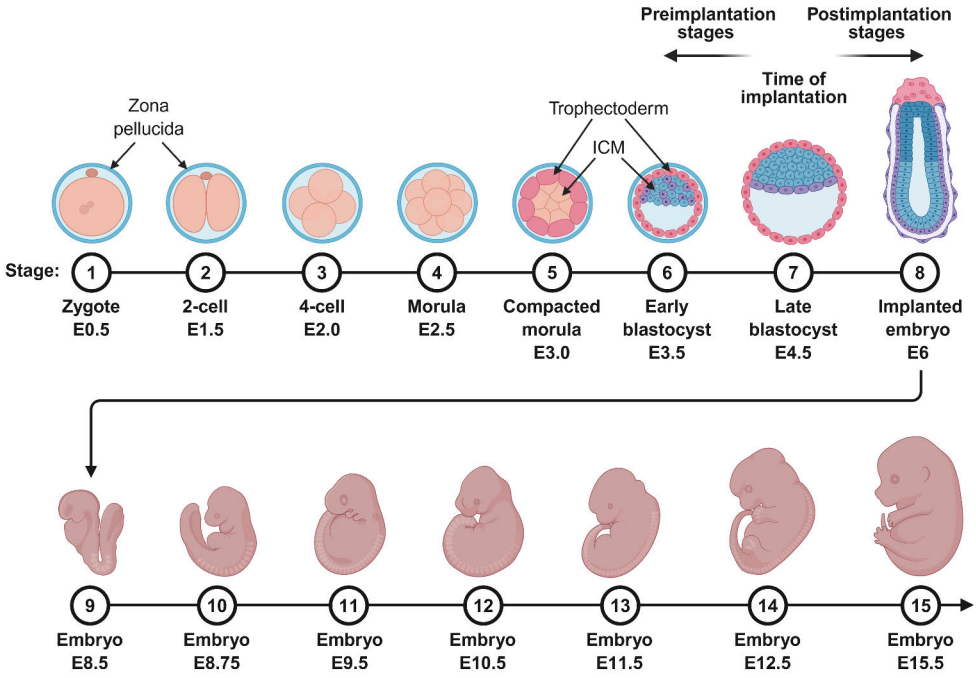

Figure 1. Schematic representation of mouse embryonic development. The embryonic stages of mouse development at embryonic days 0.5-15.5 (E0.5-E15.5) are shown. The development can be divided into preimplantation and postimplantation stages. Before the implantation, the embryo escapes the zona pellucida capsule. The inner cell mass (ICM) forms the embryo proper, and the trophectoderm generates extraembryonic tissues. ICM, inner cell mass. Adapted from BioRender.com "Mouse Development Embryonic Stages" template (https://app.biorender.com/biorender-templates/details/t-6009a97e28bf69021fdce6e1-mouse-development-embryonic-stages).

1.1.1 Implantation and gastrulation

Approximately four days after fertilization, the embryo escapes the zona pellucida capsule, allowing it to implant itself into the uterine wall around E4.5 and begin the formation of the placenta. During the implantation (Figure 2), the inner cell mass and trophectoderm of the late blastocyst produce distinctly different cell types. The inner cell mass differentiates into epiblast (primitive ectoderm) and hypoblast (primitive endoderm). The trophectoderm differentiates into trophoblast cells, which continue to encapsulate the embryo and expand to form the ectoplacental cone and generate the embryo-supporting extraembryonic tissues, such as the placenta and yolk sac. The epiblast forms almost all embryo proper tissues and the extraembryonic mesoderm, while the hypoblast serves as a precursor to parietal endoderm and visceral endoderm (Alberts et al., 2002; Kojima et al., 2014; Rivera-Pérez & Hadjantonakis, 2015).

The epiblast grows rapidly into the yolk sac cavity during the early postimplantation stages. During this cavitation process, the mouse egg cylinder transforms from a solid mass to a hollow cup-shaped structure as the epiblast forms a columnar epithelium that surrounds the proamniotic cavity (Figure 2). By E6.0, the postimplantation epiblast has formed and transformed into a pseudostratified epithelium (Kojima et al., 2014; Rivera-Pérez & Hadjantonakis, 2015). The epiblast and the extraembryonic ectoderm are two separate but coherent epithelia, the apical surface of which faces the proamniotic cavity. The visceral endoderm is a specialized extraembryonic tissue layer that functions as both a nutrient supplier and a signaling center, and it is in contact with both the epiblast and extraembryonic ectoderm (Bielinska et al., 1999; Rivera-Pérez & Hadjantonakis, 2015). The parietal endoderm and trophoblast giant cells surround the visceral endoderm (Figure 2). The parietal endoderm plays a central role in creating the extraembryonic environment by participating in the transport of nutrients (Yagi et al., 2016; Filimonow & de la Fuente, 2022). The trophoblast giant cells, derived from the trophectoderm, participate in the formation of the fetal-maternal interface by interacting with the maternal decidua and blood vessels during implantation and placentation (Hu & Cross, 2009).

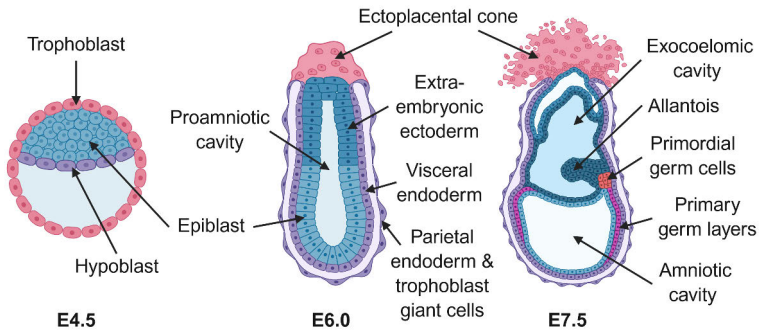

Figure 2. Embryonic structures during implantation and mid-gastrulation. During the implantation, the inner cell mass of the late blastocyst differentiates into the epiblast and hypoblast. The outer trophectoderm cell layer differentiates into the trophoblast, which expands to form the ectoplacental cone (a precursor for placental tissues). The proamniotic cavity opens and elongates. By E6.0, the embryo has implanted, and the visceral endoderm surrounds both the epiblast and extraembryonic ectoderm. In addition, the visceral endoderm is surrounded by the parietal endoderm and trophoblast giant cells. Next, the primitive streak appears, and the primordial germ cell populations form. The gastrulation begins around E6.5: cells originating from the epiblast at the primitive streak undergo an epithelial to mesenchymal transition and invade the primitive streak, forming the primary germ layers. The allantois, a crucial component in creating the chorioallantoic placenta and umbilical circulation, emerges during early gastrulation. During mid-gastrulation at E7.5, mesoderm-derived cells from the primitive streak extend around the embryo and divide the proamniotic cavity into the exocoelomic cavity and amniotic cavity. E, embryonic day. Created with BioRender.com.

A transient structure known as the primitive streak is a thickening of pluripotent cells that appears on the posterior region of the epiblast during early gastrulation. In mice, gastrulation occurs mainly from E6.25 to E9.5 and is the process that forms the primary germ layers: ectoderm, mesoderm, and endoderm (Bardot & Hadjantonakis, 2020). During gastrulation, cells from the posterior region of the epiblast migrate into the primitive streak. At this location, epiblast cells undergo an epithelial-to-mesenchymal transition (EMT), which involves changes in cell shape. As epiblast cells move into the primitive streak, they contribute to the formation of the mesoderm and endoderm, while the remaining epiblast cells develop into the ectoderm. Additionally, during mid-stage gastrulation at E7.5 (Figure 2), mesoderm-derived cells from the primitive streak extend around the embryo, and the proamniotic cavity is divided into two fluid-filled spaces: the amniotic cavity and the exocoelomic cavity (Kojima et al., 2014; Rodriguez & Downs, 2017; Muhr et al., 2025). A spatiotemporally controlled sequence of events during gastrulation leads to the generation and positioning of organ progenitors (Bardot & Hadjantonakis, 2020). The primitive streak serves as a pathway for cell migration and differentiation, which ultimately determines the body structure and the future organization of the embryo. It defines the body axis of the embryo by marking the anterior-posterior polarity of the embryo (Rivera-Pérez & Magnuson, 2005; Rodriguez & Downs, 2017; Muhr et al., 2025).

Primordial germ cells (PGCs) are the first population of germ cells to form during embryogenesis. They serve as the direct precursors to gametes, egg cells (oocytes) in females and sperm cells (spermatogonia) in males, and are responsible for passing genetic and epigenetic information across generations. In mammals, the lineage of germ cells is distinguished from the somatic lineages early in development through the induction from pluripotent embryonic cells (epigenesis). PGCs are formed outside the developing embryo and migrate to the gonads, where they mature into egg or sperm cells. In mouse embryos, the germ cell lineage first appears in the epiblast before the primary germ layers are established during gastrulation. PGCs arise from a cluster of cells at the base of the forming allantois around E7.25 (Figure 2). By E10.5, the PGCs migrate to the developing gonads, where they begin to differentiate toward either an oogenic or spermatogenic pathway (Tam & Loebel, 2009; Saitou & Yamaji, 2012).

1.1.2 Organogenesis

Simultaneously with gastrulation, newly specified cells continue to differentiate into progenitors for several organs and tissues. This process is known as organogenesis. Cells departing from the primitive streak during gastrulation are patterned into progenitors of multiple organ systems as they migrate away from the primitive streak

to their destination. These cells reach their locations at various times, resulting in exposure to distinct signaling environments. This process results in the formation of a variety of cell types, which are organized into functional units (Bardot & Hadjantonakis, 2020). Mouse organogenesis initiates around E8.0-E8.5 with the formation of the neural plate and heart tube. The organogenesis progresses rapidly over the following days, occurring primarily between E9.5 and E13.5, when almost all major organ systems start to develop. Strikingly, in a short timeframe, the cells of the three germ layers transform into an embryo that contains most of the major internal and external organs (Cao et al., 2019; Qu et al., 2023).

The lateral asymmetry of the body axis is a crucial aspect of vertebrate organogenesis. At the end of gastrulation, the heart and the primordia of the respiratory and digestive organs are positioned along the midline. The right-sided looping of the developing heart is the first noticeable sign of left-right (L-R) asymmetry (Saijoh & Hamada, 2020). In amniotes, the second noticeable asymmetrical event is referred to as axial rotation. This, also known as "turning", is a significant morphogenetic movement and occurs between E8.5 and E9.0 in mice (Figure 3). During this process, the longitudinal axis of the embryo curves into a U-shape, ultimately leading to the embryo adopting a "fetal" position. This movement is essential for establishing the final body plan and asymmetry of the embryo. The rotation also has the crucial effect of closing the region of the midgut (Faisst et al., 2002; Copp et al., 2023). In addition, the embryo gets enwrapped by its extraembryonic membranes as a result of the rotation: the amnion and visceral yolk sac (Dobreva et al., 2010). Finally, all visceral organs exhibit L-R asymmetry, either by developing as single organs, such as the heart, or by having bilateral paired organs, like the lungs, which show a difference in lobe number on each side (Faisst et al., 2002; Copp et al., 2023). Furthermore, axial rotation is closely linked to neural tube closure, which begins in the anterior region (brain) and continues during the rotation period. In mice, this process occurs in two phases. The primary neurulation takes place between E8.5 and E10.5. During this phase, the neural folds fold and close at the dorsal side to form the neural tube. The secondary neurulation occurs from E10.5 to E13.5. In this phase, the caudalmost part of the neural tube is formed through a mesenchymal-to-epithelial transition (MET) process in the tailbud (Copp et al., 2023).

After the specification and migration away from the anterior primitive streak during gastrulation, the definitive endoderm integrates into the visceral endoderm on the embryo's surface, leading to the dispersion of the visceral endoderm. Around E8.0, the epithelial endoderm aligns at the midline and undergoes involution to form the primitive gut tube. The primitive gut tube is specified into foregut, midgut, and hindgut regions around E8.5 (Bardot & Hadjantonakis, 2020; Zhao et al., 2022). The most anterior foregut region gives rise to the formation of primordia of various

visceral organs. The patterning of the foregut aligns with the future locations of organs that will emerge during organogenesis, with progenitor cells for the thymus, thyroid, esophagus, lungs, stomach, liver, and pancreas. In the more posterior regions, the midgut and hindgut develop into the primordia of small and large intestines (Mori & Cardoso, 2014; Bardot & Hadjantonakis, 2020).

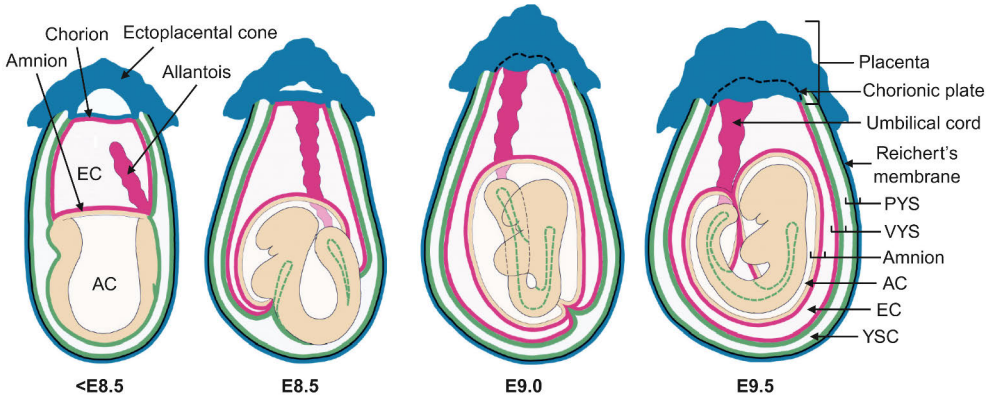

Figure 3. Extraembryonic tissues of a mouse embryo before and after axial rotation. Schematic representation of the extraembryonic tissues in mouse development from E8.5 to E9.5. The embryo becomes enclosed in its extraembryonic membranes during the process of axial rotation. The extraembryonic mesoderm is shown in magenta, the extraembryonic endoderm is shown in green, and the trophectoderm-derived extraembryonic lineages are shown in blue. AC, amniotic cavity; E, embryonic day; EC, exocoelomic cavity; PYS, parietal yolk sac; VYS, visceral yolk sac; YSC, yolk sac cavity. Adapted from Dobreva et al., 2010, 2012.

1.1.3 Extraembryonic tissues and placentation

During embryogenesis, mammals produce complex extraembryonic structures, including the placenta and "fetal membranes", which comprise the allantois, chorion, yolk sac, and amnion. They enclose and protect the embryo while facilitating the exchange of metabolic products with the mother (Alberts et al., 2002; Carter, 2016). They are also vital in organizing embryonic patterning and axial specification (Rivera-Pérez & Hadjantonakis, 2015).

In mice, the yolk sac is composed of two distinct parts: the parietal yolk sac and the visceral yolk sac, and they play crucial roles in early embryonic development. The parietal yolk sac surrounds the embryo and contains the parietal endoderm, Reichert's membrane, and trophoblast giant cells (Figure 3), which provide biomechanical protection for the embryo at early postimplantation stages (Copp, 2025). The visceral yolk sac develops into an epithelial layer over the epiblast and extraembryonic ectoderm (Figure 3). It has a visceral endoderm layer derived from the hypoblast and a mesodermal layer derived from epiblast cells. The visceral yolk

sac functions as an exchange system for nutrients, waste, and gas and is the initial site of hematopoiesis (Yagi et al., 2016; Yamane, 2018; Ornoy & Miller, 2023).

The amnion is the innermost extraembryonic membrane that surrounds the embryo in amniotic fluid and lines the fluid-filled amniotic cavity (Figure 3). It consists of two layers: an outer extraembryonic mesoderm layer and an inner amniotic ectoderm layer, which provides the embryo with a closed space and a protective, shock-resistant structure (Pereira et al., 2011; Dobreva et al., 2010, 2012; Chuva de Sousa Lopes et al., 2022).

The choriovitelline and chorioallantoic are two types of fetal membranes that play a role in placental development in mice. The choriovitelline placenta is an early placental structure and supports the embryo until the chorioallantoic placenta has formed around E10 and later acts as an accessory placenta through pregnancy (Figure 3). It is noteworthy that this structure is not established in human development. The allantois emerges from the primitive streak during early gastrulation and is a crucial part of the formation of the chorioallantoic placenta and umbilical cord blood circulation. The allantois reaches towards the chorion and merges with it, forming the chorioallantoic placental labyrinth, where the exchange with the mother takes place: the chorioallantoic placenta consists of the trophoblast-derived chorionic plate and the allantois-derived umbilical cord. The chorioallantoic placenta is the definitive placenta in mice and most other mammals (Carter, 2016; Rodriguez & Downs, 2017; Downs, 2022).

1.1.4 Branching morphogenesis during embryogenesis

Branching morphogenesis is an essential event in embryonic development that shapes the structure of various organs and tissues during organogenesis. This developmental program builds branched epithelial trees in various secretory organs and organs primarily responsible for transporting gases or fluids, including the labyrinthine structure of the placenta, the ducts of mammary glands, the airways of the lungs, and the collecting ducts of the kidneys (Rinkenberger & Werb, 2000; Alberts et al., 2002; Varner & Nelson, 2014; Caldeira et al., 2018).

The branching process is driven by exchanges of signals between mesenchymal cells and the invading epithelium. These molecular signaling pathways that regulate branching morphogenesis appear to be conserved across organs and species, although the final geometries of epithelial trees are different. The process seems to be controlled by a conserved set of molecules, such as fibroblast growth factors (FGFs) (Varner & Nelson, 2014). The mouse model has played a significant role in studying the branching morphogenesis regulation, and the effects of signaling pathways important for this process can be investigated using gene knockout experiments (Alberts et al., 2002).

The effectiveness of branching morphogenesis is significantly influenced by the composition and organization of the extracellular matrix (ECM) (Alberts et al., 2002; Caldeira et al., 2018). The local synthesis and accumulation of certain ECM proteins, such as fibronectin, collagens, and laminins, contribute to the creation of a supportive and stable microenvironment that facilitates tissue growth. Additionally, these proteins can trigger a series of molecular events that lead to changes in cell morphology, reduce cell-cell adhesion, and promote a motile phenotype that enhances cleft formation, which, in turn, may lead to epithelial bud formation and branching. For instance, fibronectin production and deposition are crucial for cleft formation in branching morphogenesis of the lungs and kidneys (Caldeira et al., 2018).

ECM remodeling is a dynamic process that delivers structural integrity and regulates various cellular processes, such as cell shape, motility, and growth. The ECM cleavage is central during branching morphogenesis, allowing the epithelial cells to proliferate, migrate, and invade the surroundings. During this process, matrix metalloproteinases (MMPs) are involved in ECM degradation and remodeling, and are, therefore, key regulators of invasion and branching. Furthermore, MMPs' proteolytic activity also leads to the release of ECM fragments and growth factors (GFs), which are crucial for enhancing epithelial cell proliferation and migration, as well as regulating branching morphogenesis (Caldeira et al., 2018).

1.1.5 Lung development

The respiratory system serves as a vital interface between the body and the external environment and has a crucial role in the efficient conduction and clearing of air, while facilitating optimal gas exchange to meet metabolic demands. Its primary function is the exchange of oxygen from the air with carbon dioxide from the cardiovascular system. Over the course of evolution, the respiratory system in mammals has developed into a complex network of branching epithelial and vascular structures, connecting to a vast network of alveolar units dedicated to gas exchange. This system can be divided into two major regions: the upper and lower respiratory tracts. The upper respiratory tract extends from the external nares to the larynx, while the lower respiratory tract continues from the larynx to the alveoli (Mori & Cardoso, 2014; Hakim & Usmani, 2014).

Mouse lung development initiates around E9.0-E9.5. The process can be divided into five stages (Figure 4): embryonic, pseudoglandular, canalicular, saccular, and alveolar (Langhe et al., 2006; Bogue et al., 2012; Herriges & Morrisey, 2014; Mori & Cardoso, 2014). The lung and trachea progenitor cells arise from the foregut endoderm. The earliest sign of endoderm specification into the respiratory lineage is the localized expression of homeobox protein Nkx2-1 in the central region of the

foregut endoderm, approximately at E9.0 in mice. During the embryonic stage, the primordial lungs emerge at midgestation at E9.5, when the epithelium of the endoderm grows into the neighboring mesenchyme to form the two initial lung buds, which eventually form the left and right main bronchi. Local Fgf10 expression in the foregut mesoderm at E9.5 activates endodermal fibroblast growth factor receptor 2b (Fgfr2b) signaling to expand the lung progenitors and develop the lung buds. The trachea develops to the point where the primary buds fuse (the future carina). There are differences in the number of lobes on each side of the lungs. In mice, the left lung consists of one lobe, and the right lung consists of four. The lung L-R patterning is related to the general body plan and begins long before lungs are formed (Mori & Cardoso, 2014; Dean & Cheong, 2023).

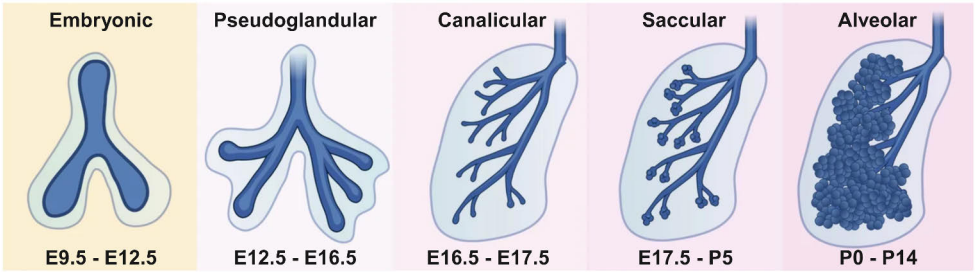

Figure 4. The stages of mouse lung development. The figure illustrates the five stages of mouse lung development: embryonic, pseudoglandular, canalicular, saccular, and alveolar. E, embryonic day; P, postnatal day. Adapted from Dean & Cheong, 2023.

During the pseudoglandular stage (E12.5-E16.5), the lung buds undergo extensive branching morphogenesis, resulting in a tree-like network of airways known as the bronchial tree. Throughout this process, epithelial tubes branch repeatedly as they extend. The lungs exhibit a glandular appearance, with thick mesenchyme separating the epithelial tubules (Alberts et al., 2002; Mori & Cardoso, 2014). Fgfr2b, which is expressed in the lung bud epithelium, is essential for the branching process that shapes the developing airways (Peters et al., 1994). Additionally, the lung endoderm differentiates into specific cell lineages along its proximal-distal axis during branching morphogenesis. Expression of Sox2 identifies the proximal endoderm progenitor lineage, while the combined presence of Sox9 and the transcriptional regulator Id2 indicates the distal endoderm progenitor lineage. These two progenitor populations have different fates: the proximal progenitors differentiate eventually into airway neuroendocrine cells, secretory cells, ciliated cells, and mucosal cells, while the distal progenitors develop into alveolar type II (ATII) and alveolar type I (ATI) epithelial cells (Herriges & Morrisey, 2014). Furthermore, endothelial cells lining blood vessels invade the mesenchyme

alongside the lung buds during branching morphogenesis, creating a system of closely spaced airways and blood vessels that is essential for gas exchange in the lungs (Alberts et al., 2002).

During the canalicular stage, which occurs around E16.5-E17.5, the branching of the airways is completed. At this point, the lung epithelium differentiates, allowing for the distinction between conducting airways and respiratory airways. The mesenchyme becomes thinner, which facilitates the convergence of epithelial tubes and blood vessels. As the branches narrow, clusters of epithelial sacs begin to form; the tips of the terminal respiratory tubules expand into the surrounding mesenchyme to create acinar and alveolar ducts. The pulmonary acinus, which is the functional unit for gas exchange, comprises the respiratory bronchioles, alveolar ducts, and alveolar sacs. Simultaneously, the capillary network continues to develop, and ATII cells start to form and synthesize surfactant proteins (Vasilescu et al., 2012; Herriges & Morrisey, 2014; Mori & Cardoso, 2014; Bartman et al., 2020). The cuboidal surfactant-producing ATII cells differentiate from distal epithelial progenitors in the terminal saccules between E16.5 and E18.5. Pulmonary surfactant is essential for proper lung function after birth, as it reduces surface tension in the alveoli. Moreover, the ATII differentiate into squamous gas-exchanging ATI cells, which ultimately cover the majority of the alveolar surface (Aspal & Zemans, 2020; Riccetti et al., 2024).

During the saccular stage, which occurs from E17.5 to postnatal day 5 (P5), the distal airways expand to form saccules. During this period, the tissue between the airspaces, known as the interstitium, becomes thinner due to the apoptosis and differentiation of mesenchymal cells. This thinning, along with an increase in extracellular matrix, allows for the expansion of the alveolar sacs, eventually leading to the alveolar stage, where dense connective tissue containing cartilage and smooth muscle surrounds the airways. Additionally, the ATII and ATI cells continue to differentiate during the saccular stage (Herriges & Morrisey, 2014; Mori & Cardoso, 2014; Domm et al., 2015; Bartman et al., 2020). Importantly, Fgfr2 signaling is critical for the differentiation of alveolar epithelial cells at the saccular stage, particularly ATII cells. This signaling pathway also influences the differentiation of other cell types, such as ATI cells and lung fibroblasts (Riccetti et al., 2024).

The alveolar stage represents the final phase of lung development, during which the alveolar region is subdivided into smaller units known as alveoli, the air sacs responsible for gas exchange. This process, known as alveologenesis, occurs around P0-P14. The formation of alveoli significantly increases the lung's surface area for respiration (Herriges & Morrisey, 2014; Branchfield et al., 2016; Bartman et al., 2020). Surfactant protein C (SPC) is vital for the formation and function of the alveoli. It is specifically expressed in ATII cells postnatally and is essential for the

pulmonary surfactant production. This substance reduces surface tension in the alveoli, helping to prevent their collapse (Branchfield et al., 2016).

When alveologenesis is disrupted, it can lead to a simplification of the alveoli, a condition commonly seen in premature infants diagnosed with bronchopulmonary dysplasia (BPD). This lung disease is often associated with lifelong breathing difficulties. Several factors contribute to the development of BPD, including genetics and conditions related to the maternal, fetal, or postnatal environment. Importantly, many preterm infants are in the saccular phase of lung development, which occurs approximately from E17.5 to P5 in mice. Therefore, mice serve as a suitable experimental model for studying how excessive oxygen exposure can negatively affect saccular development in preterm humans (Domm et al., 2015; Branchfield et al., 2016).

1.1.6 Kidney development

The mammalian kidney is a complex organ made up of thousands of nephrons, the functional units of the kidney, connected by a highly branched collecting duct system. The primary function of the kidneys is to filter waste products and excess fluid from the blood to produce urine, while maintaining the homeostasis of fluids and electrolytes in the body. Blood is filtered in the kidney by the glomerulus, which consists of a capillary loop surrounded by mesangial cells, enveloped in podocytes, and enclosed by Bowman's capsule. From the glomerular space, the produced primary urine flows through the nephron tubule, which includes the proximal tubule, loop of Henle, distal tubule, and finally, the connecting tubule, which joins a collecting duct. The collecting system comprises the cortical and medullary collecting ducts, calyces, papilla, and ureter. During embryonic development, these components are derived from the intermediate mesoderm (IM), with complex interactions between the ureteric bud (UB) and the metanephric mesenchyme (MM), leading to kidney formation. It is noteworthy that the collecting system and the nephron have distinct developmental pathways (Costantini & Kopan, 2010; Pietilä & Vainio, 2014; Kuure & Sariola, 2020).

Mammalian kidney differentiation contains three sequentially formed distinct kidneys: pronephros, mesonephros, and metanephros. The development begins around E8.5 in mice with the formation of the pronephros (Figure 5), which is a transient structure with no known function in mammals. This stage involves the development of the nephric duct (ND), also known as the Wolffian duct or mesonephric duct. In the early phases of kidney development, the IM gives rise to both the embryonic kidney and the gonads, contributing to the formation of the urogenital system. During this initial stage, the ND primordium and nephrogenic cord (NC) emerge from the IM and extend along the anterior-posterior axis of the

developing embryo. As development progresses to the mesonephros stage, which begins at E9.5, the ND forms a simple epithelial tube and undergoes epithelialization. Additionally, the MM starts to form. Subsequently, the caudal cells of the ND proliferate and convert into a pseudostratified epithelium. The pronephros and mesonephros stages are collectively referred to as the kidney primordium (Costantini & Kopan, 2010; Kuure & Sariola, 2020).

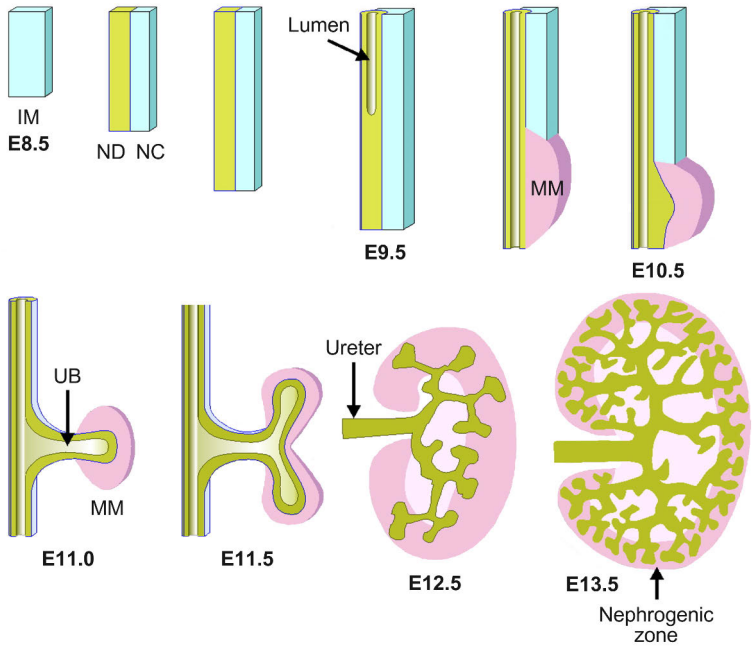

Figure 5. Early mouse kidney morphogenesis. The development of the mouse kidney starts around E8.5 with the formation of the pronephros. The intermediate mesoderm (IM) gives rise to the urogenital system. Initially, the nephric duct (ND) primordium and nephrogenic cord (NC) arise from the IM and extend along the embryo. The mesonephros starts around E9.5 when the ND forms a simple epithelial tube and the metanephric mesenchyme (MM) develops. The caudal ND cells proliferate and become a pseudostratified epithelium. Formation of the permanent kidney, metanephros, begins around E10.5, as the ureteric bud (UB) emerges from the ND and invades the MM. The UB undergoes growth and branching, leading eventually to the renal collecting duct system and the ureter. The nephrogenic zone within the kidney is where new nephrons, the kidney's functional units, are formed. E, embryonic day; IM, intermediate mesoderm; NC, nephrogenic cord; ND, nephric duct; MM, metanephric mesenchyme; UB, ureteric bud. Adapted from Costantini & Kopan, 2010.

The formation of the metanephros, which will become the permanent kidney, starts around E10.5 (Figure 5). The metanephric kidney begins to function after mid-gestation and plays a key role in fetal health by secreting primary urine into amniotic fluid. It is derived from the reciprocal interactions of two primordial mesodermal

derivatives, the UB and the MM. During this phase, the UB emerges as an outgrowth from the caudal end of the ND and invades the MM. At this stage, the UB is already divided into tip and trunk regions, which have different molecular signatures and different cellular behaviors. The UB tip is highly proliferative and surrounded by a discontinuous and sparse ECM. The UB undergoes repeated growth and branching, ultimately leading to the development of the renal collecting duct system and the ureter. The MM plays a crucial role in facilitating the continuous growth and branching of the UB (Saxén & Lehtonen, 1987; Lechner & Dressler, 1997; Vainio & Lin, 2002; Kuure & Sariola, 2020). Proper branching of these renal epithelial structures is vital for healthy kidney development; any abnormalities in UB branching can significantly impair kidney formation and function (Schedl, 2007).

Both nephron differentiation and branching morphogenesis are influenced by interactions between the UB and the surrounding mesenchyme. The nephrogenic zone is a specific area within the developing kidney where new nephrons, the functional units of the kidney, are generated (Figure 5). The tips of the UB stimulate the differentiation of nephrons from nephrogenic progenitor cells located in the MM, known as cap mesenchyme. As the UB undergoes branching morphogenesis, each tip acts simultaneously as an inductive center, triggering the formation of nephrons (Vainio & Lin, 2002; Costantini & Kopan, 2010). Homeobox protein Six2-positive nephron progenitor cells (NPCs) are a specific type of cell in the developing kidney that are crucial for forming nephrons. These cells are known for their ability to self-renew and differentiate into all the cell types of the nephron (Kobayashi et al., 2008; Costantini & Kopan, 2010). These progenitors both self-renew to maintain the cap mesenchyme until the end of nephrogenesis and differentiate through MET into specialized epithelial cells of all nephron segments. Nephrogenesis initiates with the aggregation of NPCs at the junctions of the T-shaped UB. This pretubular aggregate then undergoes morphological changes to become a secretory nephron, progressing through stages like the renal vesicle, comma-shaped bodies, and S-shaped bodies. The final number of nephrons in an individual correlates with the extent of UB branching. Importantly, all nephron segments, including podocytes, Bowman's capsule, proximal and distal tubules, loop of Henle, and the connecting piece, derive from the same NPC pool (Costantini & Kopan, 2010; Kuure & Sariola, 2020).

Congenital anomalies of the kidney and urinary tract (CAKUT) are among the most common birth defects and are associated with an increased risk of hypertension and renal failure later in life. These anomalies arise from inborn defects in the differentiation of the kidneys and urinary tract. Understanding normal organ development is crucial to uncovering the genetic, molecular, and cellular bases of these malformations. CAKUT includes a variety of conditions, such as renal aplasia, hypodysplasia, ectopia, and different ureteral abnormalities; however, many of the genetic causes remain unknown. As mentioned, the metanephric kidney plays a

central role in fetal health by secreting primary urine into amniotic fluid. Interestingly, in a condition known as Potter's sequence, reduced amounts of amniotic fluid, caused by decreased urine production, can lead to complications such as pulmonary hypoplasia, resulting in small lungs and respiratory insufficiency. Research using mutant mice has identified key genes involved in renal differentiation, which provides valuable insights into the genetic basis of kidney defects and improving diagnostic methods (Costantini & Kopan, 2010; Kuure & Sariola, 2020).

1.2 Stem cells

A stem cell is a distinctive type of cell recognized for its remarkable capacity to self-renew and differentiate into various cell types, playing an essential role in the maintenance, repair, and regeneration of tissues. Stem cells are a diverse group of cells, including embryonic stem cells, various types of adult stem cells, and induced pluripotent stem cells. All stem cells can be classified into five groups according to their differentiation potential: totipotent, pluripotent, multipotent, oligopotent, and unipotent (Kolios & Moodley, 2012; Burgess, 2016).

Stem cells utilize two primary mechanisms for self-renewal: asymmetric and symmetric self-renewal. In asymmetric self-renewal, one stem cell divides into a stem cell and a differentiated cell, maintaining a stable stem cell population under normal conditions. In symmetric self-renewal, a stem cell produces two daughter stem cells, expanding the stem cell pool, e.g., after tissue injury or in conditions that cause loss of differentiated cells. Symmetric and asymmetric divisions can coexist, with both being intermixed during subsequent cell divisions. In mid to late gestation, some mammalian progenitor cells switch from mainly symmetric to predominantly asymmetric divisions. Besides, adult stem cells typically divide asymmetrically, but they can switch to symmetric divisions to replenish stem cell pools after injury or disease (Gattazzo et al., 2014; Burgess, 2016).

1.2.1 Stem cell niches

Stem cells reside in specialized and dynamic microenvironments called "niches", which provide crucial extracellular signals and components necessary for their proper function and longevity. The niche regulates stem cell behavior, balancing their quiescence, self-renewal, and differentiation. Even though stem cells have a high potential for proliferation, the niche keeps them in a quiescent and low metabolic state to prevent exhaustion. The niche is also believed to protect stem cells from accumulating genetic mutations that could lead to malignant transformation into cancer cells (Gattazzo et al., 2014; Burgess, 2016).

Stem cell niches comprise the stem cells, supportive cells, and ECM components produced by the stem cells, such as fibronectin, collagen I, laminins, and vitronectin. Various niches have been identified, each capable of housing and nurturing specific kinds of stem cells. Given the wide variety of stem cells, each niche serves particular functions and exhibits unique structural features and compositions (Gattazzo et al., 2014; Burgess, 2016; Caldeira et al., 2018).

The maintenance of stem cell function largely depends on interactions between stem cells and ECM components. The ability of cells to adhere to their ECM niche is primarily influenced by the interactions of cell-surface receptors or co-receptors. These interactions are essential in controlling cellular processes such as proliferation, migration, and differentiation, as they anchor the extracellular microenvironment to the intracellular cytoskeleton, thereby supporting stem cell niches. For instance, E-cadherins and N-cadherins mediate the anchoring of stem cells within their niches. Stem cells also express integrins that facilitate their interaction with the ECM by directly binding to ECM proteins. The ECM in the niches also serves as a reservoir of GFs that influence stem cell behavior. ECM remodeling, aided by MMPs, releases GFs essential for stem cell migration and differentiation. Overall, ECM interactions are vital for determining stem cell fate (Gattazzo et al., 2014; Burgess, 2016; Caldeira et al., 2018).

1.2.2 Embryonic stem cells

Embryonic stem cells (ESCs) are derived from the inner cell mass of a blastocyst. They are pluripotent cells and can self-renew indefinitely and differentiate into any cell type present in the adult body (Figure 6). The pluripotent nature of ESCs allows them to contribute to all three primary germ layers, ectoderm, mesoderm, and endoderm. Thus, they have the capacity to differentiate into several organ and tissue types in the developing embryo and the adult. In contrast, the totipotent cells, which are present in the earliest stages of embryonic development, have the capacity to differentiate into all cell types in the developing embryo and extraembryonic tissues (G. Huang et al., 2015; Burgess, 2016).

Mouse, rat, and human ESCs possess a common subset of transcription factors that define their “stemness”. Among these factors, Oct4, Sox2, and Nanog are considered to be essential factors of the core circuitry responsible for maintaining pluripotency together (Zhang & Cui, 2014; G. Huang et al., 2015). Additionally, the LIF/STAT3 signaling pathway enhances self-renewal in mouse ESCs (G. Huang et al., 2015; Burgess, 2016).

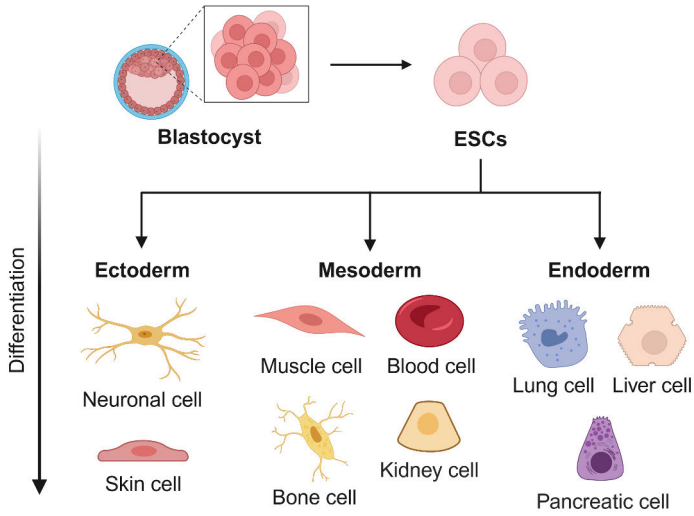

Figure 6. Embryonic stem cell differentiation. Blastocyst-derived pluripotent ESCs can differentiate into the primary germ layer cells, ectoderm, mesoderm, and endoderm, and further into several cell types. ESCs, embryonic stem cells. Created with BioRender.com.

ESCs cultured in the right conditions can be propagated indefinitely. Furthermore, ESCs can be maintained in a genetically stable state, which reduces the risk of genetic mutations. Cultured ESCs can be used in cell-based therapeutic and diagnostic platforms. ESC manipulation and their capacity to divide and produce virtually any cell type make them ideal for use in tissue engineering and regenerative medicine applications. ESCs can be used to replace damaged or diseased tissues and organs to treat various disorders. However, their use can be limited by legal and ethical considerations (G. Huang et al., 2015; Burgess, 2016).

1.2.2.1 Generation of a knockout mouse model

ESCs are also critical tools for creating knockout mice. Knockout mouse models are crucial research tools for investigating the function of genes and their roles in various biological processes and diseases. Such model can be generated using the "knockout-first" strategy to turn a desired gene off in mice (Figure 7). This strategy can also be used to create a conditional knockout mouse model (inactivation of a gene in specific tissues or at specific times). The specific target gene is inactivated by homologous recombination in a vector construct. Then, this targeting construct is introduced into ESCs by electroporation, and the cells are selected for the successful incorporation of the construct. These modified cells are then inserted into a blastocyst and subsequently implanted into a surrogate mouse. The resulting chimeric male mice

are crossbred with wild type (WT) female mice to achieve germline transmission. The obtained heterozygous mice are further bred to generate homozygous offspring that carry the desired mutation (Ney et al., 2020).

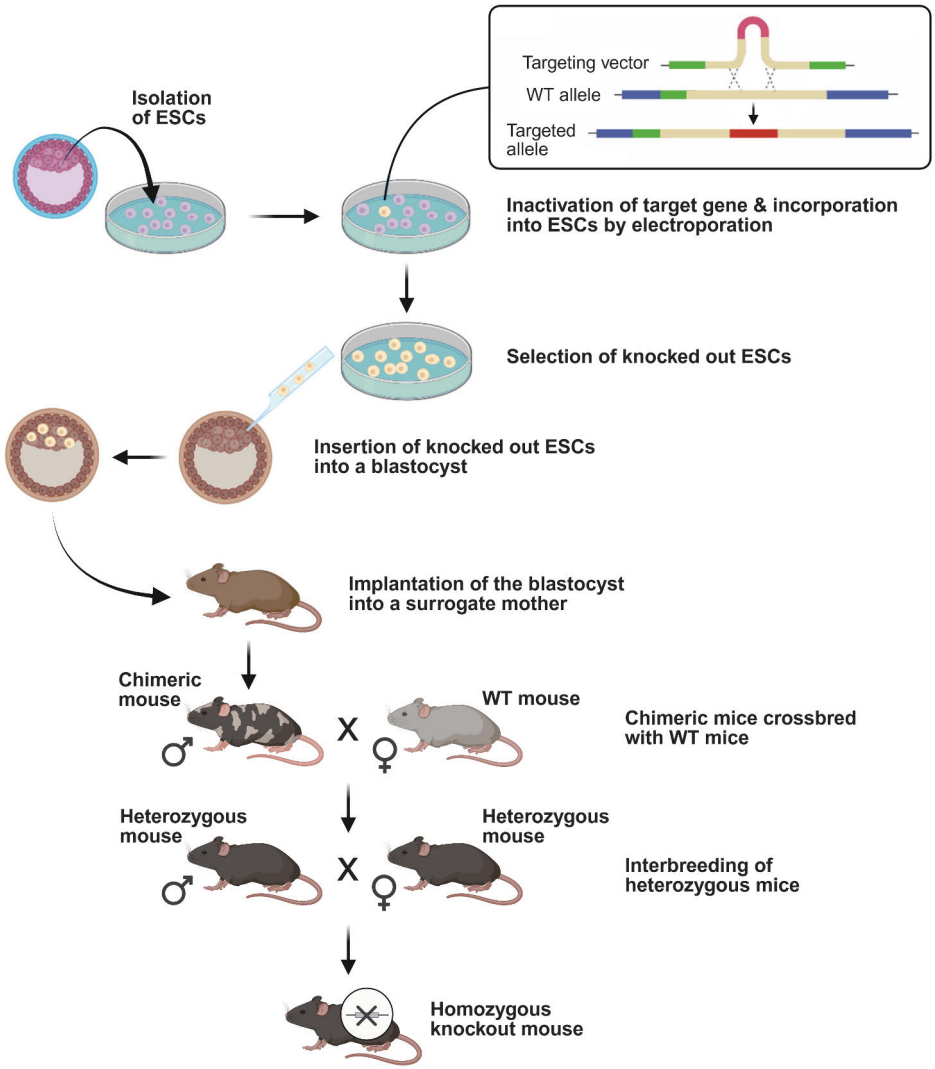

Figure 7. Creating a knockout mouse model. First, a targeting vector is created by homologous recombination, which is designed for the deletion of a specific gene. This targeting construct is then introduced into ESCs by electroporation. The ESCs are selected for the successful incorporation of the construct and are subsequently injected into a blastocyst, which is later implanted into a surrogate mouse. The resulting chimeric male offspring are then crossbred with wild type (WT) female mice. The obtained heterozygous mice are then bred again to produce homozygous offspring that carry the mutation of interest. ESCs, embryonic stem cells; WT, wild type. Adapted from Ney et al., 2020 and created with BioRender.com.

1.2.3 Adult stem cells

Stem cells for research and therapeutics can be extracted from various sources, such as bone marrow, adipose tissue, amniotic cells, umbilical cord, and placental tissue (Poliwoda et al., 2022). Adult stem cells (ASCs), also known as somatic or tissue cells, are undifferentiated cells found in various tissues and organs after birth. ASCs are capable of self-renewal and can differentiate into at least one cell type. However, ASCs have limited self-renewal capacity and can be difficult to isolate and expand in large quantities for therapeutic use. The primary role of ASCs in adults is regenerative and restorative (Avgustinova & Benitah, 2016; Burgess, 2016).

1.2.3.1 Multipotent stem cells

Multipotent stem cells have the capacity to differentiate into a limited range of cell types. For example, mesenchymal stem cells (MSCs), are multipotent cells that can differentiate into various mesoderm-derived tissues, such as adipose tissue, bone, cartilage, and muscle. The use of ESCs is often limited by legal and ethical considerations, which is why MSCs are generally preferred. MSCs can be isolated from various neonatal and adult tissues, and still possess the ability to differentiate into multiple cell types. This makes them suitable for clinical and research applications without the ethical issues associated with ESCs (D.-C. Ding et al., 2011; Kolios & Moodley, 2012; Poliwoda et al., 2022).

Another example of multipotent stem cells is hematopoietic stem cells (HSCs), which can differentiate into both myeloid and lymphoid lineages (Mesfin et al., 2023). HSCs are a well-studied type of multipotent adult stem cell that is capable of transforming into all mature blood cell forms and giving rise to common myeloid and lymphoid progenitor cells (Kaebisch et al., 2015).

Neural stem cells (NSCs) are another class of multipotent stem cells, located in the central nervous system. They are self-renewing and have the potential to differentiate into the main cell types in the brain: neurons, astrocytes, and oligodendrocytes. NSCs have a central role in both brain development and function, and have promising potential for the treatment of neurological disorders (Llorente et al., 2022).

In addition, amniotic stem cells are also classified as multipotent stem cells. These cells originate from the amniotic fluid and the membrane that surrounds the embryo during gestation. Their isolation does not require the destruction of embryos, so their use can be considered an ethically less controversial alternative to ESCs. Their ability to differentiate into various cell types makes them valuable for research and therapy (Burgess, 2016).

1.2.3.2 Oligo and unipotent stem cells

Oligopotent stem cells can self-renew and develop into two or more different cell lineages within a specific tissue. Oligo and unipotent stem cells are often called progenitor or precursor cells because they are on a defined pathway to differentiate into specific cell types. However, they have self-renewal capabilities, which set them apart from non-stem cells (Ko et al., 2010; Kolios & Moodley, 2012; Poliwoda et al., 2022; Mesfin et al., 2023).

Common myeloid and lymphoid progenitor cells are oligopotent stem cells, as they can differentiate into various types of blood and immune cells. Common myeloid progenitors give rise to erythrocytes, megakaryocytes (which differentiate to platelets), monocytes (which differentiate to macrophages), and granulocytes (neutrophils, eosinophils, basophils). Common lymphoid progenitors generate lymphocytes (B cells, T cells, and natural killer cells) (Lim et al., 2013).

Unipotent stem cells can replicate and replace aging cells, but they can only differentiate into one specific cell type. Unipotent stem cells include germline stem cells (which produce sperm or eggs), epidermal stem cells (which generate skin), and erythroid precursor cells (which differentiate into red blood cells) (Ko et al., 2010; Kolios & Moodley, 2012; Poliwoda et al., 2022; Mesfin et al., 2023).

Bronchioalveolar stem cells (BASCs) are a type of adult lung stem cell that are also considered oligopotent, meaning they may differentiate into both bronchiolar (such as club cells and ciliated cells) and alveolar epithelial cells (such as ATII and ATI cells). BASCs are located at the bronchioalveolar duct junction, an essential area for lung maintenance and repair. They coexpress both club cell marker secretoglobin 1a1 (Scgb1a1 or CC10) and ATII cell marker SPC, which indicates their potential to differentiate into either type of cell (Kim et al., 2005; Liu et al., 2020). In the distal lung, oligopotent club cells, also known as Clara cells, can self-renew and replace lost club cells or differentiate into ciliated cells (Rawlins et al., 2009). In turn, unipotent ATII cells in the alveoli also have self-renewing capabilities and, in response to injury, can transform into ATI cells, which are vital for gas exchange (Barkauskas et al., 2013).

1.2.4 Induced pluripotent stem cells

The use of ESCs can be controversial, and ASCs have restricted multi-lineage differentiation capacity. Thus, alternative cell-based therapeutics platforms have been studied. In certain cases, differentiated adult cells may be driven to lose their molecular and morphological identities and transform into other cell types. This process is known as transdifferentiation, where a non-stem cell transforms into a different cell type, or a differentiated stem cell forms other cell types beyond its normal multipotency. Additionally, in an artificial setting, in a process known as

dedifferentiation, differentiated adult somatic cells can be genetically reprogrammed to an embryonic-like state. These types of cells are known as induced pluripotent stem cells (iPSCs), which exhibit pluripotent differentiation capabilities (Kolios & Moodley, 2012; Burgess, 2016).

iPSCs are generated from somatic cells utilizing reprogramming factors, such as the transcription factors Oct3/4, Sox2, Klf4, and c-Myc. They are similar to ESCs in terms, e.g., of morphology, proliferation, gene expression, and telomerase activity, and they can differentiate into cell types of the three germ layers *in vitro*. In the future, this technique could enable personalized gene therapy where oligopotent or unipotent cells are taken from a patient, reprogrammed, and then reintroduced elsewhere in the body. Overall, iPSCs are promising tools for drug development, disease modeling, and regenerative medicine (Kolios & Moodley, 2012; Poliwoda et al., 2022).

1.3 Basigin family proteins

Basigin family members are transmembrane proteins, which are part of the immunoglobulin (Ig) superfamily consisting of diverse kinds of cell-surface and soluble proteins. The basigin subgroup consists of three type I membrane proteins (Figure 8): embigin (Emb/Gp70), basigin (Bsg/EMMPRIN/CD147), and neuroplastin (Nptn; Np65/Gp65 and Np55/Gp55) (Muramatsu & Miyauchi, 2003). These three proteins share structural and functional similarities. The proteins exhibit a common structure characterized by extracellular immunoglobulin-like (Ig-like) domains, a single hydrophobic transmembrane segment, and a short cytoplasmic tail. They are well conserved as they have 37-46% amino acid sequence identity (Hanna et al., 2003). All members have glutamate at the same position in the transmembrane domain, and the highest degree of identity seems to be within the transmembrane and intracellular domains (Beesley et al., 2014). Nevertheless, significant structural variations likely contribute to their diverse biological functions. One major difference is in the number of Ig-domain repeats within the extracellular region: embigin, basigin/basigin-2, and neuroplastin Np55 possess only two Ig-like domains, whereas basigin-1 and neuroplastin Np65 contain three (Beesley et al., 2014). The two additional basigin isoforms identified in humans, basigin-3 and basigin-4, consist of a single Ig-like domain (Liao et al., 2011). Moreover, the diversity in both the quantity and sequence of these Ig-like domains, along with the N-glycosylation state of these heavily glycosylated proteins, may play a crucial role in their function (Langnaese et al., 1997; Yoshida et al., 2000; Ochrietor et al., 2003; X.-L. Yu et al., 2008). However, very little is known about the potential role of the N-glycosylation on these proteins.

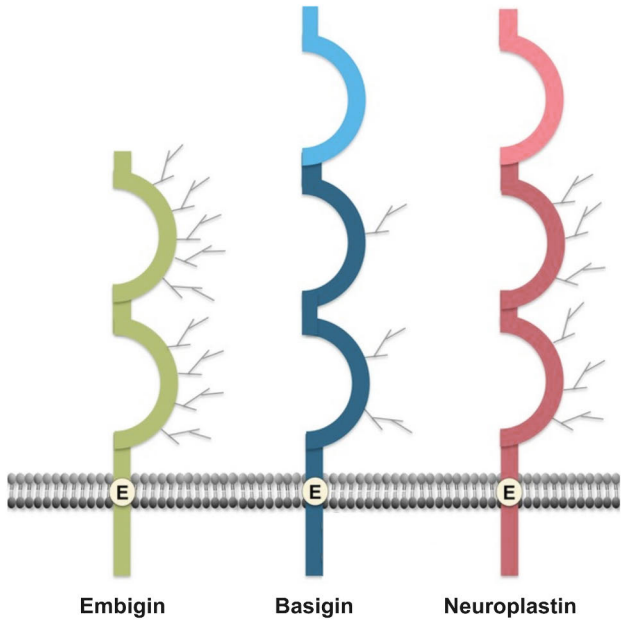

Figure 8. Structural features of basigin family proteins. Embigin contains two extracellular Ig-like domains, while basigin and neuroplastin have either two or three domains. Embigin has nine, basigin three, and neuroplastin six potential N-linked glycosylation sites in the extracellular Ig-like domains. Family members have glutamate (E) at the same position in the transmembrane domain. Adapted from Beesley et al., 2014.

1.3.1 Basigin

Basigin has been the most thoroughly studied basigin family member from physiological and pathological aspects, hence the group's name. Basigin was found independently in different laboratories around the same time and has multiple name variations: gp42, basigin, HT7, neurothelin, OX-47, M6, 5A11, EMMPRIN, and CD147 (Altruda et al., 1989; Miyauchi et al., 1990, 1991; Seulberger et al., 1990; Schlosshauer & Herzog, 1990; Fossum et al., 1991; Kasinrerk et al., 1992; Fadool & Linser, 1993; Biswas et al., 1995; Muramatsu & Miyauchi, 2003). The basigin gene symbol in humans is *BSG* and in mice *Bsg* (Muramatsu & Miyauchi, 2003).

Basigin is expressed in several embryonic and adult tissues. The basigin-1 isoform, which contains an additional Ig-like domain, is specifically expressed in human and mouse retina, while the basigin/basigin-2 isoform is more widely expressed (Hanna et al., 2003; Muramatsu, 2016). During early mouse embryonic development, basigin is very broadly expressed. During organogenesis, basigin has been detected in several epithelial tissues, including the liver, kidneys, lungs, intestine, brain, and spinal cord (Fan et al., 1998). In adults, basigin is expressed at different levels in various cell types, such as leukocytes, hematopoietic, endothelial,

and epithelial cells (Yurchenko et al., 2006). Basigin is also expressed in the testis, ovary, uterus, and placenta and is needed for normal fertility in both male and female mice. Basigin overexpression is connected to reproductive diseases, including endometriosis (K. Li & Nowak, 2020).

The majority of basigin knockout ($Bsg^{-/-}$) mice are lost, mainly around the time of implantation (Igakura et al., 1998). The few surviving $Bsg^{-/-}$ mice are defective in lymphocyte responsiveness, exhibit decreased efficiency in implantation, are sterile, and have renal fibrosis (Igakura et al., 1996, 1998; Kato et al., 2009, 2011). Additionally, abnormalities of sensory and memory functions have been observed in $Bsg^{-/-}$ mice (Naruhashi et al., 1997).

Basigin has a role in a wide variety of cellular processes. For instance, it is a carrier of Lewis X carbohydrate antigen in mouse teratocarcinoma stem cells (Miyauchi et al., 1990) and is involved in neural-glial interactions (Fadool & Linser, 1993). Basigin may also influence the function of integrin-type cell adhesion receptors (Berditchevski et al., 1997; Muramatsu, 2016). Notably, basigin has a role in cancer. In human tumor cells, basigin/extracellular matrix metalloproteinase inducer (EMMPRIN) triggers the production or release of MMPs in neighboring mesenchymal cells, and thus, contributes to tumor invasion (Biswas et al., 1995). Basigin also has a role in the immune system and inflammatory processes and is a receptor for cyclophilins (Yurchenko et al., 2006). Basigin may act as a co-receptor for viral entry into host cells in SARS-CoV-2, HIV-1, and malaria parasitic infections (Nitin et al., 2022; Pushkarsky et al., 2001; Crosnier et al., 2011).

1.3.2 Neuroplastin

Neuroplastin is enriched in neurons and synapses (Hill et al., 1988). Np65 is expressed in the brain and mainly localized in forebrain neurons, specifically the cerebral cortex, hippocampus, and striatum. Np55 is expressed in all brain regions and is also detected in various organs and cell types, such as the liver, kidneys, skeletal muscle, spleen, testis, lungs, and heart (Hill et al., 1988; Langnaese et al., 1997, 1998). Both neuroplastin isoforms are enriched in synapses (Hill et al., 1988).

The *NPTN* gene in humans, which encodes neuroplastin, may be involved in genetic susceptibility to schizophrenia (Saito et al., 2007). Neuroplastin is involved in synaptic formation, plasticity, and long-term potentiation, which are likely linked to vital cognitive functions, such as learning and memory (Smalla et al., 2000; Owczarek & Berezin, 2012; Beesley et al., 2014). Np65-deficient mice exhibit abnormal cognition and emotional behaviors (Amuti et al., 2016). Furthermore, Np65-null mice have altered brain architecture and significantly reduced Wnt3 expression (H. Li et al., 2018). Lack of Np65 also causes hearing loss in mice (Carrott et al., 2016; Newton et al., 2022).

1.3.3 Embigin

Embigin (embryo + immunoglobulin) is the founding member of the basigin family, which was discovered in murine teratocarcinoma stem cells as a carrier of *Dolichos biflorus* agglutinin carbohydrate binding sites (Ozawa et al., 1988; R.-P. Huang et al., 1990). It is a highly glycosylated transmembrane protein that has nine potential N-linked glycosylation sites in the two extracellular Ig-like domains. The size of the embigin core protein is around 30-37 kDa, and its glycosylated form is about 62-90 kDa (Ozawa et al., 1988; Fan et al., 1998; Muramatsu & Miyauchi, 2003). The embigin gene symbol in humans is *EMB*, and in mice *Emb*. The *EMB* gene is located on human chromosome region 5q11.1 and *Emb* on mouse chromosome 13 (Muramatsu & Miyauchi, 2003; J. Zhou et al., 2020).

Embigin mRNA expression has been found during early mouse development until E9, after which its expression decreases during the progression of embryogenesis (R.-P. Huang et al., 1990; Fan et al., 1998). Embigin expression seems to be more restricted than basigin's during embryonic development. Embigin mRNA is highly expressed in the endoderm during early postimplantation embryogenesis. At E8.5, strong embigin mRNA expression was found in the embryonic gut and visceral yolk sac (Fan et al., 1998). Furthermore, embigin mRNA expression has been reported in mouse and rat UB (Stuart et al., 2003; Schwab et al., 2003), and it may serve as a *Dolichos biflorus* lectin binding protein in the kidney (Stuart et al., 2003). Overall, embigin may have a role in the early stages of embryogenesis.

In adult mice, low levels of embigin mRNA have been detected in the brain, spleen, testis, kidneys, heart, small intestine, skeletal muscle, and ovaries. Additionally, the uteri of pregnant mice had higher levels of embigin expression than the uteri of nonpregnant mice (R.-P. Huang et al., 1990). Embigin mRNA expression has also been reported in various rat tissues: the brain, testis, kidneys, heart, liver, lungs, prostate glands, and mammary glands. Interestingly, during prostate gland development, increased expression of embigin has correlated with the appearance of highly organized tubular structures (Guenette et al., 1997). Embigin has also been localized in luminal sperm tails in the testis and the transition zone between corpus and cauda in the epididymis, whereas the distal cauda remained embigin-negative. Additionally, embigin was detected in the principal piece and the acrosome in spermatozoa (Mannowetz et al., 2012). In photoreceptors, embigin is present in the outer segment plasma membrane (Skiba et al., 2021). Moreover, primary astrocytes have been found to express embigin in addition to basigin. An antibody blockade of either embigin or basigin led to a significant reduction of parasite infectivity in astrocytes (Nasuhidehnavi et al., 2022). Embigin expression has also been detected in basal cells of the oral epithelium of mice (Seubert et al., 2024).

Embigin has been linked to cell adhesion regulation: it potentially enhances the function of integrin-mediated cell-substratum adhesion (R.-P. Huang et al., 1993). Our previous research has shown that embigin can function as an ECM receptor by binding with its Ig1 domain directly to type I repeats in the N-terminal domain of fibronectin (Sipilä et al., 2022). In the same paper, we defined embigin as a marker for basal sebocytes in the mouse sebaceous gland, and the loss of embigin promotes sebocyte progenitors' exit from the basal layer to suprabasal differentiation (Sipilä et al., 2022).

Concomitantly with our paper included in this thesis (Talvi et al., 2024), another group independently reported that the absence of embigin in the C57BL/6NTac background mice results in subviability, hearing deficit, and brain and cardiac defects. Interestingly, embigin also appears to interact genetically with cadherin 23 (Newton et al., 2023). The most recent study has also identified embigin as essential for the development of the enteric nervous system, as it regulates the proliferation and migration of enteric neural crest-derived cells in mice. Embigin appears to recruit PP2A enzyme to the cell membrane and activate the PI3K signaling pathway, both of which are crucial for proper enteric nervous system formation. Furthermore, embigin deficiency can severely impair enteric nervous system development, potentially leading to conditions like Hirschsprung disease (Z. Li et al., 2025).

1.3.3.1 Embigin and monocarboxylate transporters

Embigin is probably best known for its ancillary function for monocarboxylate transporters (MCTs). Cells using glycolysis as their main energy source, such as skeletal muscle, red and white blood cells, and most tumor cells, must export the accumulating lactic acid to prevent acidosis. Besides, rapid lactic acid import is required to increase respiration in the brain, heart, and red muscle, as well as gluconeogenesis in the kidneys and liver (Halestrap & Meredith, 2004). MCTs, especially MCT1-4, are necessary for carrying metabolically important monocarboxylates, including L-lactate, pyruvate, ketone bodies, acetoacetate, and β-hydroxybutyrate, across the plasma membrane (Poole & Halestrap, 1993; Halestrap, 2013b, 2013a). MCTs are encoded by SLC16 family genes, which comprise 14 members (Halestrap, 2013b, 2013a). The crucial role of MCTs in physiology and development has been shown, for example, in MCT1 knockout mice, which are embryonically lethal (Lengacher et al., 2013). All three members of the basigin group have been associated with MCTs (Wilson et al., 2005; Halestrap, 2013b; Wilson et al., 2013).

Embigin can support the function of MCT1 (gene: *Slc16a1*), MCT2 (gene: *Slc16a7*), MCT4 (gene: *Slc16a3*), and MCT7 (gene: *Slc16a6*) (Wilson et al., 2005; Halestrap, 2013b; Skiba et al., 2021; Xu et al., 2022; Higuchi, 2022; Cheng, Liu,

Gao, Zhu, et al., 2025; Cheng, Liu, Gao, Xin, et al., 2025), which are all SLC16A family members that act as proton-linked MCTs (Halestrap, 2013a). The ancillary proteins embigin or basigin are required for the correct membrane expression of MCTs (Halestrap, 2013a). For MCT2, embigin has been proposed as the primary ancillary protein, and basigin is the preferred binding partner for MCT1 and MCT4, as basigin seems to be more widely distributed in different tissues than embigin (Wilson et al., 2005; Ovens et al., 2010). Additionally, the neuroplastins are accessory proteins for MCT2 in some neuron populations (Wilson et al., 2013; Beesley et al., 2014). Recently, embigin has been associated with MCT4 regulation (Cheng, Liu, Gao, Zhu, et al., 2025; Cheng, Liu, Gao, Xin, et al., 2025). Interestingly, embigin and basigin also interact and regulate MCT7, which is a facilitative taurine receptor. MCT7, like MCT2, appears to interact with embigin rather than basigin (Higuchi, 2022). MCT7 may also transport ketone bodies (Hugo et al., 2012; Halestrap, 2013a). Notably, ancillary proteins for most MCT family members have not been reported, and their ability to interact with embigin is unknown.

Embigin has been shown to facilitate MCT1 trafficking to the plasma membrane by forming a heterodimeric complex (Xu et al., 2022). In the testis, MCT1, MCT2, and MCT4 are essential for spermatogenesis, and in sperm, MCT2 and MCT4 are central in energy metabolism (Halestrap, 2013a). However, in sperm, no interaction was detected with MCT1 or MCT2 and embigin, while these were associated with basigin (Mannowetz et al., 2012). On the contrary, in the photoreceptor outer segment plasma membrane, embigin is associated with MCT1 (Skiba et al., 2021). In mouse sebaceous glands, embigin seems to have a role in cellular metabolism, as it appears to regulate MCT1 localization. Additionally, Wnt seems to control embigin in the sebaceous gland, where embigin drives cell differentiation through a mechanism that connects cell adhesion and lactate transport (Sipilä et al., 2022). Notably, carbonic anhydrase IV (CAIV) interacts with MCT1, MCT2, and MCT4, and facilitates their function through their ancillary proteins basigin and embigin (Forero-Quintero et al., 2019).

1.3.3.2 Embigin in pathological processes

The members of the basigin family are involved in diverse cellular functions, thus, it is not surprising that they also have links to pathological processes, including cancer (Riethdorf et al., 2006; Nabeshima et al., 2006; Sumardika et al., 2019). Embigin has been reported to act as a suppressor of tumorigenesis in breast cancer (Chao et al., 2015) and promoter in pancreatic carcinoma (Jung et al., 2016), prostate cancer (Ruma et al., 2018), glioblastoma multiforme (GBM) (Cheng, Liu, Gao, Zhu, et al., 2025), and *Helicobacter pylori* infection-related stomach adenocarcinoma (STAD) (Peng et al., 2025).

In breast cancer cells, homeobox C8 (HOXC8) transcriptionally regulates embigin. Knockdown of embigin leads to an increase in proliferation, anchorage-independent growth, and migration of breast cancer cells. Additionally, HOXC8 seems to regulate breast tumorigenesis by regulating embigin expression. Moreover, low embigin expression levels correlate with the short survival of breast tumor patients. Overall, embigin seems to have a role in the progression of breast tumor (Chao et al., 2015).

In pancreatic ductal adenocarcinoma, embigin expression was elevated compared to normal pancreatic tissues. Silencing of embigin in pancreatic cancer cells resulted in reductions of cell proliferation, migration, invasion, wound healing, decreased MCT2 levels at the plasma membrane, and reduced expression of PI3K, GSK3-β, and Snail/Slug. Besides, embigin might mediate EMT in pancreatic cancer cells and be involved in pancreatic cancer progression (Jung et al., 2016).

Embigin acts as a receptor for extracellular S100A4. The interaction of extracellular S100A4 with embigin facilitates the progression of prostate cancer by orchestrating various processes. These include the suppression of AMPK activity, the activation of NF-κB, MMP9, and mTORC1 signaling, and the inhibition of autophagy, which results in increased cellular motility. Additionally, embigin seems to enhance prostate cancer growth, the ability to form spheroids and colonies, and increase resistance to chemotherapy independently of S100A4 (Ruma et al., 2018).

In GBM, embigin is highly expressed, and it is linked to poor prognosis in GBM patients. Embigin appears to accelerate GBM progression by upregulating EMT, aerobic glycolysis, and glutathione redox balance through MCT4 and GPX3 proteins (Cheng, Liu, Gao, Zhu, et al., 2025). In STAD, embigin was recognized as a prognostic “risk” gene associated with *Helicobacter pylori* infection. Embigin also showed high mRNA expression in cultured STAD cells and might be involved in the development of STAD (Peng et al., 2025). Moreover, embigin and basigin have been recognized as galectin-3 binding proteins. These proteins were identified to have a role in metastasis-related processes in melanoma cells (Dange et al., 2017).

Interestingly, embigin also enhances the growth of motor neurons and the formation and plasticity of neuromuscular junctions (Lain et al., 2009). The human embigin gene *EMB* has been identified as a susceptibility gene for schizophrenia (J. Zhou et al., 2020), as well as the human neuroplastin *NPTN* gene (Saito et al., 2007).

1.3.3.3 Embigin as a regulator of immune cells and stem cells

Embigin has been associated with immune cells. Embigin is expressed in bone marrow progenitors, T cells, and myeloid cells but not in B cells. The Pax5 transcription factor was found to repress embigin expression specifically during early B cell differentiation; however, the precise role of embigin in the process

remained unclear (Pridans et al., 2008). Notably, embigin was found to be re-expressed in activated B cells and plasma cells, and the expression was linked to the posttranslational inhibition of Pax5 function (Kallies et al., 2007). Embigin mRNA is also highly expressed in $Cd4^+$ and $Cd8^+$ T cells and lung $CD4^+$ Th17 tissue-resident memory T cells of C57BL/6 mice. However, embigin was determined to be unnecessary for both the generation of CD4 responses and the formation of $CD8^+$ T cell memory (Yang et al., 2024). In addition, the $CD69^+CD49b^-$ subset of NK cells was found to express high levels of embigin (Torcellan et al., 2024). Embigin is also specifically expressed by infiltrating macrophages of the central nervous system in mice (DePaula-Silva et al., 2019). Furthermore, embigin expression is induced in microglia during ischemic stroke, and elevated embigin levels accelerate glycolytic metabolism in microglia, worsening inflammation. In microglia, MCT4 is critical in embigin-mediated glycolytic metabolism and neuroinflammation. The EMB/MCT4 axis appears to mediate the inflammatory phenotype of microglia in stroke via the STING pathway (Cheng, Liu, Gao, Xin, et al., 2025).

Embigin has also been linked to stem and progenitor cell regulation in adult mice. Interactions between hematopoietic stem and progenitor cells (HSPCs) and hematopoietic niche cells are crucial for maintaining hematopoiesis in the bone marrow. Embigin has been recognized to serve a role in the regulation and retention of the hematopoietic niche, as embigin regulates the HSPC quiescence (Silberstein et al., 2016). Osteomacs serve as important cellular components of the niche; osteomacs interact with osteoblasts and megakaryocytes to support hematopoiesis (Mohamad et al., 2017). Interestingly, embigin has been identified as a critical component of osteomac-mediated HSC function in the niche (Mohamad et al., 2024). We have also discovered that embigin regulates cell differentiation in sebaceous gland progenitor cells in adult mice (Sipilä et al., 2022).

2 Aims of the Study

The goal of this thesis was to investigate embigin protein function during mouse embryonic development. We hypothesized that embigin mediates the interaction between cells with the ECM while also participating in the regulation of the basic metabolism of the cells through the MCT proteins, especially in stem cells. The results of the study were expected to reveal new mechanisms for mouse embryonic development and stem cell regulation. Therefore, the aims of this thesis were to:

1. Map embigin protein expression during mouse embryonic development and in adult mice.
2. Elucidate the critical stage for mouse embryonic development, when the embigin function is important.
3. Clarify the importance of embigin during lung and kidney development in mice.
4. Investigate the function of embigin during early mouse embryonic development.

3 Materials and Methods

The materials and methods have been described in detail in the original publications I-III. Here, the relevant experimental setups are summarized.

3.1 Antibodies (I-III)

Primary antibodies used in immunofluorescence stainings and western blotting (WB) are listed in Table 1.

Table 1. Primary antibodies used in this study. Abbreviations: α-SMA, alpha smooth muscle actin; IF, immunofluorescence staining; MCT, monocarboxylate transporter; WB, western blotting; WM, whole-mount immunofluorescence staining.

Antigen	Cat#/clone	Company	Type	Application	Used in
α-SMA conjugated to Alexa Fluor 488	ab184675	Abcam	mouse monoclonal	WM	I
basigin/CD147	ab188190; EPR18008-8	Abcam	rabbit monoclonal	IF, WM	I
β-tubulin I	T7816; SAP.4G	Sigma-Aldrich	mouse monoclonal	WB	I, III
calbindin D28K	sc-7691; C-20	Santa Cruz Biotechnology	goat polyclonal	WM	III
CC10/Scgb1a1	sc-365992; E-11	Santa Cruz Biotechnology	mouse monoclonal	IF	I
collagen I	NB600-408	Novus Biologicals	rabbit polyclonal	IF	I
E-cadherin	AF748	R&D systems	goat polyclonal	IF	III
embigin	14-5839-81; G7.43.1	eBioscience, Invitrogen	rat monoclonal	IF, WM, WB	I, III
fibronectin	AB2033	Sigma-Aldrich	rabbit polyclonal	IF, WM	I, III
GAPDH	ab9485	Abcam	rabbit polyclonal	WB	I

Antigen	Cat#/clone	Company	Type	Application	Used in
Hop	sc-398703; E-1	Santa Cruz Biotechnology	mouse monoclonal	IF	I
Ki67	ab16667; SP6	Abcam	rabbit monoclonal	IF	I
MCT1	AB1286-I	Sigma-Aldrich	chicken polyclonal	IF, WM	I, III
MCT4	ab308528; EPR28177-30	Abcam	rabbit monoclonal	IF, WM	I
Six2	11562-1-AP	ProteinTech	rabbit polyclonal	WM	III
prosurfactant protein C (SPC)	ab211326; EPR19839	Abcam	rabbit monoclonal	IF	I

3.2 Animal models (I-III)

C57BL/6N mice (*Mus musculus*, Charles River Laboratories, Wilmington, MA) and the generated embigin knockout ($Emb^{-/-}$) mice were maintained in the Central Animal Laboratory at the University of Turku, Finland. All animal experiments were formally reviewed and approved by the Ethical Committee for Animal Experimentation in Finland, complying with international guidelines on the care and use of laboratory animals. $Emb^{-/-}$ mice were generated in collaboration with the Turku Center for Disease Modeling.

3.2.1 Generation of embigin knockout ($Emb^{-/-}$) mice (I)

A targeting vector for the *Emb* gene, HTGR06008_A_1_E08 from The European Conditional Mouse Mutagenesis Program (Figure 9), was linearized with AsiSI restriction enzyme (NEB). This construct was then transfected into G4 embryonic stem cells, derived from 129S6/SvEvTac x C57BL/6NCrl mice, via electroporation. The cells were cultured for 7-9 days on a neomycin-resistant primary embryonic fibroblast feeder layer. To confirm successful homologous recombination, positive ES cell clones were identified through PCR and sequencing. These ES cells were subsequently injected into blastocysts from C57BL/6N mouse to create chimeric mice. Germline transmission was accomplished by breeding male chimeras with C57BL/6N females.

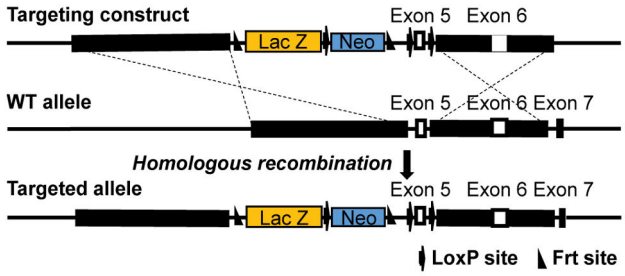

Figure 9. Embigin knockout targeting vector. The "knockout-first" strategy was used to create knockout alleles. A targeting vector was created using homologous recombination, aimed at deleting the *Emb* gene. In the schematic presentation, the structure of the targeting construct is shown at the top, the WT embigin allele with its coding exons 5, 6, and 7 in the middle, and the homologously mutated allele is shown below. A bold line presents the homologous sequences in the targeting construct, while arrows indicate the loxP sites and triangles the Frt sites. The mutated allele is expected to either produce a truncated protein or result in nonsense-mediated decay. Adapted from Figure S2 of Study I.

3.2.2 Genotype determination (I, III)

Genomic DNA was extracted with the NucleoSpin Tissue kit (Macherey-Nagel), and the genotypes of the mice were determined from genomic DNA using polymerase chain reaction (PCR) primer pairs listed in Table 2. DreamTaq polymerase (Thermo Fisher Scientific) was used according to the manufacturer's instructions using the following PCR settings: 95°C, 2 min; 35 x [95°C, 30 s; 50°C, 30 s; 72°C, 1 min]; 72 °C, 10 min.

Table 2. Primers used in this study for genotyping by PCR.

Type	Sequence	Company
Genotyping PCR primer pair 1	forward (5'-TAAGTCTCTTGTTTGCTGTG-3'; reverse 5'-CACAACGGGTTCTTCTGTTAGTCC-3')	Eurofins
Genotyping PCR primer pair 2	forward (5'-ACCCTTAAGTGCATGAACAAAA-3'; reverse 5'-GGGTTCCTTGGCATTGTTACTAA-3')	Eurofins

3.2.3 Timed mating (I-III)

In timed mating, the day of the vaginal plug appearance was considered embryonic day 0.5 (E0.5). The mouse embryos were examined at E8.5-E18.5 and pups at P0-P3 and P14-21. Young female adult mice were studied at the age of 6 weeks. Adult mice were studied at the ages of 2, 4, 6, and 12 months. The body weights of embryos at E17.5 were analyzed. Additionally, the lungs and kidneys of embryos at E17.5 were weighed and imaged with a stereo microscope.

3.3 Alkaline phosphatase in amniotic fluid (I)

Amniotic fluids were collected from WT, $Emb^{+/-}$, and $Emb^{-/-}$ embryos at E17.5 and analyzed with VetScan Comprehensive Diagnostic Profile reagent rotor used with the VetScan VS2 Chemistry Analyzer (Abaxis). Alkaline phosphatase activity (U/l) and the concentrations (mmol/l) of sodium, calcium, and glucose were determined.

3.4 Explant cultures

3.4.1 Lung explant culture (I-II)

Our version of the method for the lung explant culture is described in detail in Study II. The lung developmental branching in WT and $Emb^{-/-}$ embryos was compared in lung explant cultures at E12.5 (Figure 10). The lungs were harvested in PBS, and the explants were cultured on 8.0 mm pore size Whatman Nuclepore Track-Etched membranes (Merck) in DMEM/F12 medium supplemented with 0.5% FBS and Penicillin-Streptomycin 200 U/ml. The lung explants were cultured at 37 °C in a humidified atmosphere with 5% CO_2 for 2 days. The samples were imaged on days 0, 1, and 2 with a stereo microscope. The number of peripheral buds in lung explants was counted, and normalization was carried out to remove the size variation between different litters from various pregnant dams.

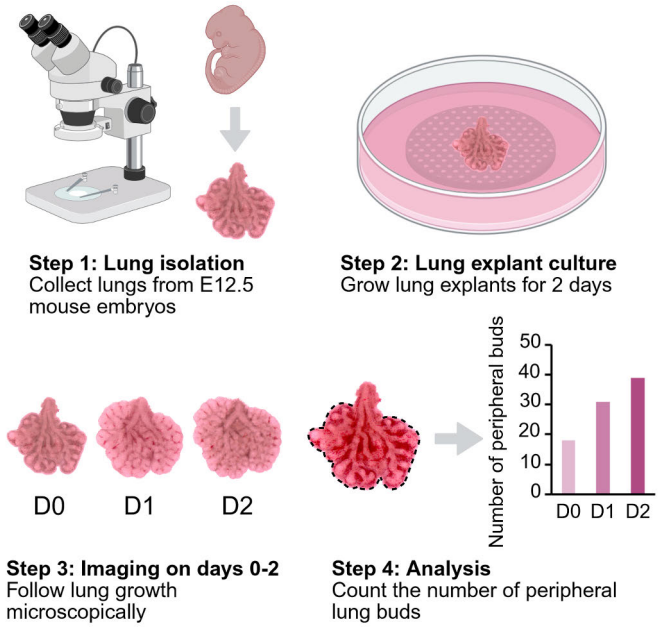

Figure 10. Analysis of lung developmental branching in mouse lung explant culture. Workflow for our version of studying early lung developmental branching using lung explant culture. D, day; E, embryonic day. The protocol is described in detail in Study II. Adapted from Study II and created with BioRender.com.

3.4.2 Kidney explant culture (III)

Embryonic kidney cultures were carried out on a Trowell-type system according to published protocols (Ihermann-Hella & Kuure, 2019; Saxén & Lehtonen, 1987). Briefly, after isolation of kidneys at E11.5, they were placed on the Transwell insert filter (Corning) and cultured in DMEM/F12 medium supplemented with 10% FBS, 2 mM L-glutamine, 100 units/ml Penicillin-Streptomycin at 37°C in a humidified atmosphere with 5% CO_2 for 48 h.

3.5 Immunostainings

3.5.1 Whole-mount immunofluorescence staining (I, III)

3.5.1.1 Staining of whole embryos (I)

The embryonic embigin expression was analyzed using a whole-mount immunofluorescence staining technique, as described previously in detail (Yokomizo et al., 2012). WT embryos at E8.5, E9.5, and E10.5 and $Emb^{-/-}$ embryos at E9.5 were stained with embigin and alpha smooth muscle actin (α-SMA) antibodies. α-SMA, which is present in smooth muscle cells of the developing heart and dorsal aorta, was used as a positive control. Additionally, the expression levels of embigin, MCT1, MCT4, and fibronectin were compared in WT and $Emb^{-/-}$ embryos at E10.5. The embryos were imaged with a confocal microscope, and image adjustments were performed with Zeiss ZEN blue software and Imaris (Bitplane).

3.5.1.2 Staining of embryonic kidneys (III)

Embigin and MCT1 or fibronectin localization were studied in WT kidneys at E13.5 using the whole-mount immunofluorescence staining technique as described previously (Yokomizo et al., 2012). The kidneys were imaged with a confocal microscope, and image adjustments were performed with ImageJ/Fiji software (Schindelin et al., 2012).

3.5.1.3 Staining of kidney explant cultures (III)

Embigin expression in early kidney development was studied in WT kidney explants isolated at E11.5 and cultured for 48 h. Additionally, the kidney UB tip formation in WT and $Emb^{-/-}$ embryos was compared in kidney explants isolated at E11.5 and cultured for 48 h. Whole-mount immunofluorescence staining was performed as previously described (Sariola et al., 1988). The kidneys were fixed in 4% paraformaldehyde for staining with embigin and Six2 primary antibodies. A methanol fixation at 4°C was used for staining with calbindin and Six2 primary antibodies. The samples were visualized with Alexa Fluor secondary antibodies and imaged with a confocal microscope. Image adjustments were performed with ImageJ/Fiji software (Schindelin et al., 2012). The number of UB tips was counted, and normalization was performed to eliminate the size variation between different litters from various pregnant dams.

3.5.2 Paraffin section immunofluorescence staining (I, III)

Formalin-fixed samples were embedded in paraffin, and 4 μm sections were cut using a microtome and immobilized on adhesion slides. The sections were deparaffinized and rehydrated. The antigen retrieval was achieved with 3 min proteinase K treatment (Agilent) for embigin, collagen I, CC10, and E-cadherin antibodies. For the SPC, Hop, Ki67, MCT1, MCT4, fibronectin, and basigin antibodies, heat-mediated antigen retrieval was done with sodium citrate buffer (pH 6.0). After antigen retrieval, the samples were washed in PBS, blocked with 1% bovine serum albumin (BSA) in PBS for 1 h, and stained with primary antibodies in the blocking buffer overnight. The samples were washed and incubated with Alexa Fluor secondary antibodies (Thermo Fisher Scientific) for 1 h. The nuclei were labeled with Hoechst 33342 stain for 10 min. Finally, the sections were rinsed and mounted in Mowiol containing 25 mg/ml DABCO anti-fading reagent. The samples were imaged with either a confocal microscope or a widefield microscope.

Image adjustments were performed with ImageJ/Fiji software (Schindelin et al., 2012). Ki67-positive cells in WT and $Emb^{-/-}$ embryonic lungs at E17.5 were analyzed as a fraction of all cells from five different areas of each lung.

3.6 Histological stainings

3.6.1 Hematoxylin and eosin staining (I, III)

Male and female WT and $Emb^{-/-}$ mice were examined at 2, 4, and 6 months. Additionally, a male and a female $Emb^{-/-}$ mouse were analyzed at the age of 1 year. The specific organs, heart, lungs, liver, spleen, kidneys, skin, small intestine, adrenal glands, epididymis, testis, and ovaries, were prepared for histological analysis. Lungs were also analyzed from WT and $Emb^{-/-}$ embryos at E17.5 and pups at P0. WT and $Emb^{-/-}$ placentas were analyzed at E17.5. Furthermore, kidneys from WT and $Emb^{-/-}$ embryos were examined at E17.5.

Organ sections were cut, immobilized to adhesion slides, and stained with conventional hematoxylin and eosin (H&E). The samples were imaged with a slide scanner. The relative area of airways in the lung section images of E17.5 embryos and P0 pups was analyzed with ImageJ/Fiji software (Schindelin et al., 2012).

3.6.2 Mammary gland whole-mount staining (III)

WT and $Emb^{-/-}$ abdominal mammary glands of 6-week-old mice at the diestrus stage of the estrous cycle were isolated, spread to adhesion slides, and fixed in Carnoy's solution for 2 h at RT. The samples were washed in 70% ethanol, hydrated by

gradually changing the solution to distilled water, and stained in carmine alum solution (Stemcell Technologies) for 1 day. The samples were dehydrated in graded solutions of ethanol, cleared in xylene for 2 days, and mounted. The mammary glands were imaged with a stereo microscope. The images were analyzed with ImageJ/Fiji software (Schindelin et al., 2012) to measure the number of branches, junctions, and terminal end-points of the mammary glands.

3.7 Transmission electron microscopy (I)

Lungs from WT and Emb$^{-/-}$ embryos at E18.5 were collected and fixed in 5% glutaraldehyde in 0.16 M s-collidine buffer, pH 7.4. The samples were post-fixed for 2 h with 2% OsO4 containing 3% potassium ferrocyanide, dehydrated, and embedded in epoxy. 70-nm sections were cut with an ultramicrotome and stained with 1% uranyl acetate and 0.3% lead citrate. The sections were examined with a transmission electron microscope. Lamellar bodies in ten cells of each section were counted, and areas were measured with ImageJ/Fiji software (Schindelin et al., 2012).

3.8 Cell lines (III)

Mouse epithelial keratinocyte cells isolated from adult dorsal skin (Carroll et al., 1995) were cultured in FAD medium containing three parts DMEM medium, one part Ham's F12 medium supplemented with 10% fetal bovine serum (FBS), 2 mM L-glutamine, 100 units/ml Penicillin-Streptomycin, 200 µM adenine, 0.5 µg/ml hydrocortisone, 5 µg/ml insulin, 16,8 ng/ml cholera toxin and 10 ng/ml epidermal growth factor. The cells were cultured at 37°C in a humidified atmosphere with 5% CO_2.

3.8.1 Embigin siRNA silencing of mouse epithelial cells (III)

Subconfluent mouse epithelial cells were transfected with three different 75 nM siRNAs (Mm_Emb_1 Flexitube (Emb1), Mm_Emb_4 Flexitube (Emb4), or AllStars Negative Control siRNA from QIAGEN) using siLentFect reagent (Bio-Rad) according to the manufacturer's instructions. After 48 h of treatment, cells were detached by scraping in PBS. The success of the transfection was verified with western blotting.

3.9 Analyses at the protein level

3.9.1 Urine analysis of newborn pups and adult mice (III)

Urine samples were collected from P0 pups and 5- to 6-month-old adult mice. The P0 mice urine samples were run on a 12% SDS-PAGE gel, and the gel was stained with InstantBlue Coomassie Protein Stain (Abcam) according to the manufacturer's instructions. BSA was used as a reference control. The protein concentrations of adult mice urine samples were analyzed with Combur 10 UX urine test strips and Urisys 1100 analyzer (Roche).

3.9.2 Protein extraction (I, III)

Protein samples were extracted from organs with the NucleoSpin RNA/Protein kit (Macherey-Nagel). Bead Tubes Type F (Macherey-Nagel) were used in tissue homogenization. Protein concentrations were measured with Pierce 660nm Protein Assay (Thermo Scientific).

3.9.3 Deglycosylation (I)

50 mg of protein extracts from either lungs, kidneys, skin, epididymis, testis, or liver of 4-month-old WT mice were deglycosylated for 4 h at 37 °C using Glycoprotein Deglycosylation Kit (Sigma-Aldrich). The results were analyzed with western blotting.

3.9.4 Western blotting (I, III)

For siRNA-transfected mouse epithelial cells, protein samples for western blotting were lysed in SDS-PAGE loading buffer, denatured by heating at 95°C for 5 min, and loaded on a 10% SDS-PAGE gel. Protein samples extracted with the NucleoSpin RNA/Protein kit were denatured by heating at 95°C for 5 min and loaded on 8% or 10% SDS-PAGE gel or 4–20% FastGene SDS-PAGE gradient gels (Nippon Genetics). Embigin and β-tubulin or GAPDH were stained in the membrane for 2 h at RT. IRDye secondary antibodies and Odyssey CLx imager (LI-COR Biosciences) were used for signal detection.

3.10 Genomic analyses

3.10.1 RNA extraction (I, III)

Total RNA was isolated using the NucleoSpin RNA kit (Macherey-Nagel) according to the manufacturer's instructions. For embryonic lungs, kidneys, and placenta, bead Tubes Type F (Macherey-Nagel) were utilized in tissue homogenization. The quality and quantity of the RNA were determined using the Nanodrop ND-2000 spectrophotometer (Thermo Scientific).

3.10.2 RNA sequencing (I, III)

In Study I, RNA sequencing (RNA-seq) analysis was done on WT and $Emb^{-/-}$ embryo lungs, kidneys, and placentas at E17.5. The libraries were prepared from 300 ng of RNA / sample using TruSeq Stranded mRNA HT Kit (Illumina). Sequencing was performed with NovaSeq 6000 SP Sequencing System (Illumina) using paired-end sequencing chemistry and 2 x 50 bp read length. Five independent biological replicates for both WT and $Emb^{-/-}$ were analyzed and run in one lane. The RNA-seq analysis is described in detail in the original publication I.

In Study III, RNA-seq analysis was performed on WT and $Emb^{-/-}$ embryo kidneys at E13.5. For each E13.5 kidney WT sample, kidneys from 4 individuals were pooled, and for each $Emb^{-/-}$ sample, kidneys from 6 individuals were pooled. The samples were prepared for the sequencing, and the RNA-seq was performed as described above. Five independent biological replicates for both WT and $Emb^{-/-}$ were analyzed and run in one lane. The RNA-seq analysis is defined in detail in the original publication III.

Furthermore, the siRNA-transfected mouse epithelial cells were analyzed with RNA-seq in Study III. The samples were prepared for the sequencing, and the RNA-seq was performed as described above. Three samples (negative control, Emb1, and Emb4 siRNA-treated samples) from four independent biological replicates were analyzed and run in one lane. Since silencing with Emb1 siRNA proved to be more effective than silencing with Emb4 siRNA, the results obtained with Emb1 siRNA were presented in the RNA-seq analysis; the Emb1 siRNA-silenced cells were compared to negative control siRNA-silenced cells. The detailed RNA-seq analysis is represented in the original publication III.

Additionally, our earlier RNA-seq results of E17.5 lungs and kidneys were reanalyzed to match the analysis workflow used in the RNA-seq of E13.5 kidneys and mouse epithelial cells in the original publication III. In short, the DeSeq2 Bioconductor package (Love et al., 2014) was used to normalize gene-wise read counts and to perform statistical tests between groups. The gene was determined as

differentially expressed when the log2 of the fold change value was above 0.6 or below -0.6, and the Benjamini-Hochberg-corrected p-value was less than 0.05 between the compared groups. Metascape, https://metascape.org (Y. Zhou et al., 2019), was used to perform over-representation analysis of downregulated genes against biological process gene ontology from the RNA-seq results. Venny 2.1, https://bioinfogp.cnb.csic.es/ tools/venny/ (Oliveros, 2007) was used to compare the downregulated genes shared between the RNA-seq results of the E13.5 or E17.5 kidneys and the mouse epithelial cells or the E17.5 lungs and the mouse epithelial cells.

3.11 Statistical analyses (I, III)

IBM SPSS Statistics software (version 25 or 29, IBM) was used for all statistical analyses. A p-value < 0.05 was considered statistically significant. The statistical details of the experiments can be found in the original publications I and III.

4 Results

4.1 Characterization of embigin protein expression in mice

Understanding of embigin expression has primarily relied on determining mRNA levels in various tissues, leaving the protein expression pattern unclear. Thus, our objective was to map the protein expression of embigin during mouse embryonic development and in adult mice.

4.1.1 Embigin expression is high in early mouse embryogenesis

We utilized whole-mount immunofluorescence staining to visualize the protein expression pattern of embigin in mouse embryos at E8.5-E10.5. Consistent with earlier mRNA studies (Fan et al., 1998; R.-P. Huang et al., 1990), the highest levels of embigin expression were observed during the early stages of embryogenesis, particularly in the developing gut (Figure 11A). Although embigin expression did not completely cease after E10.5, there was a noticeable decline. At E13.5, low levels of embigin were found in specific tissues, particularly in the kidneys, lungs, and small intestine (I, Figure S1A). At E17.5, embigin was still present in the kidneys, while in the lungs, the expression levels were almost undetectable (I, Figure 1B). Additionally, an analysis of scRNA-seq data at the mouse organogenesis spatiotemporal transcriptomic atlas (MOSTA; Chen et al., 2022) further validated that embigin expression is high at E9.5 and decreases later (Figure 11B).

We also studied the embigin protein expression in mice after the gestational period. A set of adult organs was examined at four months using an immunofluorescence staining technique in paraffin sections. The kidneys, lungs, epididymis, and skin (Figure 11C) showed high embigin levels, and embigin was located in the epithelial cells lining the tubular structures of the organs. The expression level of embigin in both the lungs and kidneys was found to increase shortly after birth at P3, and the expression was observed to be the highest in adult mice (I, Figures 1B-1C, S1C).

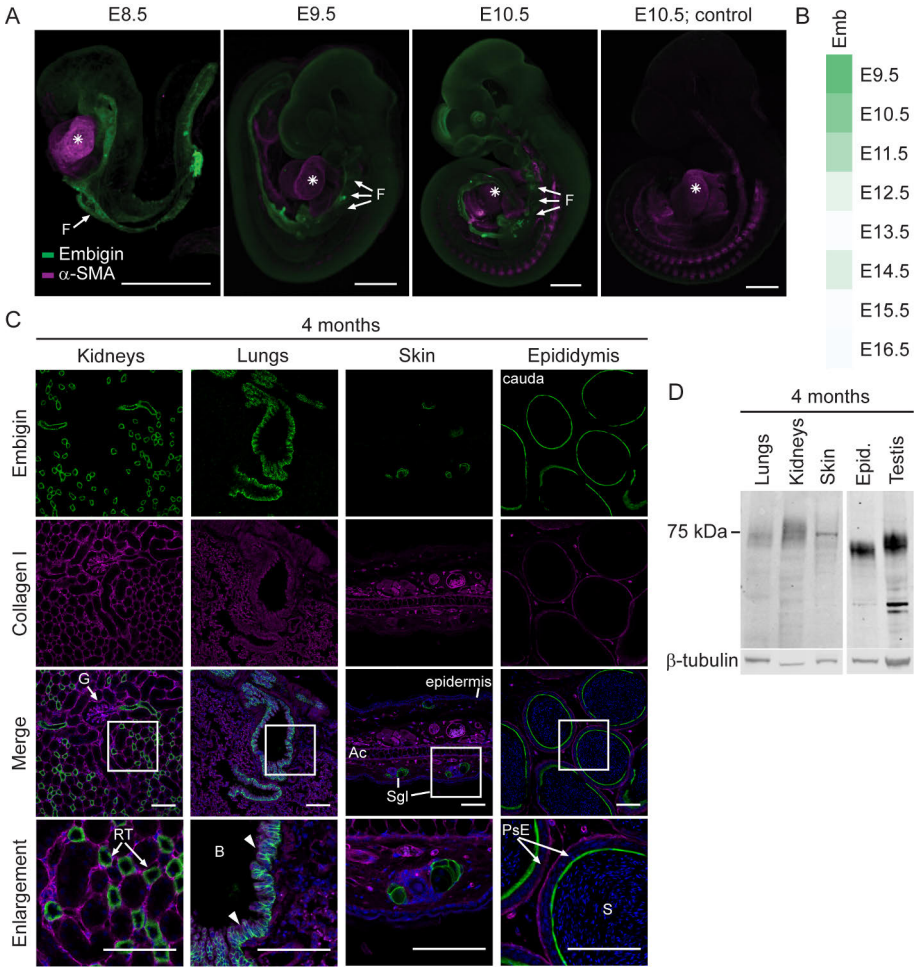

Figure 11. Embigin is widely expressed in early mouse embryogenesis and later in specific organs. A. E8.5, E9.5, and E10.5 WT mouse embryos were stained with embigin and alpha smooth muscle actin (α-SMA) antibodies using the whole-mount immunofluorescence staining. As the negative control for embigin, only a secondary antibody was used; α-SMA was stained as a positive control. An asterisk indicates a developing heart, F, foregut. Scale bars: 500 µm. **B.** Embigin mRNA expression in E9.5-E16.5 mouse embryos based on the analysis of scRNA-seq data published in the MOSTA database. **C.** The paraffin sections of the kidneys, lungs, skin, and epididymis of four-month-old mice were immunostained with embigin antibody. Collagen I was used as a positive control, and nuclei were labeled with Hoechst 33342 Fluorescent Stain. Magnifications of the embigin-positive areas are shown. G, glomerulus, RT, renal tubule; B, bronchiole, arrow heads point at the epithelial cells lining bronchioles; Ac, auricular cartilage, Sgl, sebaceous gland; PsE, pseudostratified epithelia, S, sperm cells. Scale bars: 100 µm. **D.** Embigin expression in protein samples from four-month-old WT mouse lungs, kidneys, skin, epididymis (epid.), and testis was studied with western blotting. β-tubulin was used as a loading control. E, embryonic day. Adapted from Figures 1 and S1 of Study I.

The embigin protein expression in the organs was verified through western blot analysis (Figure 11D). A significant signal was detected in the mouse testis as well, suggesting that embigin is present in the tissue. However, the other tested organs, the liver, spleen, small intestine, adrenal glands, ovaries, and heart, were determined to be embigin-negative tissues (I, Figure S1D). In the embigin-positive tissues, embigin was identified as a typical diffuse band around 75 kDa. After the protein was completely deglycosylated, its size decreased to 35 kDa, matching the expected size of the embigin core protein (I, Figure S1E). The highest molecular mass of embigin was found in the kidney, whereas the epididymis showed the lowest molecular mass, and the smallest variation was observed in the skin (I, Figure 1E). Therefore, the detected change in the molecular mass of embigin in the tissues is likely due to differential N-linked glycosylation at the nine reported glycosylation sites in the protein (Ozawa et al., 1988). However, it is not yet clear whether variations in glycosylation influence the function of embigin.

4.1.2 Embigin is expressed in the mouse lung bronchioles and kidney collecting ducts and distal tubules

As mentioned, embigin protein was found to be in the epithelial cells lining the tubular structures of the mouse lungs and kidneys. In the lungs, embigin was detected in the epithelial cells of the lung bronchioles (Figure 11C). In bronchioles, embigin was observed to colocalize with CC10 (Scgb1a1), which is a marker for club cells (I, Figure S6B). Club cells are oligopotent stem cells in the bronchi and bronchioles, essential for regulating cell proliferation in the lungs (Rawlins et al., 2009).

In the kidneys, embigin was consistently present in tubular structures (I, Figure 1B, S1A). These structures were confirmed to be collecting ducts and distal tubules, as E-cadherin (Prozialeck et al., 2004) and embigin showed colocalization in paraffin sections of WT kidneys at P3 (III, Figure 1A).

4.2 Embigin deficiency results in high neonatal mortality in mice

To investigate the role of embigin *in vivo*, knockout mice lacking exon 5 of the embigin gene were generated in collaboration with the Turku Center for Disease Modeling. The absence of embigin expression in the embigin knockout ($Emb^{-/-}$) mice was confirmed using both PCR and western blot analysis (I, Figures S2B-S2C). Additionally, the mouse embigin antibody was validated with $Emb^{-/-}$ mice, which confirmed its specificity and lack of off-target binding (I, Figures S2C-S2D).

Next, the impact of the embigin deficiency on the lifespan of $Emb^{-/-}$ mice was studied. The genotypes of 203 embryos from $Emb^{+/-}$ pairings at developmental stages

from E8.5 to E17.5 were analyzed. The relative frequency of the genotypes at stage E8.5 was found to follow the Mendelian distribution (I, Figure 2A). However, the frequency of $Emb^{-/-}$ embryos at E17.5 was discovered to be only 18% instead of the expected 25% (I, Figure 2A). The Spearman's rank correlation analysis revealed a statistical significance in the small gradual decrease in the number of $Emb^{-/-}$ embryos as the gestation progressed (I, Figure 2A). Next, the genotypes of 284 pups from $Emb^{+/-}$ pairings were examined between P14 and P21. Based on the results, only 7% of the pups were $Emb^{-/-}$ at P14-P21 (Figure 12A). Our results indicate that 72% of expected $Emb^{-/-}$ pups did not reach adulthood. To determine the time window for the lethality of $Emb^{-/-}$ mice, 100 pups from $Emb^{+/-}$ pairings were monitored after birth. The results show that the majority of $Emb^{-/-}$ pups died during days 0 and 1 of postnatal life (I, Figure 2C). Therefore, the first days after birth seem to be critical for the survival of the $Emb^{-/-}$ mice. However, some $Emb^{-/-}$ mice were already lost during the gestation and possibly the parturition.

4.2.1 Embigin deficiency seems to have no significant impact on mice after the neonatal period

To further investigate the effect of embigin deficiency on surviving mice, $Emb^{-/-}$ and WT mice were studied at 2, 4, 6, and 12 months. There was no difference in body weights of adult WT and $Emb^{-/-}$ mice (I, Figure S2E). Additionally, there was no difference in the histology or weights of specific organs (I, Figures S2F-S2I, Table S1). The embigin deficiency did not affect the fertility of mice (I, Table 1). Our findings indicate that the surviving $Emb^{-/-}$ mice are fertile, showing no significant changes in typical body and organ weights or in the histological architecture of the tissues examined.

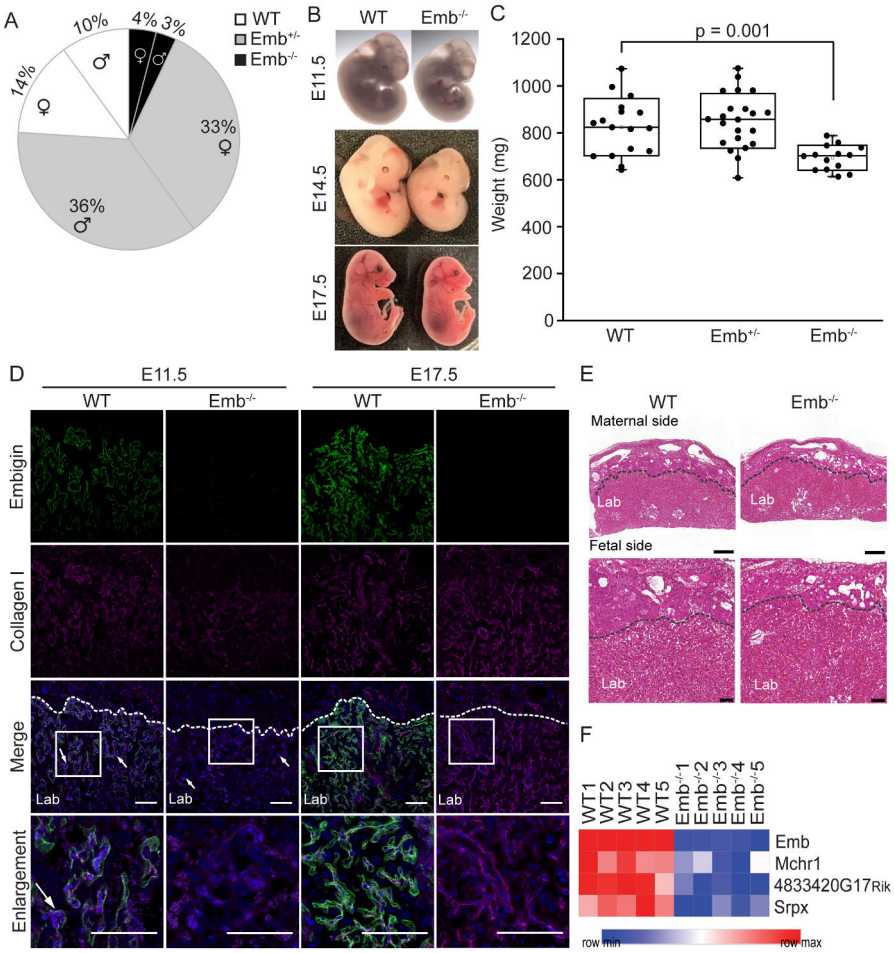

Figure 12. Embigin deficiency leads to high neonatal mortality in mice, and the growth of the Emb$^{-/-}$ embryos is delayed. A. The Mendelian frequency of the genotypes of the pups from Emb$^{+/-}$ breedings was defined. 284 pups from 40 litters were analyzed at P14-P21. **B.** The representative images of WT and Emb$^{-/-}$ embryos are shown at E11.5, E14.5, and E17.5. **C.** The weights of 53 embryos from Emb$^{+/-}$ breedings were analyzed at E17.5. The statistical significance of the weight difference between WT and Emb$^{-/-}$ embryos (p = 0.001) was analyzed with Student's T-test for independent samples. Data are represented as a Spear style boxplot. **D.** The paraffin sections of WT and Emb$^{-/-}$ placenta were immunostained with embigin and collagen I antibodies at E11.5 and E17.5. Nuclei were labeled with Hoechst 33342 Fluorescent Stain. Arrowheads show fetal-derived round nuclei. Magnifications of the embigin-positive areas are shown. Lab, labyrinth zone. Scale bars: 100 µm. **E.** WT and Emb$^{-/-}$ placentas at E17.5 were histologically analyzed with H&E staining. Scale bars: 500 µm. Below, the magnifications of the inner edges of the placental labyrinth zones are shown. Lab, labyrinth zone. Scale bars: 100 µm. **F.** Heatmap of differentially expressed genes (log2 of fold change above 0.6 or below -0.6 and Benjamini-Hochberg-corrected p value <0.05) in E17.5 WT (n = 5) and Emb$^{-/-}$ (n = 5) placenta based on the RNA-seq analysis. E, embryonic day. Adapted from Figures 2 and 3 of Study I.

4.2.2 The growth of the Emb$^{-/-}$ embryos is delayed

The body sizes of Emb$^{-/-}$ embryos appeared to be smaller than their Emb$^{+/-}$ or WT littermates (Figures 12B-12C). Since the placenta has an essential role in fetal growth, we characterized the placentas of Emb$^{-/-}$ and WT embryos. Using the immunofluorescence staining technique for paraffin sections of placentas of WT embryos at E11.5 and E17.5, we observed an increasing embigin expression in the labyrinthine layer of the placenta (Figure 12D). However, no histological differences were detected between the placentas of WT and Emb$^{-/-}$ embryos (Figure 12E). Based on the RNA-seq data, only four genes, including embigin, were differentially expressed in the placentas of Emb$^{-/-}$ embryos compared to the WT at E17.5 (Figure 12F). Thus, we did not find evidence that the lack of embigin could lead to placental dysfunction, which could explain the smallness or the mortality of the Emb$^{-/-}$ embryos. As a result, other essential organs were studied.

Based on lung and kidney weights, we observed that the lungs and kidneys were significantly smaller in Emb$^{-/-}$ embryos than in WT at E17.5 (I, Figure S3D; III, Figure 2A). However, this can be related to the observed overall growth regulatory effect for embigin during development, as the whole Emb$^{-/-}$ embryos were smaller than WT (Figures 12B-12C), and also the WT and Emb$^{-/-}$ kidney weight/embryo weight ratios resembled each other (III, Figure 2A).

4.3 Embigin is a critical protein in mouse lung development

4.3.1 The maturation of the Emb$^{-/-}$ mice lungs is delayed

When we examined the Emb$^{-/-}$ lungs at E17.5 histologically, we discovered an abnormal structure: the number and the size of the small airways and distal airspace were significantly smaller when compared to the lungs of WT embryos (Figure 13A). Additionally, the relative area of the structures in the Emb$^{-/-}$ lungs at E17.5 correlated with the size of the Emb$^{-/-}$ embryo: larger embryos exhibited more mature lungs (Figure 13B). Overall, lung development was systematically delayed in Emb$^{-/-}$ embryos at E17.5. While the Emb$^{-/-}$ lungs remained at the canalicular stage, their WT littermates had already progressed to the saccular stage of lung development.

Next, we studied the alkaline phosphatase activity from the amniotic fluid at E17.5. At the end of gestation, elevated alkaline phosphatase activity is known to indicate increasing fetal lung maturity (Brocklehurst & Wilde, 1980). The alkaline phosphatase activity in the amniotic fluid of the Emb$^{-/-}$ embryos was found to be significantly lower than the activity detected in WT embryos (Figure 13C). Furthermore, the concentrations of sodium, calcium, and glucose have been reported

to vary in the amniotic fluid during normal pregnancy (Cheung & Brace, 2005). However, the concentrations of sodium, calcium, or glucose did not significantly differ between WT and Emb$^{-/-}$ embryos at E17.5 (I, Figures S3A-S3C), suggesting that the pregnancies of Emb$^{-/-}$ embryos progressed normally.

To investigate further the delay observed in Emb$^{-/-}$ lungs, WT and Emb$^{-/-}$ lungs were harvested at E12.5 and cultured as explants for 48 h. The smaller Emb$^{-/-}$ lungs showed significantly fewer peripheral branching buds than WT lungs (Figure 13D). The results indicate that while lung branching was progressing in Emb$^{-/-}$ lungs, it continuously stayed behind the developmental program of WT lungs (Figure 13D). Notably, our version of the lung explant culture method is detailed in Study II (Figure 10). In Study I, this method was central and interesting; therefore, we made a detailed publication of it. The actual native lung tissue preserves complex structures, such as the lung microenvironment, compared to lung organoids. We have fine-tuned each step of the process to its peak and visualized the critical steps with a video we made, including placing the lung lobes in the correct orientation on the membrane. Overall, we also believe that the overall picture is clearer than in previous publications (Carraro et al., 2010; Del Moral & Warburton, 2010).

Furthermore, we discovered that the formation and maturation of distal epithelial cells were slightly delayed in Emb$^{-/-}$ lungs at E17.5: the number of both ATII and ATI cells was lower when compared to WT lungs (I, Figure 4E). However, the ATII cells present in the Emb$^{-/-}$ lungs were capable of synthesizing SPC at E17.5 (I, Figure 4E) and able to form lamellar bodies store SPC storage, as observed with transmission electron microscopy at E18.5 (I, Figure 4F). Nevertheless, the lamellar bodies found in the Emb$^{-/-}$ lungs were significantly smaller (I, Figure 4F). These results suggest that the Emb$^{-/-}$ lungs can undergo normal lung organogenesis but in a delayed manner.

We studied the developmental delay of the lungs further by analyzing transcriptomes of WT and Emb$^{-/-}$ embryonic lungs at E17.5 with RNA-seq: 161 genes of the lungs were differentially expressed between the genotypes (Figure 13E; I, Figure S4A). When comparing Emb$^{-/-}$ embryos to WT, the upregulated genes were primarily associated with cell proliferation (I, Figure 5B). Besides, many of the upregulated genes are potential transcription and growth factors that are important for lung development.

Next, we immunostained WT and Emb$^{-/-}$ lungs at E17.5 with cell proliferation marker Ki67. The levels of Ki67 were significantly elevated in Emb$^{-/-}$ lungs (I, Figure 5C). This difference in cell proliferation aligns with the observation that at E17.5, the Emb$^{-/-}$ lungs are still in the canalicular stage, while the WT lungs have already progressed to the saccular stage. Taken together, our RNA-seq analysis and Ki67 staining results support the idea that the development of Emb$^{-/-}$ lungs is rather delayed than defective.

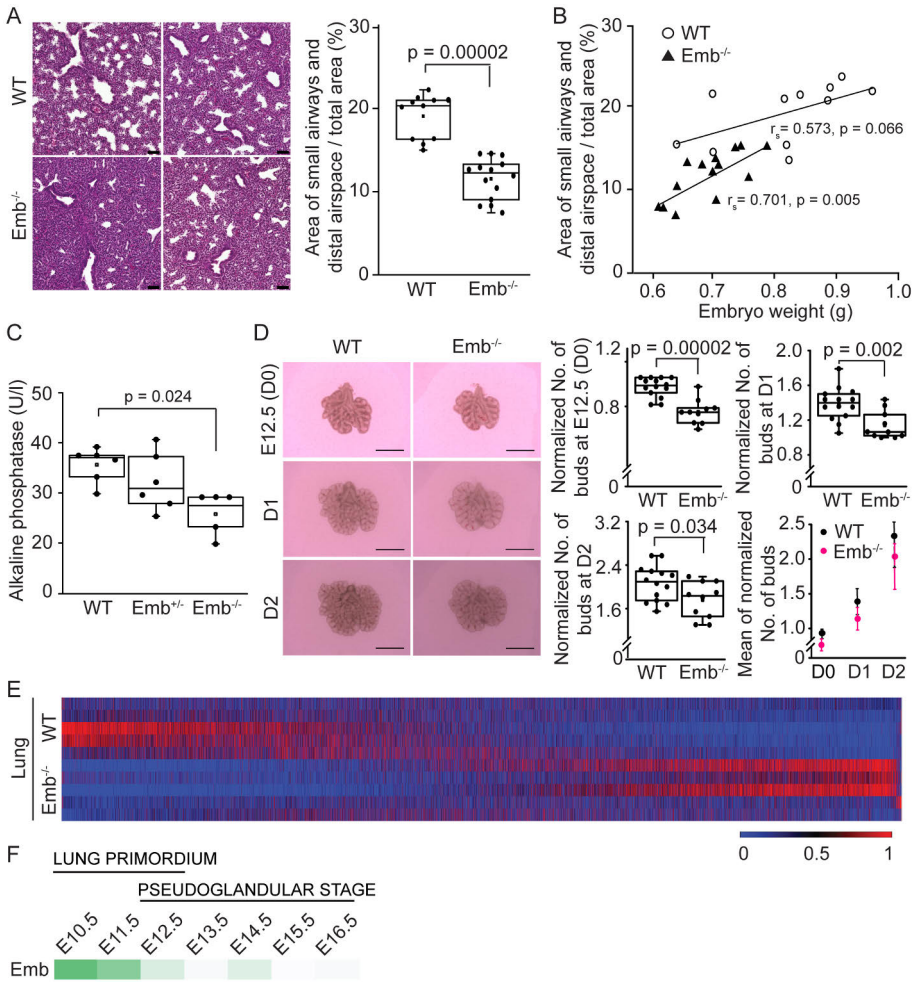

Figure 13. Lung maturation of the Emb$^{-/-}$ mice is delayed. A. Representative images of H&E-stained lung sections from two WT and two Emb$^{-/-}$ littermates at E17.5 are presented. Scale bars: 50 µm. The relative area of small airways and distal airspaces in the E17.5 lung sections was compared (n = 11 for WT and n = 14 for Emb$^{-/-}$). Statistical significance (p = 0.00002) was determined using Mann-Whitney U-test. **B.** The correlation between the body weight of the embryo and the relative area of small airways and distal airspaces in the lung sections was studied with Spearman's rank correlation coefficient (r_s) and its statistical significance. **C.** Alkaline phosphatase activity was analyzed from the amniotic fluids of E17.5 WT (n = 6), Emb$^{+/-}$ (n = 5), and Emb$^{-/-}$ (n = 5) embryos with VetScan Chemistry Analyzer. Statistical significance (p = 0.024) was determined with Dunnett's t-test. **D.** Lung explants from WT (n = 14) and Emb$^{-/-}$ (n = 10) embryos at E12.5 were cultured for 2 days and imaged on days 0, 1, and 2 (D0 – D2). The normalized count of peripheral buds in E12.5 WT and Emb$^{-/-}$ lung explants was compared. Statistical significances (D0: p = 0.00002, D1: p = 0.002, and D2: p = 0.034) were determined with Student's T-test for independent samples. Scale bars: 1000 µm. **E.** Heatmap of all expressed genes in E17.5 WT (n = 5) and Emb$^{-/-}$ (n = 5) lungs based on RNA-seq analysis. **F.** The mRNA expression of embigin in E10.5-E16.5 lungs based on the analysis of scRNA-seq data published in the MOSTA database. E, embryonic day. Data are represented as a Spear style boxplot. Adapted from Figures 4 and 5 of Study I.

4.3.2 Embigin deficiency affects inflammatory processes in the developing lungs

When the RNA-seq results of Emb$^{-/-}$ lungs were compared to WT at E17.5 using WebGestalt enrichment analysis, most of the downregulated genes were involved in the immune response (I, Figure 5B). In line with the previous analysis, another enrichment analysis of the downregulated genes using Metascape (p-value < 0.01 and ≥3 overlapping genes) revealed that these genes were mainly related to inflammatory responses (Figure 14A). Furthermore, the downregulated genes shared between the RNA-seq results of the E17.5 lungs and the mouse epithelial cells were compared. We found that *Vnn1* gene was downregulated in both results (Figure 14B; log2FC(E17.5 lungs) = -1.5, log2FC(mouse epithelial cells) = -0.7)). In the Metascape analysis, *Vnn1* was associated with acute inflammatory response. The *Vnn1* gene encodes vanin 1 (VNN1), an enzyme that participates in at least oxidative stress, inflammatory responses, cell migration, and glucose metabolism (H. Yu et al., 2024). Overall, embigin may contribute to some inflammatory events through VNN1 during mouse lung development. However, embigin expression is very low in the later stages of gestation, so its effect may be minor.

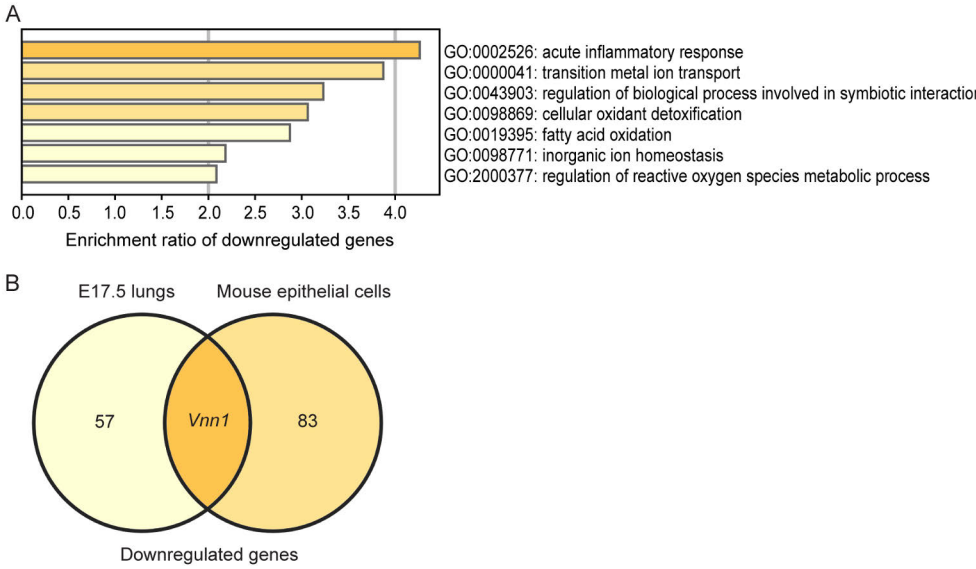

Figure 14. Embigin deficiency influences inflammatory processes in the developing lungs. **A.** The over-representation of downregulated genes in Emb$^{-/-}$ vs. WT E17.5 lungs was analyzed from RNA-seq data using Metascape. The top 7 most significantly enriched biological processes with p-values < 0.01 and ≥3 overlapping genes are shown. **B.** The downregulated genes shared between the RNA-seq results of the E17.5 lungs and the mouse epithelial cells were compared using Venny. The *Vnn1* gene was downregulated in both results (embigin knockout/knockdown vs. control). E, embryonic day.

4.3.3 Embigin is present in primordial lung cells

To get a better understanding of embigin expression in the lungs during gestation, we analyzed the MOSTA scRNA-seq data (Chen et al., 2022). Using region-specific marker genes, we found that embigin mRNA expression was highest in the lung primordium during E10.5-E12.5 (Figure 13F). Consistent with our previous observations, we noted that embigin mRNA expression gradually decreased in the lungs, reaching very low levels by E13.5.

Embigin deficiency likely affects the behavior of primordial lung cells, resulting in delayed branching morphogenesis and maturation of alveolar cells (ATI and ATII) observed at later stages of development. The delayed lung development in $Emb^{-/-}$ mice was evident at E12.5 (Figure 13D) and continued to be noticeable at E17.5 (Figure 13A). Furthermore, in P0 $Emb^{-/-}$ pups, the number and size of the small airways and distal airspaces remained smaller compared to WT mice (I, Figure S5C), although the differences were not as pronounced as seen in the E17.5 lungs. Overall, the embigin function appears to be crucial at the early pseudoglandular stage or possibly even earlier.

Embigin has been shown to facilitate the function of many MCT proteins (Wilson et al., 2005; Halestrap, 2013b; Skiba et al., 2021; Xu et al., 2022; Higuchi, 2022; Cheng, Liu, Gao, Zhu, et al., 2025; Cheng, Liu, Gao, Xin, et al., 2025), and we have previously linked embigin function to cell adhesion (Sipilä et al., 2022). Thus, we made immunostainings for MCT1, MCT4, and fibronectin during the embryonic development of mice. In both E10.5 embryos and E17.5 lungs, we did not observe any significant differences in the expression levels or tissue distributions of MCT1, MCT4, and fibronectin between WT and $Emb^{-/-}$ samples (I, Figures S5A-S5B). Additionally, differential expressions of MCT1 and MCT4 were not detected in the RNA-seq analysis of the E17.5 lungs. However, our analysis of the MOSTA scRNA-seq data (Chen et al., 2022) revealed that MCT1, MCT4, and fibronectin are expressed at higher levels in primordial lungs than in the later stages of development (I, Figure S6C). Therefore, there is a chance that embigin might assist these proteins in the primordial lungs.

It is possible that basigin may partially compensate for the function of embigin. However, we found no evidence to support this hypothesis, as there were no noticeable differences in the expression levels of basigin in either the RNA-seq analysis or the immunostaining of the E17.5 lungs (I, Figure S5B). Yet, we cannot rule out the possibility that, during the early phases of gestation, members of the basigin family may compensate for each other's functional deficiencies.

4.4 Embigin is involved in mouse kidney morphogenesis

We have shown that the markedly increased neonatal mortality (72%) of Emb$^{-/-}$ mice could be primarily explained by compromised lung maturation. However, we cannot exclude the possibility that embigin also affects the development of other mouse organs. We have observed that the embigin protein is expressed in mice in the tubular structures of kidneys at E13.5, E17.5, and P3 and in adults (I, Figures 1B, S1A, S1C). In addition, we have found that embigin is expressed in the early stages of kidney development in mice: embigin protein shows high expression in the UB and differentiating nephron precursors of mouse embryonic kidneys that have been isolated at E11.5 and cultured for 48 h (Figure 15A). Indeed, previous research has shown embigin mRNA expression in the UB of rat embryonic kidneys (Stuart et al., 2003) and also in the UB of mouse kidneys at E11.5 (Schwab et al., 2003).

Embigin has been associated with supporting the MCT proteins, especially MCT1 (Wilson et al., 2005; Halestrap, 2013b; Skiba et al., 2021; Xu et al., 2022; Higuchi, 2022; Cheng, Liu, Gao, Zhu, et al., 2025; Cheng, Liu, Gao, Xin, et al., 2025). Embigin has also been identified as a receptor for fibronectin (Sipilä et al., 2022). Thus, we studied the expression of embigin and MCT1 or fibronectin in developing mouse kidneys with the whole-mount immunofluorescence staining technique in WT kidneys at E13.5 (Figures 15B-15C). Embigin is expressed in the epithelium of the developing renal UB and nephron precursors. MCT1 is widely expressed in the developing kidney but appears not to colocalize with embigin (Figure 15B). In turn, fibronectin seems to be highly expressed in the ECM surrounding the UB (Figure 15C). Thus, embigin may facilitate the interactions between the UB and the surrounding mesenchyme, which are recognized as a key regulator of kidney development by influencing both branching morphogenesis and nephron differentiation (Kuure & Sariola, 2020).

4.4.1 Embigin deficiency delays early kidney development

In the developing rat prostate, embigin expression has been identified to correlate with the formation of well-organized tubular structures (Guenette et al., 1997), raising questions about its potential role in branching morphogenesis. Therefore, we studied whether embigin deficiency affects the UB branching morphogenesis by analyzing the tip formation of the mouse kidneys during early development. The branching of the UB tips is impaired in the Emb$^{-/-}$ kidneys compared to WT kidneys that have been isolated at E11.5 and cultured for 48 h (Figure 15D). Hence, embigin might be necessary for the UB branching during early kidney morphogenesis.

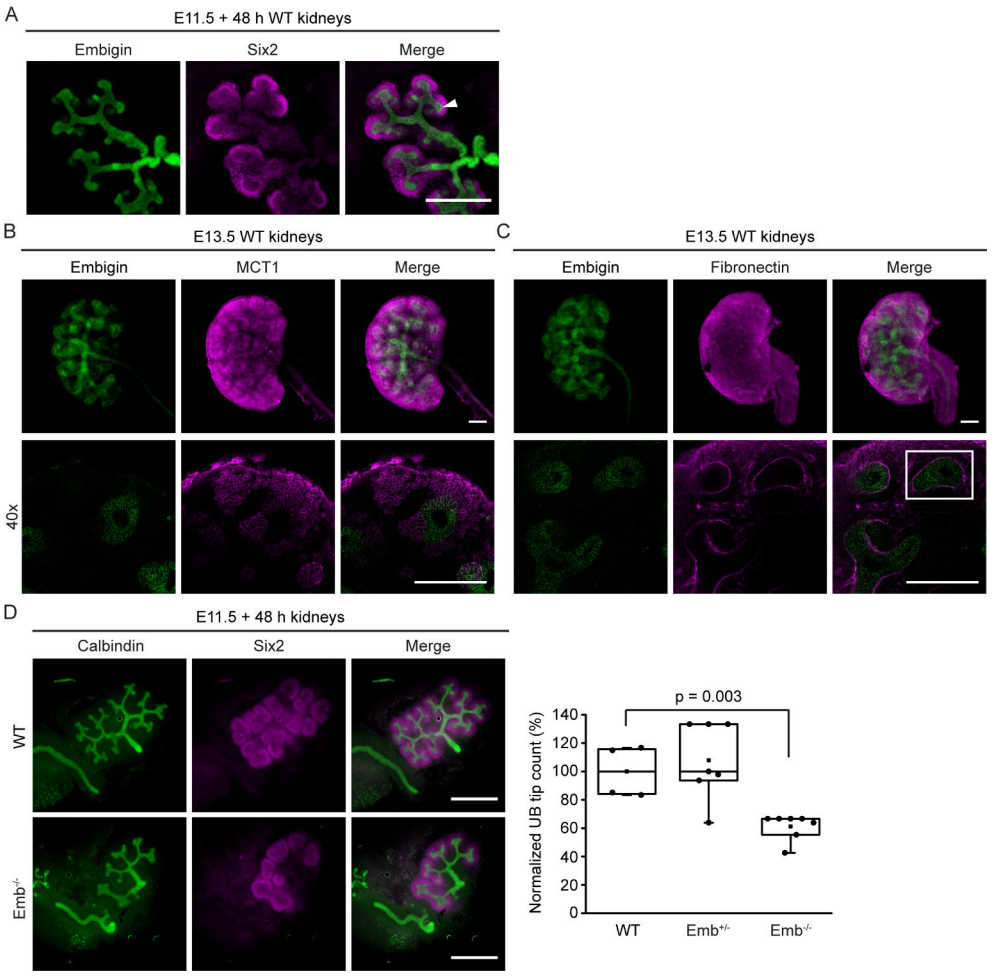

Figure 15. Embigin protein is expressed in the ureteric bud and differentiating nephron precursors. The branching of the Emb$^{-/-}$ ureteric buds is impaired. A. The kidneys from an E11.5 WT embryo were cultured for 48 h and stained using the whole-mount immunofluorescence staining technique with embigin (green) and Six2 (magenta) antibodies. Embigin is localized in the UB and differentiating nephron precursors (arrowhead) but not in Six2-positive nephron progenitor cells. Scale bar: 500 µm. **B-C.** Embigin (green) was stained with MCT1 (B, magenta) or fibronectin (C, magenta) using the whole-mount immunofluorescence staining technique in WT kidneys at E13.5. The 3D images and the 40x optical slice images from the kidney cortex area are shown. The box shows a region of the renal tubule where embigin and fibronectin expression are close together. Scale bars: 100 µm. **D.** The kidneys were isolated from WT, Emb$^{+/-}$, and Emb$^{-/-}$ embryos at E11.5, cultured for 48 h, and stained with calbindin (green) and Six2 (magenta) antibodies using the whole-mount immunofluorescence staining method. Scale bars: 500 µm. The UB tips were counted after the 48-h culture (n = 4 for WT, n = 7 for Emb$^{+/-}$, and n = 7 for Emb$^{-/-}$). The values were normalized inside each litter. Statistical significance (p = 0.003) was determined using the Mann-Whitney U-test. Data are represented as a Spear style box plot. E, embryonic day; UB, ureteric bud. Adapted from Figures 1 and 2 of Study III.

Next, we investigated whether embigin is a general regulator of tube formation and branching morphogenesis in mice. Embigin has been detected in the adult rat mammary glands (Guenette et al., 1997). When we analyzed the mammary glands of 6-week-old mice, no differences were observed in the branches, junctions, and terminal end-points between WT and $Emb^{-/-}$ mice (III, Supplementary Figure 1), indicating that embigin may have organ-specific effects during their morphogenesis.

We examined how the deficiency of embigin affected the expression of other proteins in embryonic kidneys. RNA-seq analysis conducted on mouse embryonic kidneys at E13.5 revealed primarily downregulated genes, 85 in total ($Emb^{-/-}$ E13.5 kidneys were compared to WT, log2FC > 0.6 or < -0.6 and adjusted p-value < 0.05; III, Figures 3A-3B, 4A). Additionally, 16 genes showed an increase in expression. The enrichment analysis of the RNA-seq results using Metascape (Y. Zhou et al., 2019) indicated that the downregulated genes were linked to nephron and glomerulus development, regulation of systemic arterial blood pressure, fluid and hormone balance, substance transport, and tube morphogenesis (Figure 16A). Notably, the processes identified are linked to crucial functions of mature kidneys and indicate an imbalance in the differentiation of the renal system.

Indeed, several of the downregulated genes were associated with kidney development, such as *Nphs1* and *R3hdml* (III, Supplementary Table 1). The *Nphs1* gene codes for nephrin, and *R3hdml* codes for R3h domain containing-like protein, both related to podocyte development and function (Putaala et al., 2001; Ishikawa et al., 2021). Therefore, the downregulation of these genes suggests that podocyte development is compromised in the $Emb^{-/-}$ kidneys.

Embigin is also expressed in the later stages of kidney development. The analysis of RNA-seq data from E17.5 kidneys obtained in Study I revealed that only one gene (*4833420G17Rik*) was differentially expressed between WT and $Emb^{-/-}$ embryos, in addition to embigin. Notably, the genes downregulated in the $Emb^{-/-}$ kidneys at E13.5 (III, Figure 4A) did not show statistically significant alterations in expression at E17.5, except for the lack of embigin (III, Figure 4B). This suggests that the transcriptional changes of $Emb^{-/-}$ kidneys reach the level of WT kidneys in later developmental stages. We did not notice any obvious morphological abnormalities in E17.5 $Emb^{-/-}$ kidneys either, other than the developmental stage-related differences compared to WT kidneys (III, Figure 4C). Moreover, we observed no signs of albuminuria in $Emb^{-/-}$ mice at P0 (III, Figure 4D), and no protein was found in urine samples from adult $Emb^{-/-}$ mice aged 5 to 6 months. We did not detect any obvious changes in the histology of $Emb^{-/-}$ kidneys of adult mice either (I, Figure S2F), and the $Emb^{-/-}$ mice that survive have a normal lifespan. Thus, both newborn and adult $Emb^{-/-}$ kidneys seem to be functioning normally, including podocyte-related functions.

4.4.2 Embigin regulates genes involved in kidney development and function, including *Pappa2*, *Acta2*, and *Tagln*

Differential gene expression observed in E13.5 $Emb^{-/-}$ kidneys may be partially caused by the developmental delay observed in $Emb^{-/-}$ kidneys compared to WT kidneys at E13.5. We explored whether embigin directly affects on the expression levels of kidney development-related genes in epithelial cells, using embigin-specific siRNAs to knockdown its expression in mouse keratinocyte cells. Two distinct siRNAs, Mm_Emb1 (Emb1) and Mm_Emb4 (Emb4) siRNAs, were selected for the study. After 48 hours, Emb1 siRNA-treated cells showed a reduction of embigin protein level by 88 ± 4%, while the decrease in Emb4 siRNA-treated cells was 81 ± 6%, as shown by western blot analysis (III, Figures 5A-5B).

Since Emb1 siRNA was more effective in silencing, its results were presented in the RNA-seq analysis; the Emb1 siRNA-silenced cells were compared to negative control siRNA-silenced cells. The knockdown of embigin in mouse epithelial cells resulted in the upregulation of 439 genes (III, Supplementary Figure 2A-2B) and the downregulation of 85 genes (III, Supplementary Figure 2A-2C). The differentially expressed genes from the RNA-seq data were studied with an over-representation analysis, which showed the most significantly enriched biological processes (III, Figures 5C-5D). The upregulated genes were involved in tube morphogenesis, renal system development, regulation of vasculature development, ECM organization, tissue morphogenesis, and regulation of body fluid levels (III, Figure 5C). The downregulated genes were linked to, e.g., nephron and epithelial cell development (Figure 16B). In fact, several of the downregulated genes were associated with kidney development, including *Npnt* and *Hnf1b* (III, Supplementary Table 2). In summary, the data imply that the absence of embigin in mouse epithelial cells may have a significant impact on the expression of the genes responsible for regulating the morphogenesis and function of tissues and organs, including the development of kidneys.

We investigated genes whose expression was decreased in the RNA-seq analysis of the E13.5 or E17.5 kidneys that were in common with RNA-seq data from the mouse epithelial cell samples. No common genes were observed in the data from E17.5 kidneys and mouse epithelial cells. However, we found that three genes were downregulated in both E13.5 kidney and mouse epithelial cell analyses (Figure 16C): *Pappa2*, *Acta2*, and *Tagln*. Collectively, these genes have been associated with kidney development and function (Mohrin et al., 2021; Kumar et al., 2020; Schildmeyer et al., 2000; Y. Ding et al., 2021) and represent promising regulatory targets for embigin during the early stages of kidney formation.

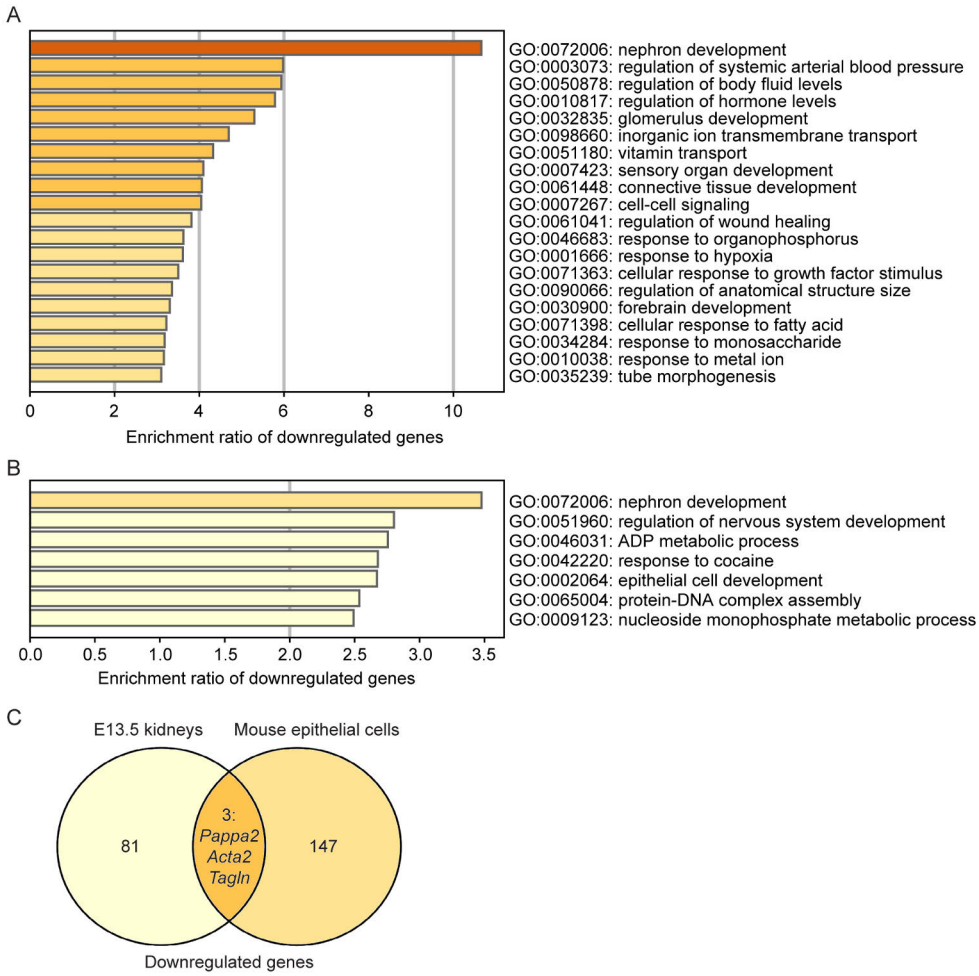

Figure 16. Embigin regulates *Pappa2*, *Acta2*, and *Tagln* genes during early kidney development. A-B. The over-representations of downregulated genes in Emb$^{-/-}$ vs. WT kidneys at E13.5 (A) and in Emb1 siRNA-treated vs. negative control siRNA-treated mouse epithelial cells (B) were analyzed from RNA-seq data using Metascape. The top 20 (A) or the top 7 (B) most enriched biological processes with p-values < 0.01 and ≥3 overlapping genes are shown. **C.** The downregulated genes shared between the RNA-seq results of the E13.5 kidneys and the mouse epithelial cells were compared using Venny. The *Pappa2*, *Acta2*, and *Tagln* genes, critical for kidney development and function, were downregulated in both results (embigin knockout/knockdown vs. control). E, embryonic day. Adapted from Figures 3 and 5 of Study III.

4.4.3 Embigin is present in the kidney primordium

In Study I, we found that embigin function is crucial in early primordium stem cells in embryonic lungs. Hence, we also wanted to study embigin expression in early mouse kidneys. When we reanalyzed single-cell RNA sequencing (scRNA-seq) data (Sanchez-Ferras et al., 2021), obtained from mouse Pax2-expressing renal cells at E8.75 and from the caudal urogenital system cells (containing the caudal nephric duct, the UB, the surrounding mesenchyme, and the cloaca) at E11.5, embigin showed expression in both time points at E8.75 and E11.5 (III, Supplementary Figure 3A-3D). Thus, embigin seems to be present in the kidneys from the pro/mesonephros stages, i.e., the kidney primordium, starting at E8.75 (Sanchez-Ferras et al., 2021).

In theory, basigin could compensate for the absence of embigin in the kidneys of $Emb^{-/-}$ mice. From the reanalysis of the scRNA-seq data (Sanchez-Ferras et al., 2021), we detected basigin in the mouse Pax2-expressing renal cells at E8.75 and the caudal urogenital system cells at E11.5 (III, Supplementary Figure 3C-3D). Notably, the majority of the cells that show embigin expression also express basigin.

Silencing of embigin in mouse epithelial cells led to the downregulation of central kidney genes that were not downregulated in E13.5 $Emb^{-/-}$ kidneys, including *Npnt*. Our reanalysis of the scRNA-seq data (Sanchez-Ferras et al., 2021) obtained from the mouse caudal urogenital system at E11.5 revealed that some of the cells of the epithelial cell-type cluster also expressed both embigin and *Npnt* (III, Supplementary Figure 4A). The *Npnt* gene codes for nephronectin, which plays a crucial role in the induction of the metanephric kidney governed by Pax2/8-Gata3-Lim1-network in the renal primordium (Boualia et al., 2013; Marcotte et al., 2014). Lim1, encoded by gene *Lhx1*, is a central protein regulating kidney primordial morphogenesis and nephronectin expression (Boualia et al., 2013; Kobayashi et al., 2005). Strikingly, the reanalysis of scRNA-seq data (Sanchez-Ferras et al., 2021) obtained from mouse Pax2-expressing renal cells at E8.75 and from the caudal urogenital system cells at E11.5 showed partial co-expression of embigin with *Lhx1* in the epithelial cell-type cluster (III, Supplementary Figure 4B-4C).

Additionally, the scRNA-seq data (Sanchez-Ferras et al., 2021) obtained from mouse Pax2-expressing renal cells at E8.75 and from the caudal urogenital system cells at E11.5 were analyzed for embigin and MCT1 (gene *Slc16a1*) expression. Interestingly, some of the cells of the epithelial cell-type cluster expressed both embigin and *Slc16a1* (III, Supplementary Figure 5A-5B).

5 Discussion

Embigin (Gp70) is part of the basigin subgroup in the immunoglobulin superfamily, which also includes basigin (CD147/EMMPRIN) and neuroplastin (Np65/Gp65 and Np55/Gp55). These three proteins share structural and functional similarities. They all play a role in facilitating the transport of MCTs to the plasma membrane (Wilson et al., 2005; Halestrap, 2013b; Skiba et al., 2021; Xu et al., 2022; Higuchi, 2022; Cheng, Liu, Gao, Zhu, et al., 2025; Cheng, Liu, Gao, Xin, et al., 2025), and embigin and basigin may influence the function of integrin-type cell adhesion receptors (R.-P. Huang et al., 1993; Muramatsu, 2016). Additionally, our previous studies have demonstrated that embigin can function as a receptor for the ECM by binding directly to fibronectin (Sipilä et al., 2022). Thus, the basigin family proteins may link the regulation of cellular metabolism to cell adhesion processes. However, the exact role of these proteins in physiological functions related to development and tissue formation is still not fully understood.

5.1 Where is embigin protein expressed in mice?

Previous knowledge of embigin expression has primarily relied on analyzing mRNA levels in mouse embryos (R.-P. Huang et al., 1990; Fan et al., 1998) and various adult mouse and rat tissues (R.-P. Huang et al., 1990; Guenette et al., 1997). Therefore, we aimed to characterize embigin protein expression during embryonic development and in adult mice. Notably, we confirmed the specific function of the mouse embigin antibody using $Emb^{-/-}$ mice. Based on our findings, the embigin protein expression was high in mouse embryonic development until E10.5, after which it decreased significantly. These results are approximately in line with previous embigin expression studies at the mRNA level, suggesting that embigin levels fall after E9 (R.-P. Huang et al., 1990; Fan et al., 1998). We observed that the embigin protein was widely expressed in the developing mouse embryo, especially in the developing gut, where expression of embigin mRNA has also been previously observed (Fan et al., 1998). Our results indicated that lower levels of embigin protein remained present in some specific organs, mainly kidneys, at E13.5 and E17.5. Interestingly, we also found that embigin is present in the labyrinthine layer of the placenta at E11.5 and E17.5, and the expression seems to increase as gestation

progresses. Based on embigin protein expression, embigin likely has a role during early mouse development and possibly in the placenta.

Using immunofluorescence stainings, we found embigin protein expression in the epithelium of tubular structures of the kidneys, lungs, sebaceous glands, and epididymis in adult mice. Previous studies have reported that embigin mRNA is expressed in various tissues of mice and rats (R.-P. Huang et al., 1990; Guenette et al., 1997), which is in line with our results in mice, except for the spleen, heart, liver, and ovaries, where we did not detect expression at the protein level.

In the lungs, we found that embigin expression varies depending on mouse age. Based on our analysis of the MOSTA scRNA-seq data (Chen et al., 2022), embigin was highly expressed during the early stages of lung development, specifically in the lung primordium. However, the expression levels declined as development progressed. Similarly, our immunofluorescence stainings and western blot analysis showed very low levels of embigin protein expression in E13.5 and E17.5 lungs. Notably, shortly after birth (P3), the expression level of embigin increased in epithelial cells of the lung bronchioles, reaching its peak in adult mice.

In the kidneys, we observed that embigin protein expression is more continuous across different age points: the tubular structures of mouse kidneys showed expression from early development to adulthood. More specifically, at P3, embigin was found to be present in the epithelium of collecting ducts and distal tubules in the kidneys. Besides, based on a reanalysis of scRNA data (Sanchez-Ferras et al., 2021), we found that embigin is present at the pro/mesonephros stage, i.e., the kidney primordium, which starts around E8.5 (Sanchez-Ferras et al., 2021).

Furthermore, embigin expression was observed in sebaceous glands of the skin, which we also reported in (Sipilä et al., 2022). Previously, embigin has been localized only in the transition zone between corpus and cauda in the epididymis, while the distal cauda remained embigin-negative (Mannowetz et al., 2012). However, we detected intense protein expression also in the epithelium of the caudal pole of the epididymis. In the western blot analysis of mouse testis, we also found a significant signal, indicating the presence of embigin in the tissue. However, our focus was on examining the lungs and kidneys in Studies I and III.

5.2 When and why are most of the embigin-deficient mice lost?

We found that the lack of embigin protein leads to significantly increased mortality (72%) in C57BL/6N mice. Our findings indicated that the first days after birth appear to be the most critical for the survival of the $Emb^{-/-}$ mice, as the majority of $Emb^{-/-}$ pups died during this neonatal period. Nevertheless, some $Emb^{-/-}$ mice may have already been lost during gestation and potentially during birth.

Some Emb$^{-/-}$ mice can survive to adulthood, although there is a significant rise in prenatal and neonatal mortality. The Emb$^{-/-}$ mice that survive past the neonatal period develop normally and are fertile. We can speculate that an adequate gestation duration, the period from conception to birth, is crucial for the survival of Emb$^{-/-}$ mice. We observed that Emb$^{-/-}$ embryos are smaller than WT embryos during development. Thus, the entire developmental process in Emb$^{-/-}$ embryos appears to be delayed. This overall growth retardation during embryonic development partly explains the mortality of Emb$^{-/-}$ mice. Thus, we investigated the placentas of Emb$^{-/-}$ and WT embryos, considering the high expression of embigin in threin and its role in fetal growth. However, we found no significant differences between the two genotypes. Therefore, embigin deficiency probably does not cause a placental dysfunction, which could explain growth restrictions or mortality of embryos.

To find out the cause of the increased mortality of the Emb$^{-/-}$ mice in terms of organ development, in Study I, we focused our research on the developing Emb$^{-/-}$ lungs, where structural abnormalities were the most evident in histological stainings. The compromised lung maturity primarily explained the high neonatal mortality of the newborn Emb$^{-/-}$ pups. In E17.5 Emb$^{-/-}$ mice, the number and the size of the small airways and distal airspace were significantly smaller. In P0 Emb$^{-/-}$ pups, these structures were still smaller than in WT pups, albeit the difference was not as evident as in E17.5 lungs. Notably, the Emb$^{-/-}$ lungs showed less peripheral branching already at E12.5. In addition, our RNA-seq analysis indicated that several genes related to cell proliferation were upregulated in the Emb$^{-/-}$ lungs at E17.5. This elevated cell proliferation, confirmed by Ki67 staining, indicated that at E17.5, the Emb$^{-/-}$ lungs were still in the late canalicular stage, whereas the WT lungs had already progressed to the subsequent saccular stage of lung maturation. The delay in lung development in E17.5 Emb$^{-/-}$ embryos was further verified by the fewer pulmonary ATI and ATII cells in the alveolar epithelium. ATI cells are essential for gas exchange and barrier function in the lungs, and ATII cells serve as progenitor cells responsible for regenerating ATI cells and secreting surfactant proteins (Ruaro et al., 2021). Additionally, the Emb$^{-/-}$ lungs at E18.5 showed smaller lamellar bodies, which are storage organelles for pulmonary surfactant found in ATII cells. Finally, we observed that alkaline phosphatase activity in the amniotic fluid was lower in E17.5 Emb$^{-/-}$ embryos. Overall, it seems that the development of Emb$^{-/-}$ lungs is rather delayed than defective. This developmental delay is likely one of the major causes for the death of most newborn Emb$^{-/-}$ pups.

We noticed that embigin protein expression is very high in the primitive gut during early mouse development. Many key organs originate from the primitive gut, including the lungs. Lung development in mice begins around E9.0-E9.5 when the trachea and two lung buds start to arise in the primitive foregut (Langhe et al., 2006; Bogue et al., 2012; Herriges & Morrisey, 2014). As noted, our analysis of the

MOSTA scRNA-seq data (Chen et al., 2022) showed high embigin expression in the lung primordium, and later its expression declined. Thus, it is improbable that embigin directly regulates cellular functions during the canalicular and saccular stages of lung development. Therefore, embigin function is most likely essential at the embryonic or early pseudoglandular stage of lung development, leading to delayed branching morphogenesis and alveolar cell maturation observed at later stages of development.

During the same time as our Study I was published, it was reported that the loss of embigin in the C57BL/6NTac mice leads to decreased viability, accelerated hearing loss, and narrowing of the brain ventricles and cardiac interventricular septum defects (Newton et al., 2023). Like us, they used a DNA targeting construct resulting in an embigin knockout mouse lacking exon 5. However, we did not observe evident cardiac defects in histological staining of the hearts of $Emb^{-/-}$ embryos or adults, nor did we detect expression of the embigin protein in the heart during development or in adult mice. Nevertheless, $Emb^{-/-}$ mice may have some heart defects that our study did not detect. Secondly, embigin appears to be strongly expressed in the brain region during early embryonic development, so $Emb^{-/-}$ mice may have some brain defects. On the other hand, we did not observe any behavioral abnormalities in our surviving mice, so the effects are at least mild or temporary. The C57BL/6N mouse strain includes several substrains, and genetic drift can result in the formation of a new substrain when a closed mouse colony is isolated from the original inbred strain (Newton et al., 2025). This may also explain variations in research results. Therefore, it is crucial to consider the genetic background and variations of the mouse strains used in scientific studies.

In addition, embigin appears to have a genetic interaction with cadherin 23 (gene: *Cdh23*) (Newton et al., 2023). The mice derived from the C57BL/6 background carry the $Cdh23^{ahl}$ allele, which has a single nucleotide change resulting in progressive hearing loss. When this allele was repaired, the embigin knockout C57BL/6NTac mice displayed normal viability, hearing, and morphology of the heart and brain. Therefore, the $Cdh23^{ahl}$ allele seems to impact more than just hearing in these mice. Repairment of this allele could also affect the survival of our $Emb^{-/-}$ C57BL/6N mice. However, the presence of the $Cdh23^{ahl}$ allele did not seem to affect the embigin expression (Newton et al., 2023). Overall, the genetic interaction between embigin and cadherin 23 could be further investigated.

Furthermore, a very recent study utilized C57BL/6J strain mice to create an embigin knockout model by targeting exon 3 (Z. Li et al., 2025). They also generated embigin knockout zebrafish, and in both models, the majority of $Emb^{-/-}$ individuals died during or shortly after birth, which aligns with our results. In zebrafish larvae, they suggested that impaired intestinal function might be responsible for the observed lethality. In mice, the loss of embigin disrupted enteric nervous system

development, leading to a Hirschsprung disease-like phenotype, a congenital disorder in which the intestine lacks nerve cells. In our Study I, we demonstrated that embigin protein is highly expressed in the developing gut. Thus, embigin may play a role in the development of several organs that arise from the primitive gut, including early gastrointestinal development.

In Study III, we observed that embigin also has a role during mouse kidney morphogenesis. During lung development, embigin expression was at its highest in the lung primordium, making it challenging to study the molecular mechanisms of embigin. By contrast, we found that embigin protein is expressed throughout mouse kidney development. We observed embigin expression in the kidney primordium starting from E8.75. Therefore, the function of embigin may also be essential for supporting primordial kidney stem cells. Besides, we discovered that embigin protein expression is strong in the epithelial UB and differentiating nephron precursors during mouse kidney development. As noted, embigin is localized in the epithelial cells of the kidney tubular structures. A previous study has found a correlation between elevated levels of embigin expression and the formation of tubular structures in developing rat prostate glands (Guenette et al., 1997). We thus investigated embigin's role in branching morphogenesis in kidney development by examining UB branching by analyzing tip formation in the early stages of mouse kidney development. After culturing isolated E11.5 kidneys for 48 h, we observed a significant impairment in UB branching in $Emb^{-/-}$ kidneys compared with WT kidneys, suggesting that embigin may be involved in early morphogenesis of kidney branching.

The RNA-seq analysis of kidneys from E13.5 $Emb^{-/-}$ embryos revealed decreased expression levels of several genes associated with especially nephron development, such as *Nphs1* and *R3hdml*. The *Nphs1* gene codes for nephrin, a protein found in podocytes, highly specialized epithelial cells located in the glomerulus of kidney nephrons that envelop capillaries (Kestilä et al., 1998; Putaala et al., 2001). Nephrin is essential for both the formation and function of the glomerular filtration barrier (Putaala et al., 2001). The *R3hdml* gene encodes R3h domain containing-like (R3hdml) protein, which also shows podocyte-specific expression during renal development and has an important role in glomerular development (Ishikawa et al., 2021). Downregulation of these genes suggests that podocyte development is delayed in the $Emb^{-/-}$ kidneys. In the analysis of RNA-seq data from E17.5 $Emb^{-/-}$ kidneys, we did not find statistically significant changes in the expression of the same genes that were downregulated in E13.5 $Emb^{-/-}$ kidneys. This suggests that the transcriptional changes of $Emb^{-/-}$ kidneys align with the WT kidneys at later developmental stages. It also appears that the kidney function is normal in surviving $Emb^{-/-}$ mice, as no significant morphological abnormalities were observed in the

E17.5 or adult Emb$^{-/-}$ kidneys, and we found no signs of albuminuria in either newborn or adult Emb$^{-/-}$ mice.

To investigate the general regulatory role of embigin in epithelial cells, we analyzed embigin-silenced mouse epithelial cells by RNA-seq. Our findings indicated that the absence of embigin significantly influences the expression of genes involved in the morphogenesis of tissues and organs, particularly in kidney development, tube morphogenesis, and epithelial cell development. However, the silencing of embigin in mouse epithelial cells led to an increase in the expression of 439 genes, which contrasts significantly with the RNA-seq results of the E13.5 kidneys. This discrepancy may be associated with the distinct origins of the samples. Because embigin is present in the renal primordium, differential regulation of certain critical embigin-related genes may no longer be present in E13.5 kidneys. Thus, silencing embigin in epithelial cells could affect vital kidney genes that remain unchanged in E13.5 Emb$^{-/-}$ kidneys. *Npnt* was found to be downregulated in embigin-silenced mouse epithelial cells. The *Npnt* gene codes for nephronectin, which has a significant role in the induction of metanephric kidneys (Boualia et al., 2013; Marcotte et al., 2014), and its deficiency in mice often leads to kidney agenesis due to delayed UB invasion (Linton et al., 2007). Nephronectin is regulated by Lim1, encoded by the *Lhx1* gene (Boualia et al., 2013), which is a key regulator of primordial kidney morphogenesis (Kobayashi et al., 2005; Marcotte et al., 2014). Notably, the reanalysis of scRNA-seq data (Sanchez-Ferras et al., 2021) revealed that some renal cells express embigin and *Npnt* in the epithelial cell-type cluster at E11.5 and embigin and *Lhx1* in the epithelial cell-type cluster at E8.75 and E11.5. In conclusion, embigin might have a role in renal lineage specification.

As noted, embigin protein expression is not limited to the gestational period; it is also present in the tubular structures of adult mouse tissues. In adult mouse lungs, embigin expression was found in stem-like club cells, which are progenitor cells lining the bronchioles (Rawlins et al., 2009). Given the normal morphology observed in adult Emb$^{-/-}$ lungs, the potential role of embigin in adult lungs may be linked to the activation of stem cells, particularly after tissue injury, rather than directly contributing to lung function. In the kidneys, embigin expression was found in the distal tubules and collecting ducts. The kidneys seem to function normally in the surviving Emb$^{-/-}$ mice. Nevertheless, the high expression levels of embigin in the epithelium of tubular structures of the lungs and kidneys suggest that its function could be uncovered if the Emb$^{-/-}$ mice were challenged.

The surviving Emb$^{-/-}$ mice may have developed some compensatory mechanism, which could explain the mild and variable phenotype observed in these mice. For example, basigin may partially compensate for the absence of embigin. However, the effects of basigin knockout on mortality differ from those seen in Emb$^{-/-}$ mice: approximately 70% of Bsg$^{-/-}$ embryos die during the early stages of embryonic

development, and about half of the surviving mice develop interstitial pneumonia and die within the first month of life, although some $Bsg^{-/-}$ individuals manage to reach adulthood (Igakura et al., 1998). In contrast, $Emb^{-/-}$ mice show better survival rates, with 28% living beyond birth compared to only 14% of $Bsg^{-/-}$ mice. We did not observe significant differences in basigin expression levels in the RNA-seq analysis or the immunostaining of the E17.5 lungs. Furthermore, the embigin deficiency did not elevate basigin mRNA levels in E13.5 or E17.5 kidneys based on RNA-seq analysis. However, our reanalysis of scRNA-seq data (Sanchez-Ferras et al., 2021) indicated that most of the embigin-positive renal cells also expressed basigin at E8.75 and E11.5, suggesting that basigin may partially compensate for the lack of embigin in $Emb^{-/-}$ mice.

5.3 How might embigin function during embryonic development?

The information about the role of embigin in cellular functions is gradually advancing. Embigin has been connected to the regulation of cancer: in some cancer types, embigin has been reported to act as a suppressor of tumorigenesis (Chao et al., 2015) and in some as a promoter (Jung et al., 2016; Ruma et al., 2018; Cheng, Liu, Gao, Zhu, et al., 2025; Peng et al., 2025). Embigin is expressed in various immune cells (Pridans et al., 2008; DePaula-Silva et al., 2019; Yang et al., 2024; Torcellan et al., 2024; Cheng, Liu, Gao, Xin, et al., 2025). Moreover, embigin is involved in stem and progenitor cell regulation in adult mice (Silberstein et al., 2016; Sipilä et al., 2022; Mohamad et al., 2024). Embigin has also been recognized as a mediator of cell adhesion (R.-P. Huang et al., 1993; Sipilä et al., 2022). Importantly, embigin has been linked to assisting many MCTs (Wilson et al., 2005; Halestrap, 2013b; Skiba et al., 2021; Xu et al., 2022; Higuchi, 2022; Cheng, Liu, Gao, Zhu, et al., 2025; Cheng, Liu, Gao, Xin, et al., 2025). However, embigin function during mouse embryonic development has remained obscure.

We found that the $Emb^{-/-}$ lungs and kidneys were significantly smaller than WT, and both the $Emb^{-/-}$ lungs and kidneys exhibited signs of developmental delays in mice. However, the whole $Emb^{-/-}$ embryos were smaller than WT embryos, which may suggest a general growth defect in $Emb^{-/-}$ mice. Moreover, embigin expression was observed at its highest level during early embryogenesis. Thus, the main effects of embigin deficiency might occur during the early phases of mouse development, possibly affecting the lung and kidney primordia. Increasing evidence suggests that embigin plays a crucial role in stem and progenitor cell function in adult mice. Embigin has been associated with the regulation of stem cell niches in the bone marrow (Silberstein et al., 2016) and progenitor cell regulation in the sebaceous gland (Sipilä et al., 2022). Recent findings indicate that embigin also participates in

the hematopoietic function of osteomac-type macrophages (Mohamad et al., 2024). We have also identified embigin in stem-like club cells that line the bronchioles of adult mouse lungs. Therefore, our findings proposing that embigin may play a role in both lung and kidney primordia align with the idea that embigin assists specific stem cells in both adult tissues and during embryonic development.

Embigin has been connected to cell adhesion regulation, particularly acting as an ECM receptor by binding to a specific domain in fibronectin (Sipilä et al., 2022) and potentially enhancing the function of integrin-mediated cell-substratum adhesion (R.-P. Huang et al., 1993). According to the MOSTA scRNA-seq data, embigin maintains a relatively high expression level in the lung primordium until E12.5. Following a 48-hour culture of E12.5 lung explants, we observed fewer peripheral branching buds in the $Emb^{-/-}$ lungs than in WT lungs. Fibronectin, an important factor in lung branching morphogenesis, is found around these lung buds (De Langhe et al., 2005; Roman & McDonald, 2012; Varner & Nelson, 2014). Interestingly, according to MOSTA scRNA-seq data, fibronectin shows higher expression in primordial lungs than during later developmental stages. Furthermore, we found strong embigin expression in the epithelial UB and differentiating nephron precursors. Fibronectin appears to be highly expressed in the ECM around the UB during kidney development, where it plays a critical role in kidney branching morphogenesis (Sakai et al., 2003) and promotes UB branching through its interaction with integrins (Ye et al., 2004). Thus, it is possible that embigin modulates cell-ECM interactions through fibronectin during lung and kidney development.

Embigin may also participate in the regulation of cellular metabolism, as previous studies have connected embigin to facilitate the function of several MCTs: MCT1, MCT2, MCT4, and MCT7 (Wilson et al., 2005; Halestrap, 2013b; Skiba et al., 2021; Xu et al., 2022; Higuchi, 2022; Cheng, Liu, Gao, Zhu, et al., 2025; Cheng, Liu, Gao, Xin, et al., 2025). Besides, we have demonstrated that embigin appears to regulate MCT1 localization in the sebaceous gland (Sipilä et al., 2022). Based on data from MOSTA scRNA-seq, MCT1 and MCT4 have higher expression levels in primordial lungs than lung cells during later developmental stages, suggesting that embigin might regulate these proteins in the primordial lungs. In addition, MCT1 is known to be present in the kidneys of adult mice (Becker et al., 2010). In kidney tubule epithelial cells, MCT1 contributes to the reabsorption of lactate, pyruvate, and ketone bodies (Halestrap, 2013a). The expression of MCT1 during early mouse embryonic kidney development has been unclear. Our reanalysis of the scRNA-seq data (Sanchez-Ferras et al., 2021) revealed that MCT1 is expressed in the kidney primordium at E8.75 and E11.5, and it is partially co-expressed with embigin in epithelial-type cells. Thus, MCT1 might be partly dependent on embigin during kidney development.

In Study III, we identified three genes, *Pappa2*, *Acta2*, and *Tagln*, that were downregulated in both E13.5 Emb$^{-/-}$ kidneys and mouse epithelial cells that were embigin-silenced. Consequently, the expression levels of these genes appear to be directly linked to embigin expression. The *Pappa2* gene codes for the pregnancy-associated plasma protein A2 (PAPP-A2), a secreted metalloprotease that enhances the availability of insulin-like growth factor (IGF) (Mohrin et al., 2021). Importantly, IGFs are essential for normal growth and development, including for pre- and postnatal kidney morphogenesis (Bach & Hale, 2015). Interestingly, similar to embigin in mice, PAPP-A2 is found in the UB of embryonic rat kidneys (Kumar et al., 2020). *Acta2* is responsible for producing alpha smooth muscle actin (α-SMA), a protein expressed in smooth muscle cells. While the absence of α-SMA in mice does not hinder normal developmental processes, it does compromise vascular contractility, leading to hypotension (Schildmeyer et al., 2000). Additionally, *Tagln* is predominantly expressed in smooth muscle cells as well (Tsuji-Tamura et al., 2021), with its protein product, transgelin, playing a significant role in the progression of proteinuria and the dynamics of podocyte foot process (Y. Ding et al., 2021). Furthermore, PAPP-A2, α-SMA, and transgelin have been associated with cell migration (Wang et al., 2016; Shinde et al., 2017; H. Yu et al., 2008), a process reliant on cell-ECM interactions. Notably, embigin also has a role in cell adhesion. Altogether, these genes are related to kidney development and function, indicating they possibly serve as potential regulatory targets for embigin during early kidney morphogenesis.

6 Conclusions

Firstly, we clarified the embigin protein expression during mouse embryonic development and in adult mice. We observed that embigin expression is high at early mouse embryogenesis until E10.5, including during the initiation of lung and kidney organogenesis, known as the primordium. Additionally, embigin expression was noted in the placental labyrinth. As development progresses, especially in the lungs, embigin expression appears to decline; however, it increases again after birth. In adult mice, embigin is present in the epithelium of tubular structures of the lungs, kidneys, epididymis, and sebaceous glands of the skin.

We created an embigin knockout ($Emb^{-/-}$) mouse model and found that these mice exhibit high neonatal mortality. $Emb^{-/-}$ mice have delayed lung maturation, which primarily explains their mortality. In particular, the onset of lung organogenesis is impaired in $Emb^{-/-}$ embryos. However, our findings indicate that embigin is not essential for specific cellular functions during the later stages of lung cell differentiation. Instead, the overall developmental process of $Emb^{-/-}$ embryos appears to be delayed, as the $Emb^{-/-}$ embryos are smaller compared to WT embryos. Given the high expression of embigin from early embryogenesis to the formation of the lung primordium, it seems that embigin's primary effects occur during the early stages of mouse development. Thus, the delay in the onset of lung development may be due to altered behavior of lung primordial cells in $Emb^{-/-}$ embryos.

Our research also indicated that the absence of embigin in mice impacts cellular behavior from the early stages of kidney development. In early kidney development, embigin protein is highly expressed in the ureteric bud (UB) and differentiating nephron precursors. $Emb^{-/-}$ embryos displayed delayed branching of the UB and downregulation of nephron development-related genes during this early stage. However, this delay in kidney development appeared to be temporary, as no significant morphological differences were detected later. *Pappa2*, *Acta2*, and *Tagln* genes, which are essential for kidney development and function, were associated with embigin expression, suggesting that embigin may directly regulate these genes. Finally, embigin was identified in the kidney primordium, indicating that it may support primordial kidney stem cells and play a role in renal lineage specification.

The exact function of embigin in adult tissues remains unclear, as the major organs of $Emb^{-/-}$ mice show normal morphology. However, the high levels of embigin expression in tubular structures of the mouse lungs and kidneys suggest that the function of embigin could be revealed if the $Emb^{-/-}$ mice were challenged. Additionally, the mild and variable phenotype observed in surviving $Emb^{-/-}$ mice could result from partial compensation by basigin. Notably, embigin is detected in stem-like club cells in adult mouse lungs, supporting the idea that embigin plays a role in stem cell regulation.

The central results of this thesis and the possible functions of embigin are summarized in Figure 17. In summary, our findings suggest that embigin plays a supportive role for tissue-specific stem cells during early embryogenesis. We hypothesize that the biological function of embigin is to enhance stem cell activities during both embryonic development and in adult mice, particularly concerning cell-ECM interactions, as embigin has been identified to bind to fibronectin. Previous studies have also linked embigin to support various MCT proteins, which participate in cellular metabolism. Interestingly, primordial lungs seem to express MCT1, MCT4, and fibronectin at the mRNA level. Besides, in the developing kidneys, embigin expression appears to be surrounded by fibronectin expression. Additionally, MCT1 is expressed in the kidney primordium, partially co-expressing with embigin. Therefore, the interactions of embigin with MCTs and fibronectin could be further studied in mouse embryos.

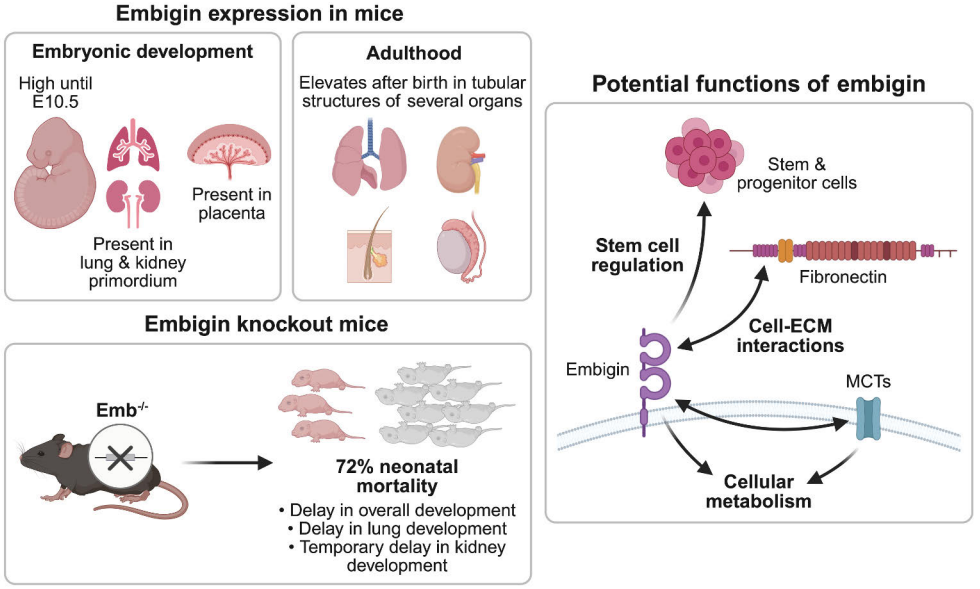

Figure 17. Summary of the main results of the thesis and the likely functions of embigin. Embigin is expressed highly and broadly in mouse embryos until E10.5. Embigin is also present in the lung and kidney primordium, proposing that embigin may play a role in them. In addition, embigin is expressed in the placental labyrinth. During later stages of development, particularly in the lungs, the expression of embigin declines. After birth, its expression increases. In adult mice, embigin is found in the epithelial cells of tubular epithelial structures in the lungs, kidneys, epididymis, and sebaceous glands of the skin. Embigin deficiency causes 72% mortality in newborn Emb$^{-/-}$ pups. Delayed lung development and general underdevelopment of the mice are the most likely causes of their death. Besides, embigin deficiency temporarily affects early kidney development. Our results and others' previously published results suggest that embigin supports tissue-specific stem cells both during embryonic development and in adult mice. Moreover, the function of embigin has been connected to mediating cell-ECM interactions, particularly through fibronectin. The embigin-fibronectin interaction may also be present during early lung and kidney development. Furthermore, increasing evidence suggests that embigin assists monocarboxylate transporters (MCTs) and thus embigin may influence cellular metabolism, possibly during development. E, embryonic day; Emb$^{-/-}$, embigin knockout; MCTs, monocarboxylate transporters. Created with BioRender.com.

Acknowledgements

This doctoral thesis work was carried out in the Interaction of Cells with Extracellular Matrix group at the Department of Life Technologies, Faculty of Technology, University of Turku. The work was conducted in BioCity, Turku, utilizing the facilities and equipment provided by the Department of Life Technologies, the MediCity Research Laboratory, the Central Animal Laboratory of the University of Turku, and the Cell Imaging and Cytometry Core of Turku Bioscience Centre. The AI-powered Grammarly writing assistant was used for language checking and improvement in this dissertation.

The work has been financially supported by several organizations, including the Research Council of Finland, the Research Council of Finland's Flagship InFLAMES, the Sigrid Jusélius Foundation, the Cancer Foundation Finland, the Finnish Foundation for Cardiovascular Research, the Orion Research Foundation, the K. Albin Johansson Stiftelse, the Ella and Georg Ehrnrooth Foundation, the Emil Aaltonen Foundation, the Finnish Cultural Foundation, and the Instrumentarium Science Foundation. I am extremely grateful to the Doctoral Programme in Technology (formerly the Doctoral Programme in Molecular Life Sciences) for the research and travel grants awarded to me and to the InFLAMES Research Flagship for accepting me for the InFLAMES doctoral module.

I would like to acknowledge the Director of the Department of Life Technologies, Prof. Paula Mulo, and the former Director of the department, Prof. Jyrki Heino, for their leadership. I am sincerely grateful to my principal supervisor, Jyrki, for all the opportunities and guidance over the years. Your wisdom and passion for this project have been truly inspiring. I also extend my gratitude to my other supervisors, Dr. Johanna Jokinen and Accoc. Prof. Pia Rantakari, for their knowledge and support, teaching of various techniques, and assistance in conducting experiments.

I would like to thank Docent Ulla Pirvola and Docent Keijo Viiri for reviewing this thesis. I am deeply grateful to Prof. Seppo Vainio for agreeing to be my opponent in the doctoral dissertation. I would also like to express my gratitude to the members of the advisory committee, Prof. Lea Sistonen and Prof. Noora Kotaja, for their wisdom and advice throughout this work.

I am very thankful for our scientific collaborators for their support in this work, and I would especially like to thank Docent Satu Kuure for her contributions to our kidney collaboration. I would also like to express my gratitude to Prof. Matti Poutanen and Docent Fu-Ping Zhang for their assistance in creating the embigin knockout mouse model. My appreciation extends to the personnel of the Turku Center for Disease Modeling and the Central Animal Laboratory of the University of Turku. I acknowledge Etta-Liisa Virtomaa, Heidi Gerke, and Agnés Viherä for their technical support. Additionally, I wish to thank Henok Karvonen for filming and editing the lung isolation video.

I am very grateful for the support, assistance, and companionship of both current and former members of the Heino group: Docent Pekka Rappu, Docent Elina Siljamäki, Docent Jarmo Käpylä, Maria Tuominen, Dr. Ujjwal Suwal, Liisa Pösö, Emmi Virtanen, Sajad Rahmani, Dr. Kalle Sipilä, Roni Leppäkoski, Anna-Brita Puranen, Dr. Marjaana Ojalill, and Dr. Maria Salmela. I also want to thank the former and current members of Elenius and Kurppa labs: Johannes, Marika, Katri, Veera, Anne, Meija, Mari, Meri, Iman, Kamal, Farid, Nikol, Zejia, Mahtab, and Sara. My gratitude also goes to many others from the Department of Life Technologies and the MediCity Research Laboratory for their assistance. Controller Satu Jasu deserves special acknowledgement for helping me navigate numerous administrative issues.

Throughout this journey, I have shared many joyful moments with my study friends from the Biostanists and Polvivammaiset groups: Marjaana, Noora, Milla, Satu, Janne, Topi, Suski, and Annis. I want to thank my parents, Jaana and Heikki; my sister Jenni and her spouse Petteri; and my parents-in-law, Marja and Jouni, for their unwavering support throughout this process. I am also grateful to my late grandparents, Alli and Mauri, for always encouraging me to study and explore the world. Most importantly, my precious dog Mörkö has provided me with unconditional love, companionship, and mental support. Finally, I would like to thank my dear husband Mikko for his support on this journey and for finding us a dream home, sustaining us financially, preparing delicious meals, and being there through all the ups and downs.

Tarvasjoki, October 2025
Salli Talvi

References

Alberts, B., Johnson, A., Lewis, J., Raff, M., Roberts, K., & Walter, P. (2002). The Mouse. In *Molecular Biology of the Cell. 4th edition*. Garland Science. https://www.ncbi.nlm.nih.gov/books/NBK26939/

Altruda, F., Cervella, P., Lou Gaeta, M., Daniele, A., Giancotti, F., Tarone, G., Stefanuto, G., & Silengo, L. (1989). Cloning of cDNA for a novel mouse membrane glycoprotein (gp42): Shared identity to histocompatibility antigens, immunoglobulins and neural-cell adhesion molecules. *Gene*, *85*(2), 445–451. https://doi.org/10.1016/0378-1119(89)90438-1

Amuti, S., Tang, Y., Wu, S., Liu, L., Huang, L., Zhang, H., Li, H., Jiang, F., Wang, G., Liu, X., & Yuan, Q. (2016). Neuroplastin 65 mediates cognitive functions via excitatory/inhibitory synapse imbalance and ERK signal pathway. *Neurobiology of Learning and Memory*, *127*, 72–83. https://doi.org/10.1016/j.nlm.2015.11.020

Aspal, M., & Zemans, R. L. (2020). Mechanisms of ATII-to-ATI Cell Differentiation during Lung Regeneration. *International Journal of Molecular Sciences*, *21*(9), 3188. https://doi.org/10.3390/ijms21093188

Avgustinova, A., & Benitah, S. A. (2016). Epigenetic control of adult stem cell function. *Nature Reviews Molecular Cell Biology*, *17*(10), 643–658. https://doi.org/10.1038/nrm.2016.76

Bach, L. A., & Hale, L. J. (2015). Insulin-like Growth Factors and Kidney Disease. *American Journal of Kidney Diseases*, *65*(2), 327–336. https://doi.org/10.1053/j.ajkd.2014.05.024

Bardot, E. S., & Hadjantonakis, A.-K. (2020). Mouse gastrulation: Coordination of tissue patterning, specification and diversification of cell fate. *Mechanisms of Development*, *163*, 103617. https://doi.org/10.1016/j.mod.2020.103617

Barkauskas, C. E., Cronce, M. J., Rackley, C. R., Bowie, E. J., Keene, D. R., Stripp, B. R., Randell, S. H., Noble, P. W., & Hogan, B. L. M. (2013). Type 2 alveolar cells are stem cells in adult lung. *The Journal of Clinical Investigation*, *123*(7), 3025–3036. https://doi.org/10.1172/JCI68782

Bartman, C. M., Matveyenko, A., & Prakash, Y. S. (2020). It's about time: Clocks in the developing lung. *The Journal of Clinical Investigation*, *130*(1), 39–50. https://doi.org/10.1172/JCI130143

Becker, H. M., Mohebbi, N., Perna, A., Ganapathy, V., Capasso, G., & Wagner, C. A. (2010). Localization of members of MCT monocarboxylate transporter family Slc16 in the kidney and regulation during metabolic acidosis. *American Journal of Physiology-Renal Physiology*, *299*(1), F141–F154. https://doi.org/10.1152/ajprenal.00488.2009

Beesley, P. W., Herrera-Molina, R., Smalla, K.-H., & Seidenbecher, C. (2014). The Neuroplastin adhesion molecules: Key regulators of neuronal plasticity and synaptic function. *Journal of Neurochemistry*, *131*(3), 268–283. https://doi.org/10.1111/jnc.12816

Berditchevski, F., Chang, S., Bodorova, J., & Hemler, M. E. (1997). Generation of Monoclonal Antibodies to Integrin-associated Proteins: EVIDENCE THAT α3β1 COMPLEXES WITH EMMPRIN/BASIGIN/OX47/M6*. *Journal of Biological Chemistry*, *272*(46), 29174–29180. https://doi.org/10.1074/jbc.272.46.29174

Bielinska, M., Narita, N., & Wilson, D. B. (1999). Distinct roles for visceral endoderm during embryonic mouse development. *The International Journal of Developmental Biology*, *43*(3), 183–205.

Biswas, C., Zhang, Y., DeCastro, R., Guo, H., Nakamura, T., Kataoka, H., & Nabeshima, K. (1995). The Human Tumor Cell-derived Collagenase Stimulatory Factor (Renamed EMMPRIN) Is a Member of the Immunoglobulin Superfamily1. *Cancer Research*, *55*(2), 434–439.

Bogue, C. W., Lou, L. J., Vasavada, H., Wilson, C. M., & Jacobs, H. C. (2012). Expression of Hoxb genes in the developing mouse foregut and lung. *American Journal of Respiratory Cell and Molecular Biology*. https://doi.org/10.1165/ajrcmb.15.2.8703472

Boualia, S. K., Gaitan, Y., Tremblay, M., Sharma, R., Cardin, J., Kania, A., & Bouchard, M. (2013). A core transcriptional network composed of Pax2/8, Gata3 and Lim1 regulates key players of pro/mesonephros morphogenesis. *Developmental Biology*, *382*(2), 555–566. https://doi.org/10.1016/j.ydbio.2013.07.028

Branchfield, K., Li, R., Lungova, V., Verheyden, J. M., McCulley, D., & Sun, X. (2016). A three-dimensional study of alveologenesis in mouse lung. *Developmental Biology*, *409*(2), 429–441. https://doi.org/10.1016/j.ydbio.2015.11.017

Brocklehurst, D., & Wilde, C. E. (1980). Amniotic fluid alkaline phosphatase, gamma-glutamyltransferase, and 5'-nucleotidase activity from 13 to 40 weeks' gestation, and alkaline phosphatase as an index of fetal lung maturity. *Clinical Chemistry*, *26*(5), 588–591. Scopus. https://doi.org/10.1093/clinchem/26.5.0588

Burgess, R. (2016). *Stem Cells: A Short Course*. John Wiley & Sons.

Caldeira, J., Sousa, A., Sousa, D. M., & Barros, D. (2018). 2—Extracellular matrix constitution and function for tissue regeneration and repair. In M. A. Barbosa & M. C. L. Martins (Eds.), *Peptides and Proteins as Biomaterials for Tissue Regeneration and Repair* (pp. 29–72). Woodhead Publishing. https://doi.org/10.1016/B978-0-08-100803-4.00002-4

Cao, J., Spielmann, M., Qiu, X., Huang, X., Ibrahim, D. M., Hill, A. J., Zhang, F., Mundlos, S., Christiansen, L., Steemers, F. J., Trapnell, C., & Shendure, J. (2019). The single-cell transcriptional landscape of mammalian organogenesis. *Nature*, *566*(7745), 496–502. https://doi.org/10.1038/s41586-019-0969-x

Carraro, G., Moral, P.-M. del, & Warburton, D. (2010). Mouse Embryonic Lung Culture, A System to Evaluate the Molecular Mechanisms of Branching. *Journal of Visualized Experiments (JoVE)*, *40*, e2035. https://doi.org/10.3791/2035

Carroll, J. M., Romero, M. R., & Watt, F. M. (1995). Suprabasal integrin expression in the epidermis of transgenic mice results in developmental defects and a phenotype resembling psoriasis. *Cell*, *83*(6), 957–968. https://doi.org/10.1016/0092-8674(95)90211-2

Carrott, L., Bowl, M. R., Aguilar, C., Johnson, S. L., Chessum, L., West, M., Morse, S., Dorning, J., Smart, E., Hardisty-Hughes, R., Ball, G., Parker, A., Barnard, A. R., MacLaren, R. E., Wells, S., Marcotti, W., & Brown, S. D. M. (2016). Absence of Neuroplastin-65 Affects Synaptogenesis in Mouse Inner Hair Cells and Causes Profound Hearing Loss. *Journal of Neuroscience*, *36*(1), 222–234. https://doi.org/10.1523/JNEUROSCI.1808-15.2016

Carter, A. M. (2016). IFPA Senior Award Lecture: Mammalian fetal membranes. *Placenta*, *48*, S21–S30. https://doi.org/10.1016/j.placenta.2015.10.012

Chao, F., Zhang, J., Zhang, Y., Liu, H., Yang, C., Wang, J., Guo, Y., Wen, X., Zhang, K., Huang, B., Liu, D., & Li, Y. (2015). Embigin, regulated by HOXC8, plays a suppressive role in breast tumorigenesis. *Oncotarget*, *6*(27), 23496–23509. https://doi.org/10.18632/oncotarget.4360

Chen, A., Liao, S., Cheng, M., Ma, K., Wu, L., Lai, Y., Qiu, X., Yang, J., Xu, J., Hao, S., Wang, X., Lu, H., Chen, X., Liu, X., Huang, X., Li, Z., Hong, Y., Jiang, Y., Peng, J., … Wang, J. (2022). Spatiotemporal transcriptomic atlas of mouse organogenesis using DNA nanoball-patterned arrays. *Cell*, *185*(10), 1777-1792.e21. https://doi.org/10.1016/j.cell.2022.04.003

Cheng, B., Liu, J., Gao, L., Zhu, Z., Yang, Y., Liu, S., & Wu, X. (2025). EMB-driven glioblastoma multiforme progression via the MCT4/GPX3 axis: Therapeutic inhibition by Ganxintriol A. *Journal of Translational Medicine*, *23*(1), 272. https://doi.org/10.1186/s12967-025-06290-z

Cheng, B., Liu, S., Gao, L., Xin, N., Shang, Z., Zhu, Z., Yang, Y., Ma, R., Xu, Z., Liu, J., & Wang, D. (2025). Long-Term Minocycline Treatment Exhibits Enhanced Therapeutic Effects on Ischemic

Stroke by Suppressing Inflammatory Phenotype of Microglia Through the EMB/MCT4/STING Pathway. *CNS Neuroscience & Therapeutics*, *31*(3), e70328. https://doi.org/10.1111/cns.70328

Cheung, C. Y., & Brace, R. A. (2005). Amniotic Fluid Volume and Composition in Mouse Pregnancy. *Journal of the Society for Gynecologic Investigation*, *12*(8), 558–562. https://doi.org/10.1016/j.jsgi.2005.08.008

Chuva de Sousa Lopes, S. M., Roelen, B. A. J., Lawson, K. A., & Zwijsen, A. (2022). The development of the amnion in mice and other amniotes. *Philosophical Transactions of the Royal Society B: Biological Sciences*, *377*(1865), 20210258. https://doi.org/10.1098/rstb.2021.0258

Copp, A. J. (2025). Reichert's membrane – A continuing enigma for developmental biologists. *Developmental Biology*, *520*, 75–81. https://doi.org/10.1016/j.ydbio.2025.01.007

Copp, A. J., Clark, M., & Greene, N. D. E. (2023). Morphological phenotyping after mouse whole embryo culture. *Frontiers in Cell and Developmental Biology*, *11*. https://doi.org/10.3389/fcell.2023.1223849

Costantini, F., & Kopan, R. (2010). Patterning a Complex Organ: Branching Morphogenesis and Nephron Segmentation in Kidney Development. *Developmental Cell*, *18*(5), 698–712. https://doi.org/10.1016/j.devcel.2010.04.008

Crosnier, C., Bustamante, L. Y., Bartholdson, S. J., Bei, A. K., Theron, M., Uchikawa, M., Mboup, S., Ndir, O., Kwiatkowski, D. P., Duraisingh, M. T., Rayner, J. C., & Wright, G. J. (2011). Basigin is a receptor essential for erythrocyte invasion by Plasmodium falciparum. *Nature*, *480*(7378), 534–537. https://doi.org/10.1038/nature10606

Dange, M. C., Bhonsle, H. S., Godbole, R. K., More, S. K., Bane, S. M., Kulkarni, M. J., & Kalraiya, R. D. (2017). Mass spectrometry based identification of galectin-3 interacting proteins potentially involved in lung melanoma metastasis. *Molecular BioSystems*, *13*(11), 2303–2309. https://doi.org/10.1039/C7MB00260B

De Langhe, S. P., Sala, F. G., Del Moral, P.-M., Fairbanks, T. J., Yamada, K. M., Warburton, D., Burns, R. C., & Bellusci, S. (2005). Dickkopf-1 (DKK1) reveals that fibronectin is a major target of Wnt signaling in branching morphogenesis of the mouse embryonic lung. *Developmental Biology*, *277*(2), 316–331. https://doi.org/10.1016/j.ydbio.2004.09.023

Dean, C. H., & Cheong, S.-S. (2023). Simple Models of Lung Development. In C. M. Magin (Ed.), *Engineering Translational Models of Lung Homeostasis and Disease* (pp. 17–28). Springer International Publishing. https://doi.org/10.1007/978-3-031-26625-6_2

Del Moral, P.-M., & Warburton, D. (2010). Explant Culture of Mouse Embryonic Whole Lung, Isolated Epithelium, or Mesenchyme Under Chemically Defined Conditions as a System to Evaluate the Molecular Mechanism of Branching Morphogenesis and Cellular Differentiation. In A. Ward & D. Tosh (Eds.), *Mouse Cell Culture* (Vol. 633, pp. 71–79). Humana Press. https://doi.org/10.1007/978-1-59745-019-5_5

DePaula-Silva, A. B., Gorbea, C., Doty, D. J., Libbey, J. E., Sanchez, J. M. S., Hanak, T. J., Cazalla, D., & Fujinami, R. S. (2019). Differential transcriptional profiles identify microglial- and macrophage-specific gene markers expressed during virus-induced neuroinflammation. *Journal of Neuroinflammation*, *16*(1), 152. https://doi.org/10.1186/s12974-019-1545-x

Ding, D.-C., Shyu, W.-C., & Lin, S.-Z. (2011). Mesenchymal Stem Cells. *Cell Transplantation*, *20*(1), 5–14. https://doi.org/10.3727/096368910X

Ding, Y., Diao, Z., Cui, H., Yang, A., Liu, W., & Jiang, L. (2021). Bioinformatics analysis reveals the roles of cytoskeleton protein transgelin in occurrence and development of proteinuria. *Translational Pediatrics*, *10*(9), 2250. https://doi.org/10.21037/tp-21-83

Dobreva, M. P., Lhoest, L., Pereira, P. N. G., Umans, L., Chuva de Sousa Lopes, S. M., & Zwijsen, A. (2012). Periostin as a Biomarker of the Amniotic Membrane. *Stem Cells International*, *2012*(1), 987185. https://doi.org/10.1155/2012/987185

Dobreva, M. P., Pereira, P. N. G., Deprest, J., & Zwijsen, A. (2010). On the origin of amniotic stem cells: Of mice and men. *The International Journal of Developmental Biology*, *54*(5), Article 5. https://doi.org/10.1387/ijdb.092935md

Domm, W., Misra, R. S., & O'Reilly, M. A. (2015). Affect of Early Life Oxygen Exposure on Proper Lung Development and Response to Respiratory Viral Infections. *Frontiers in Medicine*, *2*. https://doi.org/10.3389/fmed.2015.00055

Downs, K. M. (2022). The mouse allantois: New insights at the embryonic–extraembryonic interface. *Philosophical Transactions of the Royal Society B*. https://doi.org/10.1098/rstb.2021.0251

Fadool, J. M., & Linser, P. J. (1993). 5A11 antigen is a cell recognition molecule which is involved in neuronal-glial interactions in avian neural retina. *Developmental Dynamics*, *196*(4), 252–262. https://doi.org/10.1002/aja.1001960406

Faisst, A. M., Alvarez-Bolado, G., Treichel, D., & Gruss, P. (2002). *Rotatin* is a novel gene required for axial rotation and left–right specification in mouse embryos. *Mechanisms of Development*, *113*(1), 15–28. https://doi.org/10.1016/S0925-4773(02)00003-5

Fan, Q.-W., Kadomatsu, K., Uchimura, K., & Muramatsu, T. (1998). Embigin/basigin subgroup of the immunoglobulin superfamily: Different modes of expression during mouse embryogenesis and correlated expression with carbohydrate antigenic markers. *Development, Growth & Differentiation*, *40*(3), 277–286. https://doi.org/10.1046/j.1440-169X.1998.t01-1-00003.x

Filimonow, K., & de la Fuente, R. (2022). Specification and role of extraembryonic endoderm lineages in the periimplantation mouse embryo. *Theriogenology*, *180*, 189–206. https://doi.org/10.1016/j.theriogenology.2021.12.021

Forero-Quintero, L. S., Ames, S., Schneider, H.-P., Thyssen, A., Boone, C. D., Andring, J. T., McKenna, R., Casey, J. R., Deitmer, J. W., & Becker, H. M. (2019). Membrane-anchored carbonic anhydrase IV interacts with monocarboxylate transporters via their chaperones CD147 and GP70. *Journal of Biological Chemistry*, *294*(2), 593–607. https://doi.org/10.1074/jbc.RA118.005536

Fossum, S., Mallett, S., & Neil Barclay, A. (1991). The MRC OX-47 antigen is a member of the immunoglobulin superfamily with an unusual transmembrane sequence. *European Journal of Immunology*, *21*(3), 671–679. https://doi.org/10.1002/eji.1830210320

Gattazzo, F., Urciuolo, A., & Bonaldo, P. (2014). Extracellular matrix: A dynamic microenvironment for stem cell niche. *Biochimica et Biophysica Acta*, *1840*(8), 2506–2519. https://doi.org/10.1016/j.bbagen.2014.01.010

Guenette, R. S., Sridhar, S., Herley, M., Mooibroek, M., Wong, P., & Tenniswood, M. (1997). Embigin, a developmentally expressed member of the immunoglobulin super family, is also expressed during regression of prostate and mammary gland. *Developmental Genetics*, *21*(4), 268–278. https://doi.org/10.1002/(SICI)1520-6408(1997)21:4%253C268::AID-DVG4%253E3.0.CO;2-5

Hakim, A., & Usmani, O. S. (2014). Structure of the Lower Respiratory Tract. In *Reference Module in Biomedical Sciences*. Elsevier. https://doi.org/10.1016/B978-0-12-801238-3.00215-4

Halestrap, A. P. (2013a). Monocarboxylic Acid Transport. In *Comprehensive Physiology* (pp. 1611–1643). John Wiley & Sons, Ltd. https://doi.org/10.1002/cphy.c130008

Halestrap, A. P. (2013b). The SLC16 gene family – Structure, role and regulation in health and disease. *Molecular Aspects of Medicine*, *34*(2), 337–349. https://doi.org/10.1016/j.mam.2012.05.003

Halestrap, A. P., & Meredith, D. (2004). The SLC16 gene family—From monocarboxylate transporters (MCTs) to aromatic amino acid transporters and beyond. *Pflügers Archiv*, *447*(5), 619–628. https://doi.org/10.1007/s00424-003-1067-2

Hanna, S. M., Kirk, P., Holt, O. J., Puklavec, M. J., Brown, M. H., & Barclay, A. N. (2003). A novel form of the membrane protein CD147 that contains an extra Ig-like domain and interacts homophilically. *BMC Biochemistry*, *4*(1), 17. https://doi.org/10.1186/1471-2091-4-17

Haque, R., Song, A. D., Lee, J., Lee, S.-J. V., & Suh, J. M. (2025). Essential resources and best practices for laboratory mouse research. *Molecules and Cells*, *48*(2), 100178. https://doi.org/10.1016/j.mocell.2025.100178

Herriges, M., & Morrisey, E. E. (2014). Lung development: Orchestrating the generation and regeneration of a complex organ. *Development*, *141*(3), 502–513. https://doi.org/10.1242/dev.098186

Higuchi, K. (2022). Mammalian monocarboxylate transporter 7 (MCT7/Slc16a6) is a novel facilitative taurine transporter. *Journal of Biological Chemistry*, *298*(4), 101800. https://doi.org/10.1016/j.jbc.2022.101800

Hill, I. E., Selkirk, C. P., Hawkes, R. B., & Beesley, P. W. (1988). Characterization of novel glycoprotein components of synaptic membranes and postsynaptic densities, gp65 and gp55, with a monoclonal antibody. *Brain Research*, *461*(1), 27–43. https://doi.org/10.1016/0006-8993(88)90722-6

Hu, D., & Cross, J. C. (2009). Development and function of trophoblast giant cells in the rodent placenta. *The International Journal of Developmental Biology*, *54*(2–3), Article 2–3. https://doi.org/10.1387/ijdb.082768dh

Huang, G., Ye, S., Zhou, X., Liu, D., & Ying, Q.-L. (2015). Molecular basis of embryonic stem cell self-renewal: From signaling pathways to pluripotency network. *Cellular and Molecular Life Sciences: CMLS*, *72*(9), 1741–1757. https://doi.org/10.1007/s00018-015-1833-2

Huang, R.-P., Ozawa, M., Kadomatsu, K., & Muramatsu, T. (1990). Developmentally regulated expression of embigin, a member of the immunoglobulin superfamily found in embryonal carcinoma cells. *Differentiation*, *45*(2), 76–83. https://doi.org/10.1111/j.1432-0436.1990.tb00460.x

Huang, R.-P., Ozawa, M., Kadomatsu, K., & Muramatsu, T. (1993). Embigin, a Member of the Immunoglobulin Superfamily Expressed in Embryonic Cells, Enhances Cell-Substratum Adhesion. *Developmental Biology*, *155*(2), 307–314. https://doi.org/10.1006/dbio.1993.1030

Hugo, S. E., Cruz-Garcia, L., Karanth, S., Anderson, R. M., Stainier, D. Y. R., & Schlegel, A. (2012). A monocarboxylate transporter required for hepatocyte secretion of ketone bodies during fasting. *Genes & Development*, *26*(3), 282–293. https://doi.org/10.1101/gad.180968.111

Igakura, T., Kadomatsu, K., Kaname, T., Muramatsu, H., Fan, Q.-W., Miyauchi, T., Toyama, Y., Kuno, N., Yuasa, S., Takahashi, M., Senda, T., Taguchi, O., Yamamura, K., Arimura, K., & Muramatsu, T. (1998). A Null Mutation in Basigin, an Immunoglobulin Superfamily Member, Indicates Its Important Roles in Peri-implantation Development and Spermatogenesis. *Developmental Biology*, *194*(2), 152–165. https://doi.org/10.1006/dbio.1997.8819

Igakura, T., Kadomatsu, K., Taguchi, O., Muramatsu, H., Kaname, T., Miyauchi, T., Yamamura, K., Arimura, K., & Muramatsu, T. (1996). Roles of Basigin, a Member of the Immunoglobulin Superfamily, in Behavior as to an Irritating Odor, Lymphocyte Response, and Blood–Brain Barrier. *Biochemical and Biophysical Research Communications*, *224*(1), 33–36. https://doi.org/10.1006/bbrc.1996.0980

Ihermann-Hella, A., & Kuure, S. (2019). Mouse Ex Vivo Kidney Culture Methods. In S. Vainio (Ed.), *Kidney Organogenesis: Methods and Protocols* (pp. 23–30). Springer. https://doi.org/10.1007/978-1-4939-9021-4_2

Ishikawa, T., Takemoto, M., Akimoto, Y., Takada-Watanabe, A., Yan, K., Sakamoto, K., Maezawa, Y., Suguro, M., He, L., Tryggvason, K., Betsholtz, C., & Yokote, K. (2021). A novel podocyte protein, R3h domain containing-like, inhibits TGF-β-induced p38 MAPK and regulates the structure of podocytes and glomerular basement membrane. *Journal of Molecular Medicine*, *99*(6), 859–876. https://doi.org/10.1007/s00109-021-02050-w

Jung, D. E., Kim, J. M., Kim, C., & Song, S. Y. (2016). Embigin is overexpressed in pancreatic ductal adenocarcinoma and regulates cell motility through epithelial to mesenchymal transition via the TGF-β pathway. *Molecular Carcinogenesis*, *55*(5), 633–645. https://doi.org/10.1002/mc.22309

Kaebisch, C., Schipper, D., Babczyk, P., & Tobiasch, E. (2015). The role of purinergic receptors in stem cell differentiation. *Computational and Structural Biotechnology Journal*, *13*, 75–84. https://doi.org/10.1016/j.csbj.2014.11.003

Kallies, A., Hasbold, J., Fairfax, K., Pridans, C., Emslie, D., McKenzie, B. S., Lew, A. M., Corcoran, L. M., Hodgkin, P. D., Tarlinton, D. M., & Nutt, S. L. (2007). Initiation of Plasma-Cell Differentiation Is Independent of the Transcription Factor Blimp-1. *Immunity*, *26*(5), 555–566. https://doi.org/10.1016/j.immuni.2007.04.007

Kasinrerk, W., Fiebiger, E., Stefanová, I., Baumruker, T., Knapp, W., & Stockinger, H. (1992). Human leukocyte activation antigen M6, a member of the Ig superfamily, is the species homologue of rat OX-47, mouse basigin, and chicken HT7 molecule. *The Journal of Immunology*, *149*(3), 847–854. https://doi.org/10.4049/jimmunol.149.3.847

Kato, N., Kosugi, T., Sato, W., Ishimoto, T., Kojima, H., Sato, Y., Sakamoto, K., Maruyama, S., Yuzawa, Y., Matsuo, S., & Kadomatsu, K. (2011). Basigin/CD147 Promotes Renal Fibrosis after Unilateral Ureteral Obstruction. *The American Journal of Pathology*, *178*(2), 572–579. https://doi.org/10.1016/j.ajpath.2010.10.009

Kato, N., Yuzawa, Y., Kosugi, T., Hobo, A., Sato, W., Miwa, Y., Sakamoto, K., Matsuo, S., & Kadomatsu, K. (2009). The E-Selectin Ligand Basigin/CD147 Is Responsible for Neutrophil Recruitment in Renal Ischemia/Reperfusion. *Journal of the American Society of Nephrology*, *20*(7), 1565. https://doi.org/10.1681/ASN.2008090957

Kestilä, M., Lenkkeri, U., Männikkö, M., Lamerdin, J., McCready, P., Putaala, H., Ruotsalainen, V., Morita, T., Nissinen, M., Herva, R., Kashtan, C. E., Peltonen, L., Holmberg, C., Olsen, A., & Tryggvason, K. (1998). Positionally Cloned Gene for a Novel Glomerular Protein—Nephrin—Is Mutated in Congenital Nephrotic Syndrome. *Molecular Cell*, *1*(4), 575–582. https://doi.org/10.1016/S1097-2765(00)80057-X

Kim, C. F. B., Jackson, E. L., Woolfenden, A. E., Lawrence, S., Babar, I., Vogel, S., Crowley, D., Bronson, R. T., & Jacks, T. (2005). Identification of Bronchioalveolar Stem Cells in Normal Lung and Lung Cancer. *Cell*, *121*(6), 823–835. https://doi.org/10.1016/j.cell.2005.03.032

Ko, K., Araúzo-Bravo, M. J., Kim, J., Stehling, M., & Schöler, H. R. (2010). Conversion of adult mouse unipotent germline stem cells into pluripotent stem cells. *Nature Protocols*, *5*(5), 921–928. https://doi.org/10.1038/nprot.2010.44

Kobayashi, A., Kwan, K.-M., Carroll, T. J., McMahon, A. P., Mendelsohn, C. L., & Behringer, R. R. (2005). Distinct and sequential tissue-specific activities of the LIM-class homeobox gene Lim1 for tubular morphogenesis during kidney development. *Development*, *132*(12), 2809–2823. https://doi.org/10.1242/dev.01858

Kobayashi, A., Valerius, M. T., Mugford, J. W., Carroll, T. J., Self, M., Oliver, G., & McMahon, A. P. (2008). Six2 defines and regulates a multipotent self-renewing nephron progenitor population throughout mammalian kidney development. *Cell Stem Cell*, *3*(2), 169–181. https://doi.org/10.1016/j.stem.2008.05.020

Kojima, Y., Tam, O. H., & Tam, P. P. L. (2014). Timing of developmental events in the early mouse embryo. *Seminars in Cell & Developmental Biology*, *34*, 65–75. https://doi.org/10.1016/j.semcdb.2014.06.010

Kolios, G., & Moodley, Y. (2012). Introduction to Stem Cells and Regenerative Medicine. *Respiration*, *85*(1), 3–10. https://doi.org/10.1159/000345615

Kumar, V., Yang, C., & Cowley, A. W. (2020). Temporal Expression and Cellular Localization of PAPPA2 in the Developing Kidney of Rat. *Journal of Histochemistry and Cytochemistry*, *68*(3), 209–222. https://doi.org/10.1369/0022155420904478

Kuure, S., & Sariola, H. (2020). Mouse Models of Congenital Kidney Anomalies. In A. Liu (Ed.), *Animal Models of Human Birth Defects* (pp. 109–136). Springer. https://doi.org/10.1007/978-981-15-2389-2_5

Lain, E., Carnejac, S., Escher, P., Wilson, M. C., Lømo, T., Gajendran, N., & Brenner, H. R. (2009). A Novel Role for Embigin to Promote Sprouting of Motor Nerve Terminals at the Neuromuscular Junction*. *Journal of Biological Chemistry*, *284*(13), 8930–8939. https://doi.org/10.1074/jbc.M809491200

Langhe, S. D., Sala, F. G., Mailleux, A. A., & Bellusci, S. (2006). Lung. In *Encyclopedic Reference of Genomics and Proteomics in Molecular Medicine* (pp. 993–998). Springer, Berlin, Heidelberg. https://doi.org/10.1007/3-540-29623-9_3330

Langnaese, K., Beesley, P. W., & Gundelfinger, E. D. (1997). Synaptic Membrane Glycoproteins gp65 and gp55 Are New Members of the Immunoglobulin Superfamily*. *Journal of Biological Chemistry*, *272*(2), 821–827. https://doi.org/10.1074/jbc.272.2.821

Langnaese, K., Mummery, R., Gundelfinger, E. D., & Beesley, P. W. (1998). Immunoglobulin superfamily members gp65 and gp55: Tissue distribution of glycoforms. *FEBS Letters*, *429*(3), 284–288. https://doi.org/10.1016/S0014-5793(98)00616-4

Lechner, M. S., & Dressler, G. R. (1997). The molecular basis of embryonic kidney development. *Mechanisms of Development*, *62*(2), 105–120. https://doi.org/10.1016/S0925-4773(97)00667-9

Lengacher, S., Nehiri-Sitayeb, T., Steiner, N., Carneiro, L., Favrod, C., Preitner, F., Thorens, B., Stehle, J.-C., Dix, L., Pralong, F., Magistretti, P. J., & Pellerin, L. (2013). Resistance to Diet-Induced Obesity and Associated Metabolic Perturbations in Haploinsufficient Monocarboxylate Transporter 1 Mice. *PLOS ONE*, *8*(12), e82505. https://doi.org/10.1371/journal.pone.0082505

Li, H., Zeng, J., Huang, L., Wu, D., Liu, L., Liu, Y., & Yuan, Q. (2018). Microarray Analysis of Gene Expression Changes in Neuroplastin 65-Knockout Mice: Implications for Abnormal Cognition and Emotional Disorders. *Neuroscience Bulletin*, *34*(5), 779–788. https://doi.org/10.1007/s12264-018-0251-5

Li, K., & Nowak, R. A. (2020). The role of basigin in reproduction. *Reproduction*, *159*(2), R97–R109. https://doi.org/10.1530/REP-19-0268

Li, Z., Zhuansun, D., Meng, X., Yang, H., Xiao, J., Chen, Y., Wang, J., Yu, X., Li, Z., You, J., Chen, X., Feng, C., Wu, L., Chu, X., Duan, W., Wang, K., Li, Z., Tou, J., Yu, L., … Feng, J. (2025). EMB is essential for enteric nervous system development mediated by PI3K signaling. *Genome Medicine*, *17*(1), 102. https://doi.org/10.1186/s13073-025-01538-1

Liao, C.-G., Kong, L.-M., Song, F., Xing, J.-L., Wang, L.-X., Sun, Z.-J., Tang, H., Yao, H., Zhang, Y., Wang, L., Wang, Y., Yang, X.-M., Li, Y., & Chen, Z.-N. (2011). Characterization of basigin isoforms and the inhibitory function of basigin-3 in human hepatocellular carcinoma proliferation and invasion. *Molecular and Cellular Biology*, *31*(13), 2591–2604. Scopus. https://doi.org/10.1128/MCB.05160-11

Lim, W. F., Inoue-Yokoo, T., Tan, K. S., Lai, M. I., & Sugiyama, D. (2013). Hematopoietic cell differentiation from embryonic and induced pluripotent stem cells. *Stem Cell Research & Therapy*, *4*(3), 71. https://doi.org/10.1186/scrt222

Linton, J. M., Martin, G. R., & Reichardt, L. F. (2007). The ECM protein nephronectin promotes kidney development via integrinα8β1-mediated stimulation of Gdnf expression. *Development*, *134*(13), 2501–2509. https://doi.org/10.1242/dev.005033

Liu, K., Tang, M., Liu, Q., Han, X., Jin, H., Zhu, H., Li, Y., He, L., Ji, H., & Zhou, B. (2020). Bi-directional differentiation of single bronchioalveolar stem cells during lung repair. *Cell Discovery*, *6*(1), 1. https://doi.org/10.1038/s41421-019-0132-8

Llorente, V., Velarde, P., Desco, M., & Gómez-Gaviro, M. V. (2022). Current Understanding of the Neural Stem Cell Niches. *Cells*, *11*(19), 3002. https://doi.org/10.3390/cells11193002

Love, M. I., Huber, W., & Anders, S. (2014). Moderated estimation of fold change and dispersion for RNA-seq data with DESeq2. *Genome Biology*, *15*(12), 550. https://doi.org/10.1186/s13059-014-0550-8

Mannowetz, N., Wandernoth, P., & Wennemuth, G. (2012). Basigin interacts with both MCT1 and MCT2 in murine spermatozoa. *Journal of Cellular Physiology*, *227*(5), 2154–2162. https://doi.org/10.1002/jcp.22949

Marcotte, M., Sharma, R., & Bouchard, M. (2014). Gene regulatory network of renal primordium development. *Pediatric Nephrology*, *29*(4), 637–644. https://doi.org/10.1007/s00467-013-2635-0

Mesfin, F. M., Manohar, K., Hunter, C. E., Shelley, W. C., Brokaw, J. P., Liu, J., Ma, M., & Markel, T. A. (2023). Stem cell derived therapies to preserve and repair the developing intestine. *Seminars in Perinatology*, *47*(3), 151727. https://doi.org/10.1016/j.semperi.2023.151727

Miyauchi, T., Kanekura, T., Yamaoka, A., Ozawa, M., Miyazawa, S., & Muramatasu, T. (1990). Basigin, a New, Broadly Distributed Member of the Immunoglobulin Superfamily, Has Strong

Homology with Both the Immunoglobulin V Domain and the β-Chain of Major Histocompatibility Complex Class II Antigen. *The Journal of Biochemistry*, *107*(2), 316–323. https://doi.org/10.1093/oxfordjournals.jbchem.a123045

Miyauchi, T., Masuzawa, Y., & Muramatsu, T. (1991). The Basigin Group of the Immunoglobulin Superfamily: Complete Conservation of a Segment in and around Transmembrane Domains of Human and Mouse Basigin and Chicken HT7 Antigen. *The Journal of Biochemistry*, *110*(5), 770–774. https://doi.org/10.1093/oxfordjournals.jbchem.a123657

Mohamad, S. F., El Koussa, R., Ghosh, J., Blosser, R., Gunawan, A., Layer, J., Zhang, C., Karnik, S., Davé, U., Kacena, M. A., & Srour, E. F. (2024). Osteomacs promote maintenance of murine hematopoiesis through megakaryocyte-induced upregulation of Embigin and CD166. *Stem Cell Reports*, *19*(4), 486–500. https://doi.org/10.1016/j.stemcr.2024.02.004

Mohamad, S. F., Xu, L., Ghosh, J., Childress, P. J., Abeysekera, I., Himes, E. R., Wu, H., Alvarez, M. B., Davis, K. M., Aguilar-Perez, A., Hong, J. M., Bruzzaniti, A., Kacena, M. A., & Srour, E. F. (2017). Osteomacs interact with megakaryocytes and osteoblasts to regulate murine hematopoietic stem cell function. *Blood Advances*, *1*(26), 2520–2528. https://doi.org/10.1182/bloodadvances.2017011304

Mohrin, M., Liu, J., Zavala-Solorio, J., Bhargava, S., Maxwell Trumble, J., Brito, A., Hu, D., Brooks, D., Koukos, G., Alabdulaaly, L., Paw, J. S., Hake, K., Kolumam, G., Bouxsein, M. L., Baron, R., Kutskova, Y., & Freund, A. (2021). Inhibition of longevity regulator PAPP-A modulates tissue homeostasis via restraint of mesenchymal stromal cells. *Aging Cell*, *20*(3), e13313. https://doi.org/10.1111/acel.13313

Mori, M., & Cardoso, W. V. (2014). Chapter 1—Lung Progenitor Cell Specification and Morphogenesis. In R. Harding & K. E. Pinkerton (Eds.), *The Lung (Second Edition)* (pp. 3–9). Academic Press. https://doi.org/10.1016/B978-0-12-799941-8.00001-8

Muhr, J., Arbor, T. C., & Ackerman, K. M. (2025). Embryology, Gastrulation. In *StatPearls*. StatPearls Publishing. http://www.ncbi.nlm.nih.gov/books/NBK554394/

Muramatsu, T. (2016). Basigin (CD147), a multifunctional transmembrane glycoprotein with various binding partners. *The Journal of Biochemistry*, *159*(5), 481–490. https://doi.org/10.1093/jb/mvv127

Muramatsu, T., & Miyauchi, T. (2003). Basigin (CD147): A multifunctional transmembrane protien involved in reproduction, neural function, inflammation and tumor invasion. *Histology and Histopathology*, *18*(3), 981–987. Scopus.

Nabeshima, K., Iwasaki, H., Koga, K., Hojo, H., Suzumiya, J., & Kikuchi, M. (2006). Emmprin (basigin/CD147): Matrix metalloproteinase modulator and multifunctional cell recognition molecule that plays a critical role in cancer progression. *Pathology International*, *56*(7), 359–367. https://doi.org/10.1111/j.1440-1827.2006.01972.x

Naruhashi, K., Kadomatsu, K., Igakura, T., Fan, Q.-W., Kuno, N., Muramatsu, H., Miyauchi, T., Hasegawa, T., Itoh, A., Muramatsu, T., & Nabeshima, T. (1997). Abnormalities of Sensory and Memory Functions in Mice Lacking*Bsg*Gene. *Biochemical and Biophysical Research Communications*, *236*(3), 733–737. https://doi.org/10.1006/bbrc.1997.6993

Nasuhidehnavi, A., Zhao, Y., Punetha, A., Hemphill, A., Li, H., Bechtel, T. J., Rager, T., Xiong, B., Petrou, V. I., Gubbels, M.-J., Weerapana, E., & Yap, G. S. (2022). A Role for Basigin in Toxoplasma gondii Infection. *Infection and Immunity*, *90*(8), e00205-22. https://doi.org/10.1128/iai.00205-22

Newton, S., Aguilar, C., & Bowl, M. R. (2025). C57BL/6-derived mice and the *Cdh23ahl* allele – Background matters. *Hearing Research*, *462*, 109278. https://doi.org/10.1016/j.heares.2025.109278

Newton, S., Aguilar, C., Bunton-Stasyshyn, R. K., Flook, M., Stewart, M., Marcotti, W., Brown, S., & Bowl, M. R. (2023). Absence of Embigin accelerates hearing loss and causes sub-viability, brain and heart defects in C57BL/6N mice due to interaction with Cdh23ahl. *iScience*, *26*(10), 108056. https://doi.org/10.1016/j.isci.2023.108056

Newton, S., Kong, F., Carlton, A. J., Aguilar, C., Parker, A., Codner, G. F., Teboul, L., Wells, S., Brown, S. D. M., Marcotti, W., & Bowl, M. R. (2022). Neuroplastin genetically interacts with Cadherin 23 and the encoded isoform Np55 is sufficient for cochlear hair cell function and hearing. *PLOS Genetics*, *18*(1), e1009937. https://doi.org/10.1371/journal.pgen.1009937

Ney, A., Canciani, G., Hsuan, J. J., & Pereira, S. P. (2020). Modelling Pancreatic Neuroendocrine Cancer: From Bench Side to Clinic. *Cancers*, *12*(11), Article 11. https://doi.org/10.3390/cancers12113170

Nitin, P., Nandhakumar, R., Vidhya, B., Rajesh, S., & Sakunthala, A. (2022). COVID-19: Invasion, pathogenesis and possible cure – A review. *Journal of Virological Methods*, *300*, 114434. https://doi.org/10.1016/j.jviromet.2021.114434

Ochrietor, J. D., Moroz, T. P., van Ekeris, L., Clamp, M. F., Jefferson, S. C., deCarvalho, A. C., Fadool, J. M., Wistow, G., Muramatsu, T., & Linser, P. J. (2003). Retina-specific expression of 5A11/Basigin-2, a member of the immunoglobulin gene superfamily. *Investigative Ophthalmology & Visual Science*, *44*(9), 4086–4096. https://doi.org/10.1167/iovs.02-0995

Oliveros, J. C. (2007). *Venny. An Interactive Tool for Comparing Lists with Venn's Diagrams* [Computer software]. https://bioinfogp.cnb.csic.es/tools/venny/

Ornoy, A., & Miller, R. K. (2023). Yolk sac development, function and role in rodent pregnancy. *Birth Defects Research*, *115*(14), 1243–1254. https://doi.org/10.1002/bdr2.2172

Ovens, M. J., Manoharan, C., Wilson, M. C., Murray, C. M., & Halestrap, A. P. (2010). The inhibition of monocarboxylate transporter 2 (MCT2) by AR-C155858 is modulated by the associated ancillary protein. *Biochemical Journal*, *431*(2), 217–225. https://doi.org/10.1042/BJ20100890

Owczarek, S., & Berezin, V. (2012). Neuroplastin: Cell adhesion molecule and signaling receptor. *The International Journal of Biochemistry & Cell Biology*, *44*(1), 1–5. https://doi.org/10.1016/j.biocel.2011.10.006

Ozawa, M., Huang, R. P., Furukawa, T., & Muramatsu, T. (1988). A teratocarcinoma glycoprotein carrying a developmentally regulated carbohydrate marker is a member of the immunoglobulin gene superfamily. *Journal of Biological Chemistry*, *263*(7), 3059–3062. https://doi.org/10.1016/S0021-9258(18)69032-5

Peng, J., Yan, Q., Pei, W., Jiang, Y., Zhou, L., & Li, R. (2025). A Prognostic Riskscore Model Related to Helicobacter pylori Infection in Stomach Adenocarcinoma. *International Journal of Genomics*, *2025*(1), 5554610. https://doi.org/10.1155/ijog/5554610

Pereira, P. N., Dobreva, M. P., Graham, L., Huylebroeck, D., Lawson, K. A., & Zwijsen, A. (2011). Amnion formation in the mouse embryo: The single amniochorionic fold model. *BMC Developmental Biology*, *11*(1), 48. https://doi.org/10.1186/1471-213X-11-48

Peters, K., Werner, S., Liao, X., Wert, S., Whitsett, J., & Williams, L. (1994). Targeted expression of a dominant negative FGF receptor blocks branching morphogenesis and epithelial differentiation of the mouse lung. *The EMBO Journal*, *13*(14), 3296–3301. https://doi.org/10.1002/j.1460-2075.1994.tb06631.x

Pietilä, I., & Vainio, S. J. (2014). Kidney Development: An Overview. *Nephron Experimental Nephrology*, *126*(2), 40–44. https://doi.org/10.1159/000360659

Poliwoda, S., Noor, N., Downs, E., Schaaf, A., Cantwell, A., Ganti, L., Kaye, A. D., Mosel, L. I., Carroll, C. B., Viswanath, O., & Urits, I. (2022). Stem cells: A comprehensive review of origins and emerging clinical roles in medical practice. *Orthopedic Reviews*, *14*(3). https://doi.org/10.52965/001c.37498

Poole, R. C., & Halestrap, A. P. (1993). Transport of lactate and other monocarboxylates across mammalian plasma membranes. *American Journal of Physiology-Cell Physiology*, *264*(4), C761–C782. https://doi.org/10.1152/ajpcell.1993.264.4.C761

Pridans, C., Holmes, M. L., Polli, M., Wettenhall, J. M., Dakic, A., Corcoran, L. M., Smyth, G. K., & Nutt, S. L. (2008). Identification of Pax5 Target Genes in Early B Cell Differentiation1. *The Journal of Immunology*, *180*(3), 1719–1728. https://doi.org/10.4049/jimmunol.180.3.1719

Prozialeck, W. C., Lamar, P. C., & Appelt, D. M. (2004). Differential expression of E-cadherin, N-cadherin and beta-catenin in proximal and distal segments of the rat nephron. *BMC Physiology*, *4*(1), 10. https://doi.org/10.1186/1472-6793-4-10

Pushkarsky, T., Zybarth, G., Dubrovsky, L., Yurchenko, V., Tang, H., Guo, H., Toole, B., Sherry, B., & Bukrinsky, M. (2001). CD147 facilitates HIV-1 infection by interacting with virus-associated cyclophilin A. *Proceedings of the National Academy of Sciences*, *98*(11), 6360–6365. https://doi.org/10.1073/pnas.111583198

Putaala, H., Soininen, R., Kilpeläinen, P., Wartiovaara, J., & Tryggvason, K. (2001). The murine nephrin gene is specifically expressed in kidney, brain and pancreas: Inactivation of the gene leads to massive proteinuria and neonatal death. *Human Molecular Genetics*, *10*(1), 1–8. https://doi.org/10.1093/hmg/10.1.1

Qu, F., Li, W., Xu, J., Zhang, R., Ke, J., Ren, X., Meng, X., Qin, L., Zhang, J., Lu, F., Zhou, X., Luo, X., Zhang, Z., Wang, M., Wu, G., Pei, D., Chen, J., Cui, G., Suo, S., & Peng, G. (2023). Three-dimensional molecular architecture of mouse organogenesis. *Nature Communications*, *14*(1), 4599. https://doi.org/10.1038/s41467-023-40155-7

Rawlins, E. L., Okubo, T., Xue, Y., Brass, D. M., Auten, R. L., Hasegawa, H., Wang, F., & Hogan, B. L. M. (2009). The Role of Scgb1a1+ Clara Cells in the Long-Term Maintenance and Repair of Lung Airway, but Not Alveolar, Epithelium. *Cell Stem Cell*, *4*(6), 525–534. https://doi.org/10.1016/j.stem.2009.04.002

Riccetti, M. R., Green, J., Taylor, T. J., & Perl, A.-K. T. (2024). Prenatal FGFR2 Signaling via PI3K/AKT Specifies the PDGFRA+ Myofibroblast. *American Journal of Respiratory Cell and Molecular Biology*, *70*(1), 63–77. https://doi.org/10.1165/rcmb.2023-0245OC

Riethdorf, S., Reimers, N., Assmann, V., Kornfeld, J.-W., Terracciano, L., Sauter, G., & Pantel, K. (2006). High incidence of EMMPRIN expression in human tumors. *International Journal of Cancer*, *119*(8), 1800–1810. https://doi.org/10.1002/ijc.22062

Rinkenberger, J., & Werb, Z. (2000). The labyrinthine placenta. *Nature Genetics*, *25*(3), 248–250. https://doi.org/10.1038/76985

Rivera-Pérez, J. A., & Hadjantonakis, A.-K. (2015). The Dynamics of Morphogenesis in the Early Mouse Embryo. *Cold Spring Harbor Perspectives in Biology*, *7*(11), a015867. https://doi.org/10.1101/cshperspect.a015867

Rivera-Pérez, J. A., & Magnuson, T. (2005). Primitive streak formation in mice is preceded by localized activation of *Brachyury* and *Wnt3*. *Developmental Biology*, *288*(2), 363–371. https://doi.org/10.1016/j.ydbio.2005.09.012

Rodriguez, A. M., & Downs, K. M. (2017). Visceral endoderm and the primitive streak interact to build the fetal-placental interface of the mouse gastrula. *Developmental Biology*, *432*(1), 98–124. https://doi.org/10.1016/j.ydbio.2017.08.026

Roman, J., & McDonald, J. A. (2012). Expression of Fibronectin, the Integrin α5, and α-Smooth Muscle Actin in Heart and Lung Development. *American Journal of Respiratory Cell and Molecular Biology*. https://doi.org/10.1165/ajrcmb/6.5.472

Ruaro, B., Salton, F., Braga, L., Wade, B., Confalonieri, P., Volpe, M. C., Baratella, E., Maiocchi, S., & Confalonieri, M. (2021). The History and Mystery of Alveolar Epithelial Type II Cells: Focus on Their Physiologic and Pathologic Role in Lung. *International Journal of Molecular Sciences*, *22*(5), 2566. https://doi.org/10.3390/ijms22052566

Ruma, I. M. W., Kinoshita, R., Tomonobu, N., Inoue, Y., Kondo, E., Yamauchi, A., Sato, H., Sumardika, I. W., Chen, Y., Yamamoto, K.-I., Murata, H., Toyooka, S., Nishibori, M., & Sakaguchi, M. (2018). Embigin Promotes Prostate Cancer Progression by S100A4-Dependent and-Independent Mechanisms. *Cancers*, *10*(7), Article 7. https://doi.org/10.3390/cancers10070239

Saijoh, Y., & Hamada, H. (2020). Making the Right Loop for the heart. *Developmental Cell*, *55*(4), 383–384. https://doi.org/10.1016/j.devcel.2020.10.018

Saito, A., Fujikura-Ouchi, Y., Kuramasu, A., Shimoda, K., Akiyama, K., Matsuoka, H., & Ito, C. (2007). Association study of putative promoter polymorphisms in the neuroplastin gene and schizophrenia. *Neuroscience Letters*, *411*(3), 168–173. https://doi.org/10.1016/j.neulet.2006.08.042

Saitou, M., & Yamaji, M. (2012). Primordial Germ Cells in Mice. *Cold Spring Harbor Perspectives in Biology*, *4*(11), a008375. https://doi.org/10.1101/cshperspect.a008375

Sakai, T., Larsen, M., & Yamada, K. M. (2003). Fibronectin requirement in branching morphogenesis. *Nature*, *423*(6942), 876–881. https://doi.org/10.1038/nature01712

Sanchez-Ferras, O., Pacis, A., Sotiropoulou, M., Zhang, Y., Wang, Y. C., Bourgey, M., Bourque, G., Ragoussis, J., & Bouchard, M. (2021). A coordinated progression of progenitor cell states initiates urinary tract development. *Nature Communications*, *12*(1), 2627. https://doi.org/10.1038/s41467-021-22931-5

Sariola, H., Holm, K., & Henke-Fahle, S. (1988). Early innervation of the metanephric kidney. *Development*, *104*(4), 589–599. https://doi.org/10.1242/dev.104.4.589

Saxén, L., & Lehtonen, E. (1987). Embryonic kidney in organ culture. *Differentiation*, *36*(1), 2–11. https://doi.org/10.1111/j.1432-0436.1987.tb00176.x

Schedl, A. (2007). Renal abnormalities and their developmental origin. *Nature Reviews Genetics*, *8*(10), 791–802. https://doi.org/10.1038/nrg2205

Schildmeyer, L. A., Braun, R., Taffet, G., Debiasi, M., Burns, A. E., Bradley, A., & Schwartz, R. J. (2000). Impaired vascular contractility and blood pressure homeostasis in the smooth muscle α-actin null mouse. *The FASEB Journal*, *14*(14), 2213–2220. https://doi.org/10.1096/fj.99-0927com

Schindelin, J., Arganda-Carreras, I., Frise, E., Kaynig, V., Longair, M., Pietzsch, T., Preibisch, S., Rueden, C., Saalfeld, S., Schmid, B., Tinevez, J.-Y., White, D. J., Hartenstein, V., Eliceiri, K., Tomancak, P., & Cardona, A. (2012). Fiji: An open-source platform for biological-image analysis. *Nature Methods*, *9*(7), 676–682. https://doi.org/10.1038/nmeth.2019

Schlosshauer, B., & Herzog, K. H. (1990). Neurothelin: An inducible cell surface glycoprotein of blood-brain barrier-specific endothelial cells and distinct neurons. *Journal of Cell Biology*, *110*(4), 1261–1274. https://doi.org/10.1083/jcb.110.4.1261

Schwab, K., Patterson, L. T., Aronow, B. J., Luckas, R., Liang, H.-C., & Potter, S. S. (2003). A catalogue of gene expression in the developing kidney. *Kidney International*, *64*(5), 1588–1604. https://doi.org/10.1046/j.1523-1755.2003.00276.x

Seubert, A. C., Krafft, M., Bopp, S., Helal, M., Bhandare, P., Wolf, E., Alemany, A., Riedel, A., & Kretzschmar, K. (2024). Spatial transcriptomics reveals molecular cues underlying the site specificity of the adult mouse oral mucosa and its stem cell niches. *Stem Cell Reports*, *19*(12), 1706–1719. https://doi.org/10.1016/j.stemcr.2024.10.007

Seulberger, H., Lottspeich, F., & Risau, W. (1990). The inducible blood–brain barrier specific molecule HT7 is a novel immunoglobulin-like cell surface glycoprotein. *The EMBO Journal*, *9*(7), 2151–2158. https://doi.org/10.1002/j.1460-2075.1990.tb07384.x

Shinde, A. V., Humeres, C., & Frangogiannis, N. G. (2017). The role of α-smooth muscle actin in fibroblast-mediated matrix contraction and remodeling. *Biochimica et Biophysica Acta*, *1863*(1), 298–309. https://doi.org/10.1016/j.bbadis.2016.11.006

Silberstein, L., Goncalves, K. A., Kharchenko, P. V., Turcotte, R., Kfoury, Y., Mercier, F., Baryawno, N., Severe, N., Bachand, J., Spencer, J. A., Papazian, A., Lee, D., Chitteti, B. R., Srour, E. F., Hoggatt, J., Tate, T., Lo Celso, C., Ono, N., Nutt, S., … Scadden, D. T. (2016). Proximity-Based Differential Single-Cell Analysis of the Niche to Identify Stem/Progenitor Cell Regulators. *Cell Stem Cell*, *19*(4), 530–543. https://doi.org/10.1016/j.stem.2016.07.004

Sipilä, K., Rognoni, E., Jokinen, J., Tewary, M., Vietri Rudan, M., Talvi, S., Jokinen, V., Dahlström, K. M., Liakath-Ali, K., Mobasseri, A., Du-Harpur, X., Käpylä, J., Nutt, S. L., Salminen, T. A., Heino, J., & Watt, F. M. (2022). Embigin is a fibronectin receptor that affects sebaceous gland differentiation and metabolism. *Developmental Cell*, *57*(12), 1453-1465.e7. https://doi.org/10.1016/j.devcel.2022.05.011

Skiba, N. P., Cady, M. A., Molday, L., Han, J. Y. S., Lewis, T. R., Spencer, W. J., Thompson, W. J., Hiles, S., Philp, N. J., Molday, R. S., & Arshavsky, V. Y. (2021). TMEM67, TMEM237, and Embigin in Complex With Monocarboxylate Transporter MCT1 Are Unique Components of the Photoreceptor Outer Segment Plasma Membrane. *Molecular & Cellular Proteomics*, *20*, 100088. https://doi.org/10.1016/j.mcpro.2021.100088

Smalla, K.-H., Matthies, H., Langnäse, K., Shabir, S., Böckers, T. M., Wyneken, U., Staak, S., Krug, M., Beesley, P. W., & Gundelfinger, E. D. (2000). The synaptic glycoprotein neuroplastin is involved in long-term potentiation at hippocampal CA1 synapses. *Proceedings of the National Academy of Sciences*, *97*(8), 4327–4332. https://doi.org/10.1073/pnas.080389297

Stuart, R. O., Bush, K. T., & Nigam, S. K. (2003). Changes in gene expression patterns in the ureteric bud and metanephric mesenchyme in models of kidney development. *Kidney International*, *64*(6), 1997–2008. https://doi.org/10.1046/j.1523-1755.2003.00383.x

Sumardika, I. W., Chen, Y., Tomonobu, N., Kinoshita, R., Ruma, I. M. W., Sato, H., Kondo, E., Inoue, Y., Yamauchi, A., Murata, H., Yamamoto, K., Tomida, S., Shien, K., Yamamoto, H., Soh, J., Futami, J., Putranto, E. W., Hibino, T., Nishibori, M., … Sakaguchi, M. (2019). Neuroplastin-β mediates S100A8/A9-induced lung cancer disseminative progression. *Molecular Carcinogenesis*, *58*(6), 980–995. https://doi.org/10.1002/mc.22987

Talvi, S., Jokinen, J., Sipilä, K., Rappu, P., Zhang, F.-P., Poutanen, M., Rantakari, P., & Heino, J. (2024). Embigin deficiency leads to delayed embryonic lung development and high neonatal mortality in mice. *iScience*, *27*(2), 108914. https://doi.org/10.1016/j.isci.2024.108914

Tam, P. P. L., & Loebel, D. A. F. (2009). Specifying Mouse Embryonic Germ Cells. *Cell*, *137*(3), 398–400. https://doi.org/10.1016/j.cell.2009.04.016

Torcellan, T., Friedrich, C., Doucet-Ladevèze, R., Ossner, T., Solé, V. V., Riedmann, S., Ugur, M., Imdahl, F., Rosshart, S. P., Arnold, S. J., Gomez de Agüero, M., Gagliani, N., Flavell, R. A., Backes, S., Kastenmüller, W., & Gasteiger, G. (2024). Circulating NK cells establish tissue residency upon acute infection of skin and mediate accelerated effector responses to secondary infection. *Immunity*, *57*(1), 124-140.e7. https://doi.org/10.1016/j.immuni.2023.11.018

Tsuji-Tamura, K., Morino-Koga, S., Suzuki, S., & Ogawa, M. (2021). The canonical smooth muscle cell marker TAGLN is present in endothelial cells and is involved in angiogenesis. *Journal of Cell Science*, *134*(15), jcs254920. https://doi.org/10.1242/jcs.254920

Vainio, S., & Lin, Y. (2002). Coordinating early kidney development: Lessons from gene targeting. *Nature Reviews Genetics*, *3*(7), 533–543. https://doi.org/10.1038/nrg842

Varner, V. D., & Nelson, C. M. (2014). Cellular and physical mechanisms of branching morphogenesis. *Development*, *141*(14), 2750–2759. https://doi.org/10.1242/dev.104794

Vasilescu, D. M., Gao, Z., Saha, P. K., Yin, L., Wang, G., Haefeli-Bleuer, B., Ochs, M., Weibel, E. R., & Hoffman, E. A. (2012). Assessment of morphometry of pulmonary acini in mouse lungs by nondestructive imaging using multiscale microcomputed tomography. *Proceedings of the National Academy of Sciences of the United States of America*, *109*(42), 17105–17110. https://doi.org/10.1073/pnas.1215112109

Wang, H. Y., Zhang, Z., & Yu, S. (2016). Expression of PAPPA2 in human fetomaternal interface and involvement in trophoblast invasion and migration. *Genetics and Molecular Research: GMR*, *15*(3). https://doi.org/10.4238/gmr.15038075

Wilson, M. C., Kraus, M., Marzban, H., Sarna, J. R., Wang, Y., Hawkes, R., Halestrap, A. P., & Beesley, P. W. (2013). The Neuroplastin Adhesion Molecules Are Accessory Proteins That Chaperone the Monocarboxylate Transporter MCT2 to the Neuronal Cell Surface. *PLOS ONE*, *8*(11), e78654. https://doi.org/10.1371/journal.pone.0078654

Wilson, M. C., Meredith, D., Fox, J. E. M., Manoharan, C., Davies, A. J., & Halestrap, A. P. (2005). Basigin (CD147) Is the Target for Organomercurial Inhibition of Monocarboxylate Transporter Isoforms 1 and 4: THE ANCILLARY PROTEIN FOR THE INSENSITIVE MCT2 IS EMBIGIN (gp70)*. *Journal of Biological Chemistry*, *280*(29), 27213–27221. https://doi.org/10.1074/jbc.M411950200

Xu, B., Zhang, M., Zhang, B., Chi, W., Ma, X., Zhang, W., Dong, M., Sheng, L., Zhang, Y., Jiao, W., Shan, Y., Chang, W., Wang, P., Wen, S., Pei, D., Chen, L., Zhang, X., Yan, H., & Ye, S. (2022). Embigin facilitates monocarboxylate transporter 1 localization to the plasma membrane and transition to a decoupling state. *Cell Reports*, *40*(11), 111343. https://doi.org/10.1016/j.celrep.2022.111343

Yagi, S., Tagawa, Y., & Shiojiri, N. (2016). Transdifferentiation of mouse visceral yolk sac cells into parietal yolk sac cells *in vitro*. *Biochemical and Biophysical Research Communications*, *470*(4), 917–923. https://doi.org/10.1016/j.bbrc.2016.01.149

Yamane, T. (2018). Mouse Yolk Sac Hematopoiesis. *Frontiers in Cell and Developmental Biology*, *6*. https://doi.org/10.3389/fcell.2018.00080

Yang, H., Iwanaga, N., Katz, A. R., Ridley, A. R., Miller, H. D., Allen, M. J., Pociask, D., & Kolls, J. K. (2024). Embigin Is Highly Expressed on CD4+ and CD8+ T Cells but Is Dispensable for Several T Cell Effector Responses. *ImmunoHorizons*, *8*(3), 242–253. https://doi.org/10.4049/immunohorizons.2300083

Ye, P., Habib, S. L., Ricono, J. M., Kim, N.-H., Choudhury, G. G., Barnes, J. L., Abboud, H. E., & Arar, M. Y. (2004). Fibronectin induces ureteric bud cells branching and cellular cord and tubule formation. *Kidney International*, *66*(4), 1356–1364. https://doi.org/10.1111/j.1523-1755.2004.00897.x

Yokomizo, T., Yamada-Inagawa, T., Yzaguirre, A. D., Chen, M. J., Speck, N. A., & Dzierzak, E. (2012). Whole-mount three-dimensional imaging of internally localized immunostained cells within mouse embryos. *Nature Protocols*, *7*(3), 421–431. https://doi.org/10.1038/nprot.2011.441

Yoshida, S., Shibata, M., Yamamoto, S., Hagihara, M., Asai, N., Takahashi, M., Mizutani, S., Muramatsu, T., & Kadomatsu, K. (2000). Homo-oligomer formation by basigin, an immunoglobulin superfamily member, via its N-terminal immunoglobulin domain. *European Journal of Biochemistry*, *267*(14), 4372–4380. https://doi.org/10.1046/j.1432-1327.2000.01482.x

Yu, H., Cui, Y., Guo, F., Zhu, Y., Zhang, X., Shang, D., Dong, D., & Xiang, H. (2024). Vanin1 (VNN1) in chronic diseases: Future directions for targeted therapy. *European Journal of Pharmacology*, *962*, 176220. https://doi.org/10.1016/j.ejphar.2023.176220

Yu, H., Königshoff, M., Jayachandran, A., Handley, D., Seeger, W., Kaminski, N., & Eickelberg, O. (2008). Transgelin is a direct target of TGF-β/Smad3-dependent epithelial cell migration in lung fibrosis. *The FASEB Journal*, *22*(6), 1778–1789. https://doi.org/10.1096/fj.07-083857

Yu, X.-L., Hu, T., Du, J.-M., Ding, J.-P., Yang, X.-M., Zhang, J., Yang, B., Shen, X., Zhang, Z., Zhong, W.-D., Wen, N., Jiang, H., Zhu, P., & Chen, Z.-N. (2008). Crystal Structure of HAb18G/CD147: IMPLICATIONS FOR IMMUNOGLOBULIN SUPERFAMILY HOMOPHILIC ADHESION*. *Journal of Biological Chemistry*, *283*(26), 18056–18065. https://doi.org/10.1074/jbc.M802694200

Yurchenko, V., Constant, S., & Bukrinsky, M. (2006). Dealing with the family: CD147 interactions with cyclophilins. *Immunology*, *117*(3), 301–309. https://doi.org/10.1111/j.1365-2567.2005.02316.x

Zhang, S., & Cui, W. (2014). Sox2, a key factor in the regulation of pluripotency and neural differentiation. *World Journal of Stem Cells*, *6*(3), 305–311. https://doi.org/10.4252/wjsc.v6.i3.305

Zhao, L., Song, W., & Chen, Y.-G. (2022). Mesenchymal-epithelial interaction regulates gastrointestinal tract development in mouse embryos. *Cell Reports*, *40*(2), 111053. https://doi.org/10.1016/j.celrep.2022.111053

Zhou, J., Ma, C., Wang, K., Li, X., Zhang, H., Chen, J., Li, Z., & Shi, Y. (2020). Rare and common variants analysis of the EMB gene in patients with schizophrenia. *BMC Psychiatry*, *20*(1), 135. https://doi.org/10.1186/s12888-020-02513-3

Zhou, Y., Zhou, B., Pache, L., Chang, M., Khodabakhshi, A. H., Tanaseichuk, O., Benner, C., & Chanda, S. K. (2019). Metascape provides a biologist-oriented resource for the analysis of systems-level datasets. *Nature Communications*, *10*(1), 1523. https://doi.org/10.1038/s41467-019-09234-6

List of Figures and Tables

Figures

Tables

TURUN
YLIOPISTO
UNIVERSITY
OF TURKU

Painosalama, Turku, Finland 2025

ISBN 978-952-02-0436-5 (PRINT)
ISBN 978-952-02-0437-2 (PDF)
ISSN 0082-7002 (Print)
ISSN 2343-3175 (Online)